DESIGN AND INVESTIGATION OF A NEW TYPE ROTARY VANE AIR COMPRESSOR AND EXPANDER

A MASTER'S THESIS

in

Mechanical Engineering

Middle East Technical University

By

A. Selim OKUTUR

August 1984

Approval of the Graduate Schcol of Natural and Applied Sciences

Director

I certify that this thesis satisfies all the requirements as a thesis for the degree of Master of Science.

Chairman of the Department

I certify that I have read this thesis and in my opinion it is fully adequate, in scope and quality, as a thesis for the degree of Master of Science

Supervisor

Examining Committee ir Charge :

Doç. Dr. Ömer Göksel .....

Doç. Dr. Mazhar Ünsal .....

Y.Doç. Dr. Arif İleri .....

Y.Doç. Dr. İ. Hüseyin Filiz .....

Prof. Dr. Alp Esin .....

Committee Chairman

A B S T R A C T

DESIGN AND INVESTIGATION OF A NEW TYPE ROTARY VANE AIR COMPRESSOR AND EXPANDER

OKUTUR, A. Selim

M.S. in Mechanical Engineering

Supervisor: Assoc. Prof. Dr. Ömer Göksel

August 1984, 212 pages

In this study an attempt was made to design a new sliding vane type rotary compressor and determine its performance characteristics. In addition to the experimental investigation, a new method for prediction of the performance characteristics of the positive displacement gas machinery was developed.

To overcome the problem of rapid vane wear in the vane type compressor, the rollers were added to the root of the vanes, thus transforming the sliding friction on tip of the vanes to the rolling resistance.The addition of the

roller follower to the root of the vanes reduces the friction losses especially at high speeds. By connecting this compressor to an expander, which is similar in design and dimensions, an air-conditioning unit operating on an air cycle may be attained. In order to meet the experimental testing requirements the compressor and the expander were designed as versatile as possible, so that most of the parameters affecting the performance of the units and the air-conditioning cycle could be investigated.

It was observed that the new compressor operates with good efficiency when it is used independently. However, due to the very high efficiency requierements for the air-conditioning cycle, there still remain some difficulties to overcome before the compressor and expander couple can operate as an air-conditioning unit.

Key words : compressor, expander, circulator, vane, unit, positive displacement, air-conditioning unit, air cycle.

ÖZET

YENİ BİR TİP DÖNER KANATLI KOMPRESÖR VE GENLEŞME MAKİNESİNİN TASARIMI , İMALATI VE İNCELENMESİ

OKUTUR, A. Selim

Yüksek Lisans Tezi, Mak. Müh. Bölümü

Tez Yöneticisi : Doç. Dr. Ömer Göksel

Agustos 1984, 212 sahife

Bu çalışmada yeni bir döner kanatlı tip kompresör tasarımı yapılmasına ve performansının saptanmasına çalışılmaktadır. Deneysel araştırmalara ilaveten, pozitif iletimli gaz makinelerinin performanslarını tahmin edebilmek için yeni bir metod geliştirilmiştir.

Kanatlı tip kompresörlerdeki hızlı kanat aşınımı problemini önlemek için , kanat diplerine rulman ilave edilmiş ve böylece kanat uçlarındaki kayma sürtünmesi dönme rezistansına dönüştürülmüştür . Kanat diplerine rulman ilave edilmesi sürtünme kayiplarını özellikle

yüksek hızlarda azaltmıştır. Bu kompresörün tasarım ve boyut bakımından benzer bir genleşme makinesiyle birleştirilmesiyle, hava çevrimli bir klima cihazı olarak kullanımı mümkün olabilmektedir. Deneysel çalışmalardaki değişiklikleri sağlayabilmek için kompresör ve genleşme makinesi mümkün olduğu kadar degişken tasarlanmıştır, böylece cihazların ve soğutma çevriminin performansını etkileyen birçok parametre incelenebilmiştir.

Yeni kompresörün , bağımsız kullanıldığı zamanlarda verimliliğinin iyi olduğu gözlenmiştir. Fakat , bu ünitelerin klima cihazı olarak kulanılabilmesi çok yüksek verimlilik gerektirdiğinden , kompresör ve genleşme makinesi çiftinin bir klima cihazı olarak çalışabilmesi için hali hazırda giderilmesi gerekli bazı zorluklar bulunmaktadır.

Anahtar Kelimeler : kompresör, genleşme makinesi, dolaşım makinesi, kanat, ünite (cihaz), pozitif iletim, klima cihazı, hava çevrimi.

ACKNOWLEDGEMENT

The author wishes to express his deep gratitude to his supervisor, Assoc. Prof. Dr. Ömer Göksel , for his close guide and invaluable support as well as his supervision throughout study.

He would also like to thank to his friends Dr. Kahraman Albayrak and Mr. Sadettin Özyazıcı for their helpful interest to the work and also Yaşar Aksit and Mehmet Abuş Aksoy for their continucus help during this work.

The author also thanks to the staff members of the Computing Centers, who contributed their efforts towards the completion of this manuscript.

Last, but not least, the author also wishes to thank to his wife for her patience, understanding and support during the investigation and preperation of this manuscript.

TABLE OF CONTENTS

TABLE OF CONTENTS (CONT.)

TABLE OF CONTENTS (CONT.)

TABLE OF CONTENTS (CONT.)

LIST OF FIGURES

LIST OF FIGURES (CONT.)

LIST OF FIGURES (CONT.)

LIST OF FIGURES (CONT.)

LIST OF FIGURES (CONT.)

LIST OF FIGURES (CONT.)

LIST OF FIGURES (CONT.)

LIST OF TABLES

LIST CF SYMBOLS

A	area
a	acceleration, crossection area of vane
B	pressure ratic correction factor
b	length of vane
C	coefficient, constant
C_p	specific heat
c	distance at the root of vane
D	diameter of the casing
d	shaft diameter
d_o	roller follower diameter
E	heat exchanger efectivenes
e	eccentricity
F	force
g	gravitational acceleration
H	adiabatic head
h	head, height of the clearance
k	ratio of specific heats, constant
L	length
l	height of the vane

LIST OF SYMBOLS (CONT.)

M	torque
m	molecular weight
N	rotational speed in rpm
N_s	specific speed
n	polytropic constant
P	pressure
PD	pressure drop at ports
PR	pressure ratio
ΔP	pressure difference
p	pulse in radial direction
Q	volume flowrate
q	heat flow
R	radius of the casing, universal gas constant
r	radius, ratio
r_r	radius of the rotor
s	entropy, stroke
T	temperature
t	thickness
U	tip velocity
V	volume
v	specific volume, radial velocity
W	work

x	exponent
Y	characteristic dimension
α	non-dimensional area
γ	specific weight
ϵ	non-dimensional eccentricity
φ	angular position
μ	absolute viscosity
μ_s	friction coefficient
η	efficiency
Ω	digital reading
θ	non-dimensional pressure drop

SUBSCRIPTS

0	atmospheric, zero-speed
1,2,3,4	stages
a	actual
b	breathing
c	compression, compressor, constant friction
d	displacements, discharge
e	expansion, expander
f	pressure dependent friction

g	center of gravity
H	high
hx	heat exchanger
i	inlet, internal
L	low
l	leakage
n	net
m	mechanical
r	speed dependent friction
s	slip
t	ideal
v	volumetric

CHAPTERS

C H A P T E R O N E

INTRODUCTION

The sharp increase in the cost of the available sources of energy, which has taken place in recent years, has dramatically indicated the need for improved overall system efficiency in all systems.

Today most of the factories use the low pressure pneumatic systems. In addition to the factories, low pressure and high capacity machinary are used in some residential applications. So, the demand for the low pressure and high capacity air supply is increasing from day to day.

The aim of this study is to design and construction of a machinery which supplies air at high flowrate but low in pressure. With an additional study the design was also carried out for the production of an expander which has similar construction with the compressor. The purpose in the production of an expander was to couple the compressor to the expander and use them as an air-conditioning unit.

To start the design of the compressor some specifications, such as the flowrate, the pressure developed and the rotational speed of the compressor, were needed. These specifications were selected to meet the requirements of an air conditioning unit when installed on a passenger car. Since the working fluid of this machinery is air, the use of this compressor expander couple as an air conditioning unit might be satisfied if the reverse Brayton open air cycle is selected as the operation cycle of the unit.

The reverse Brayton air cyle, which has been known since 19th century, was used for some residential applications in the last decade. In addition to the system simplicity, the reverse Brayton air cycle has some advantages which the other vapor cycles do not have. Two of them are ; the usage of air as a refrigerant which is a non-toxic fluid, and the system performance is not affected significiantly by the operation temperatures.

The results of analytical models predict that the ideal performance of the reverse Brayton air cycle is greater than the well-known fluorocarbon reverse Rankine cycle which is currently the ' backbone ' of the air conditioning, heat pump and the refrigeration industry. To achieve the results of theoretical analysis, the thermodynamical processes and mechanical components have

to approximate closely the ideal processes as much as possible . The results are only good to the extend that the actual hardware conforms to the assumptions made in the analysis. So, the harcware must be built and tested under actual temperature and pressure conditions.

In this study an attempt was made to develop a compressor and an expander, which can also be used as an air conditioning unit in automotive vehicles which uses air as refrigerant. Tc investigate the advantages of this cycle, and to obtain some design parameters, a prototype unit which has a versatility on some parameters effecting the cycle performance was manufactured, constructed and tested.

The literature surveyed about the reverse Brayton air cycle, the general description of the types of the existing compressors and expanders , anc the attempts to develop the vane type machinary are presented in the next chapter.

Before the design of the prototype compressor and expander which are generally referred as 'units' in this thesis, the design criterion had to be decidec. In the third chapter the design requirements for the compressor-expander couple which from now on will be called as the circulator, as an automobile air conditioning unit is determined. After the discussion of thermodynamics of the

reverse Brayton air cycle, in order to assist the design, a general analysis about the parameters affecting the performance of the positive displacement gas machinery is presented and a new method for prediction of the performance characteristics of the positive displacement gas machinery is developed in the same chapter.

In the fourth chapter, the design of the compressor and the expander as a positive displacement gas machinery is carried out.

The results of the experiments carried out with the prototype units are presented in chapter five.

Conclusion and suggestion for further work are presented in the sixth chapter.

CHAPTER TWO

LITERATURE SURVEY

2.1. GENERAL COMMENTS ON THE AIR CYCLE

When a fixed quantity of a gas is compressed, as is air in a bicycle pump, it becomes warmer. If it is expanded, it cools. For any gas the basic relationships between pressure (P), volume (V) and temperature (T) are described by the gas laws, the absolute temperature of the gas being proportional to the product of its pressure and volume, PV/T=constant. These principles were used by Thomson (13)/*/ when he first proposed the possibility of heat pumping in 19th century. The basic componerts of Thomson's air cycle heat pump is shown in Fig.2.1 . This is the simplest form of the open heat pump cycle, using air as the working fluid.

An open air-cycle or reversed Brayton cycle, that was studied, has been known for many years, and air cycle machines was been used succesfully for refrigeration in

* - Numbers in parenthesis refer the references

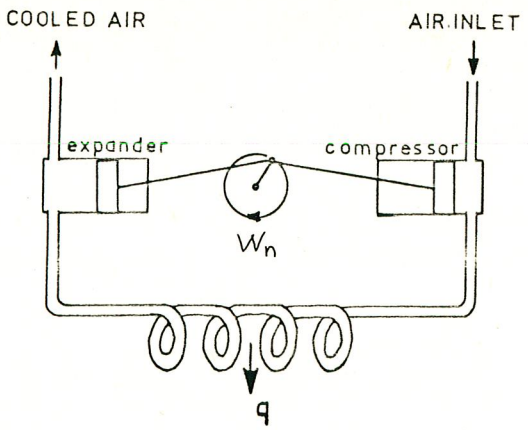

Fig.2. 1. Thomson's Heat Pump

ships in the last century, where the absence of toxic fluids was the main advantage. Modern applications have been limited to cooling cevices using compressed air produced as a by-product of other proceses, as in aircraft air conditioning units in which the jet engine provides the necessary compression. But, in recent years, a reversed Brayton air-cycle was used for some residential applications ; such as for water heating, ice making and air conditioning purposes.

The air-cycle heat pumps have many advantages. Some of them are :

i) The working fluid is air which has no adverse effect on the ozone layer surrounding the earth.

ii) The open air-cycle refrigeration system does not have an indoor heat exchanger installation with fans, refrigeration lines and defrosting mechanism.

iii) The prime mover, and the compressor-expander units need not be hermetically sealed or thermally coupled.

Consequently each component may be optimally designed and maintained independently.

iv) The coefficient of performance, C.O.P., and capacity do not vary significantly with the ambient temperature. Therefore if the system proves to be effective at standart ambient conditions, it can be considered for operation in any climate.

v) The system also does not need any thermostatic or pressure swicth, expansion valve, suction throttling valve and high pressure refrigeration lines, ... in fact , none of the many controls that a freon system needs.

The basic cycle, whether it is an open or closed cycle, embodies one or two heat transfer processes coupled with both a compression and an expansion process. The system configuration, that was studied, was an open polytropic, reverse Brayton cycle, shown in Fig.2.2 .

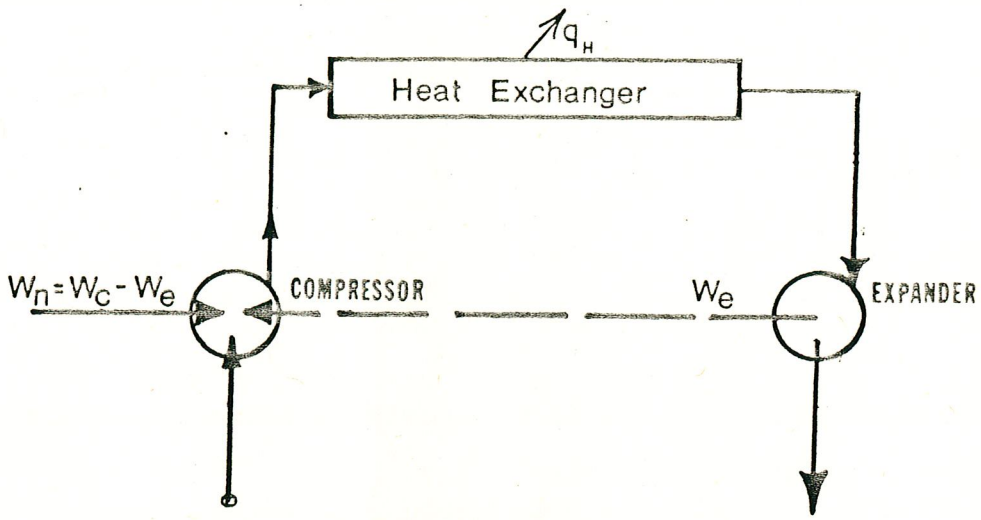

Fig.2. 2. Reverse Brayton Open Air Cycle

Ambient air is drawn into the system and compressed at constant entropy, resulting an increase in its temperature and pressure. After it is cooled to nearly ambient temperature at high pressure in the heat exchanger, the compressed air is allowed to expand in the expander. The energy given up by expanding the air helps to compress the air in the compressor. While the air expanding at constant entropy in the expander, its temperature drops below the ambient temperature and the cooled air is exhausted to the conditioned space. The corresponding T-s and P-v diagrams are shown in Fig.2.3 .

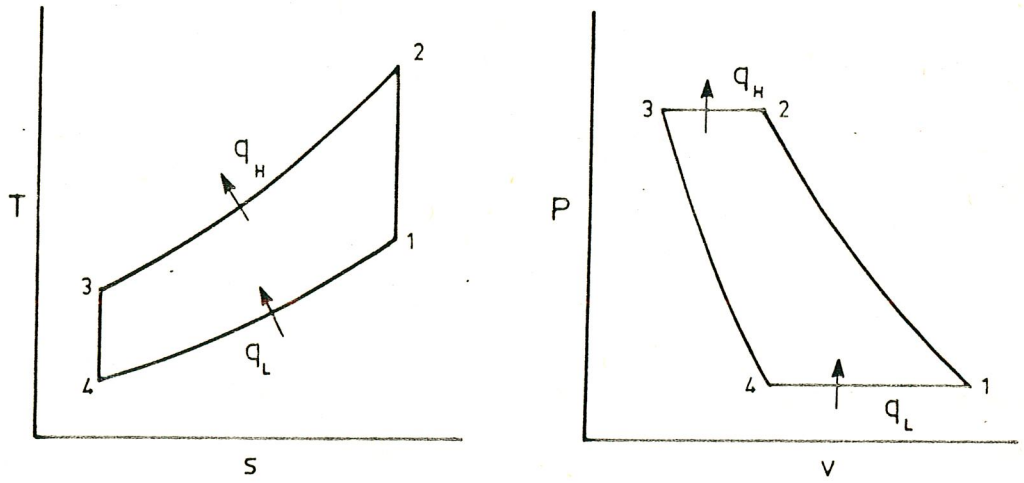

Fig.2. 3. T-s and P-v Diagrams of Air Cycle

The refrigerant of the air cycle, does not have phase change during cycling. It transfers the heat by thermal capacity of its molecules, which is very low when compared to the fluids which has phase change . This means that a very high mass flow rate is nedded through the compressor, therefore an air cycle compressor must have a

displacement of 70 times greater than a Freon 22 system needs. This disadvantage of the air cyle restricts the applications of this system where high cooling requirements are nedded.

2.2. PREVIOUS WORKS ON AIR CYCLE

After Thomson , the air cycle was first developed by Lebre (13) who used a multi cellular rotary machine to exract heat from stale ventilation air in Zurich Congress Hall in late 1930's.

There was a design study that had been performed recently by Ericson, Harwey and Toscano (18), to determine the mechanical and economic viability of reverse Brayton air-cycle water heater. A summary of the prototype design specifications are presented in Table 2.1 .

TABLE 2.1

SPECIFICATIONS OF AIR-CYCLE HEAT-PUMP WATER HEATER

WATER USAGE RATE	300 Lt/Day
HOT WATER TEMPERATURE	60 °C
HEAT PUMP HEAT RATE	2.3 KW
ENGINE ELECTRIC CONSUMPTION	1.7 KW
COMPRESSOR/EXPANDER FLOW CAPACITY	156 Lt/s
COMPRESSOR SUCTION PRESSURE	103 kPa
COMPRESSOR DISCHARGE PRESSURE	310 kPa
THERMODYNAMIC C.O.P.(HEATING)	1.7 or greater
EXPERIMENTAL C.O.P.(HEATING)	1.2-1.4

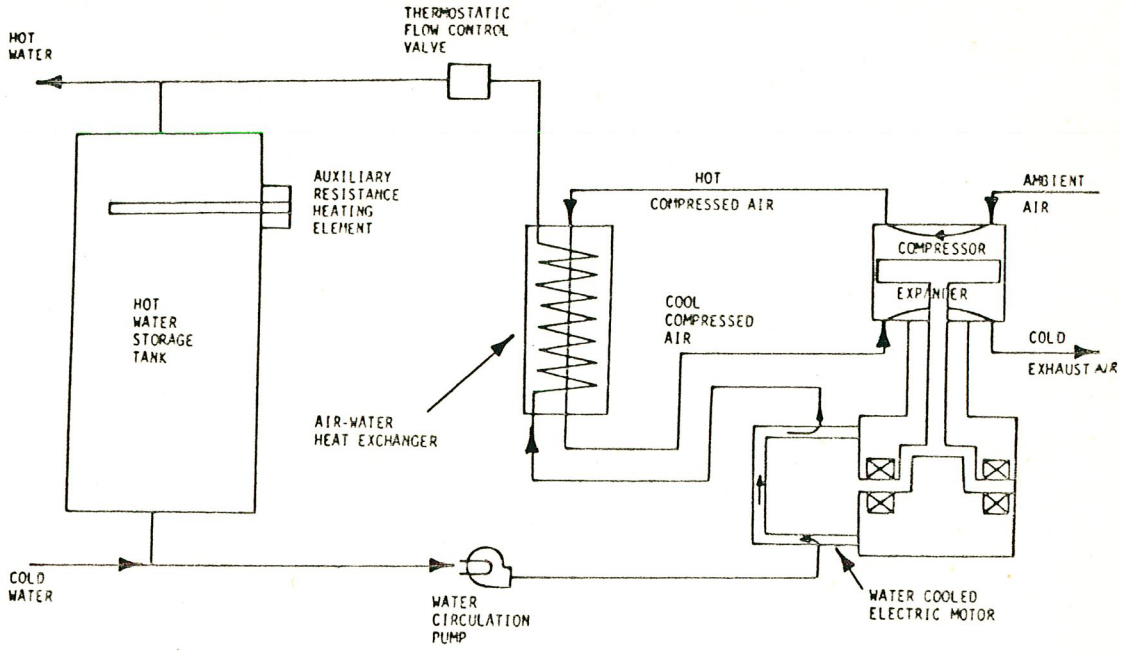

Fig.2. 4. Flow Diagrams of Air Cycle Heat Pump Water Heater

As is shown in Fig.2.4, the system configuration that was studied, was an open polytropic, reverse Brayton cycle. Ambient air is drawn into the system and compressed, thus increasing its temperature. The hot compressed air then passes trough the air water, counter flow heat exchanger, thus cooling the air and heating the water to the desired temperature. The compressed air is then expanded, with the recovered work helping to drive the compressor. Air is exhausted from the expander at temperatures between 217 °K and 267 °K. It can be used to augment air conditioning during summer. At further studies of Ericson, Harvey and Toscano, a regenerator was used to increase the cycle efficiency. Compressed air which had passed trough the water-air heat

exchanger is subsequently used to preheat the incoming ambient air.They also performed a preliminary mechanical design study, in order to reduce the losses in the compressor expancer couple. Various valve types, valve drive mechanisms and crosshead mechanisms were investigated. The selected mechanical configuration was a reciprocating compressor expander system with reed valves for the compressor and the poppet valves for the expander. The reed valves are pressure actuated and the poppet valves are operated by levers which were directly coupled to cam lobes located on the crankshaft. An external view of this compressor-expander system is shown in Fig.2.5 .

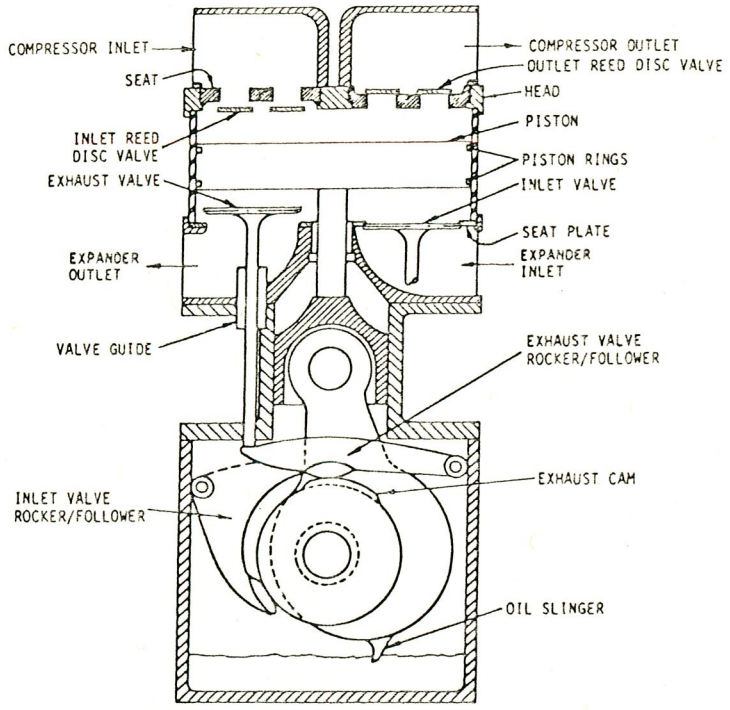

Fig.2.5.Schematic of the Compressor-Expander of Water Heater

At the end of their work it was concluded that the compressor and expancer isentropic efficiencies strongly effect the C.O.P. of the cycle . The differences between experimental results and thermodyramic performance calculations, on which the design of the machine was based, were attributed tc the mass transfer losses. In addition it was suggested that the mechanism of the transient heat transfer and flow leakage which occurs in the compressor and expander must be investigated.

Usually in the open air-cycle moist air is used as the refrigerant. The effect of moisture content of air on the cycle performance was investigated by Cooper and Sumner (5). They investigated several variations of the open air-cycle and presented their results graphically in the form of carpet plots. An example of their graphs is shown in Fig.2.6 .

A carpet plot is basically graphical means that allows double interpolation as well as consistency with a minumum amount of data. In such carpet plots, a line of constant isentropic compressor efficiency has a negative slope. As one moves along this line to the right, isentropic expansion efficiency decreases as indicated by the intersection of lines of constant isentropic expansion efficiency, which have positive slope.

Fig.2.6 shows the C.O.P. variation on a carpet plot

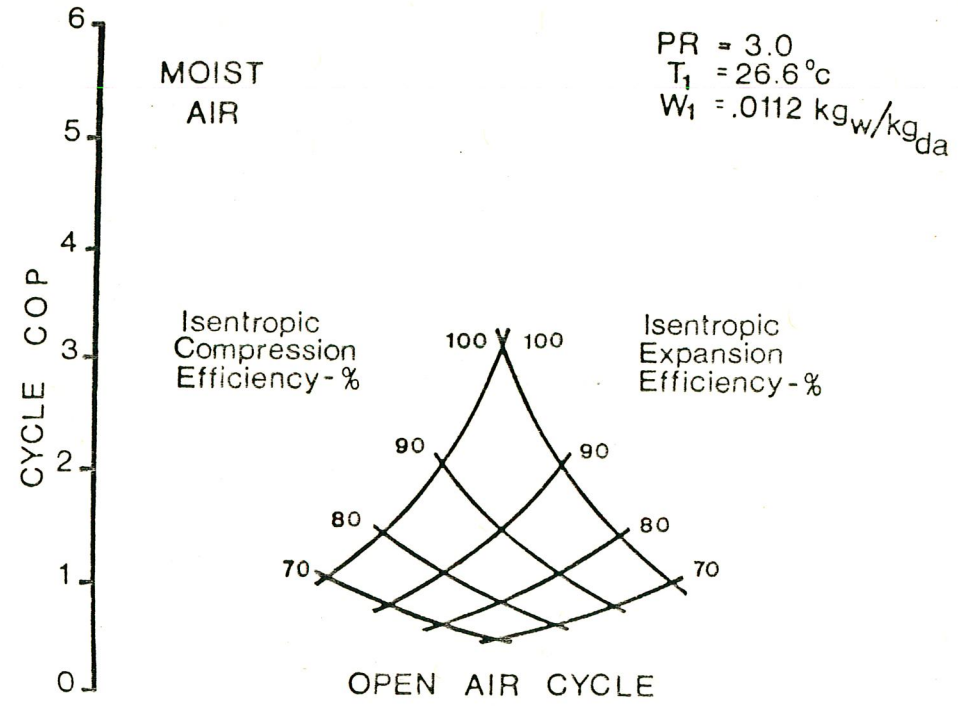

Fig.2. 6. C.O.P. Variation of Air Cyle With Moist Air

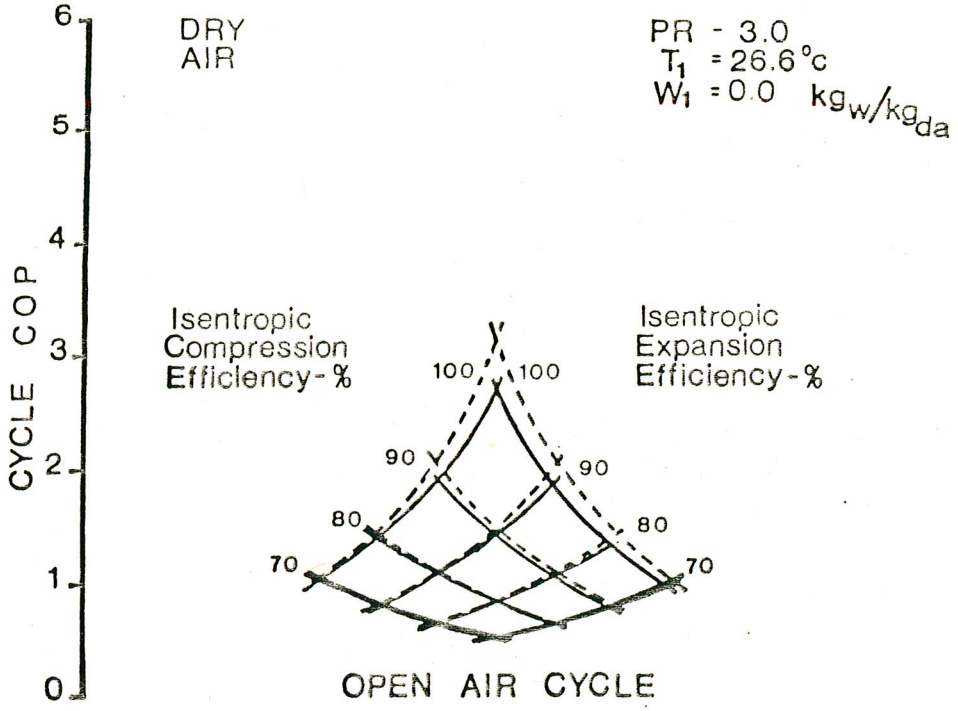

Fig.2. 7. C.O.P. Variation of Air Cyle With Dry Air

with a pressure ratio of 3.0 and 0.0112 kg of water per kg of dry air (kgw/kgda) moisture content. This plot is preapered by Cooper and Sumner for standart A.R.I. cooling rating condition of 26.6 °C (80 °F) indoor dry-bulb temperature, 19.5 °C (67 °F) indoor wet-bulb temperature, and 35 °C (95 °F) outdoor dry-bulb temperature.

The comparison between C.O.P. of dry air and C.O.P. of moist air can be seen in Fig.2.7 . Here the dashed lines indicate the moist air. As is seen in Fig.2.7 C.O.P. of moist air is greater than that of dry air, with a narrowing C.O.P. difference at lower isentropic efficiencies.

On the other hand, Fig.2.8 shows a markec increase in C.O.P. for the isentropic case when 0.020 kg of liquid

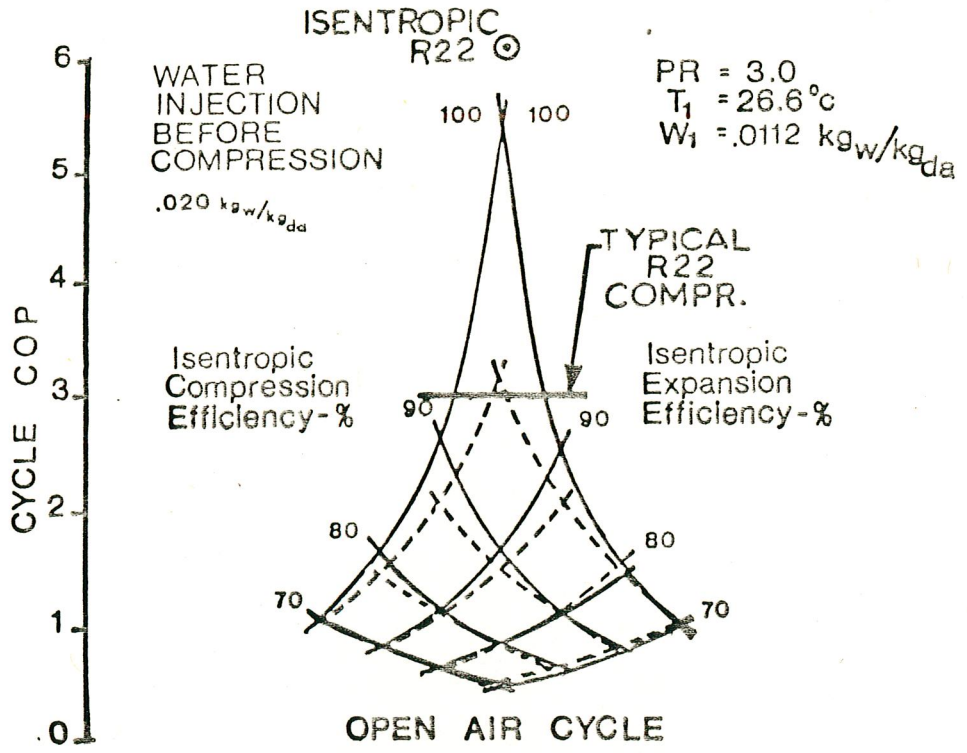

Fig.2. 8. C.O.P. Variation of Air Cyle With Water Injection

water per kg of dry air is sprayed into the air stream entering the compressor.

If the moisture content of the air in the cooled space is increased, resulting in a dry-bulb temperature of 26.6 °C (80 °F) and wet-bulb temperature of 25.6 °C (78 °F), the cycle C.O.P. is again increased as indicated by Fig.2.9 .

These figures indicate that, while the cycle C.O.P. is sensitive to moisture content at high isentropic efficiencies, much of the difference between C.O.P. of moist air and C.O.P. of dry air disappears as the compression and expansion efficiencies drop off. In other words, for an air-cycle, if the isentropic compressor and expander efficiencies are below 80 percent, the effect of moist air

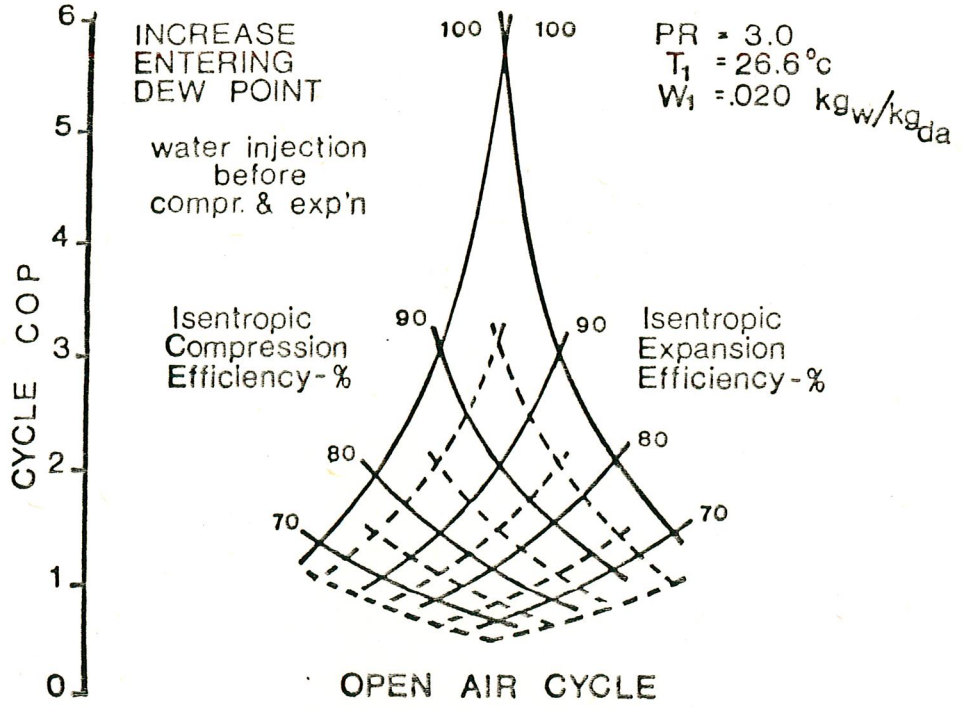

Fig.2. 9. C.O.P. Variation of Air Cyle With Increased Moisture Content

and the effect of water injection on air cycle performance are small.

Cooper and Sumner also investigated the effects of pressure drop in the heat exchanger. As is shown in Fig.2.10 a pressure drop of only 13.8 kpa (2 psi) in the heat exchanger produces a significant C.O.P. degredation.

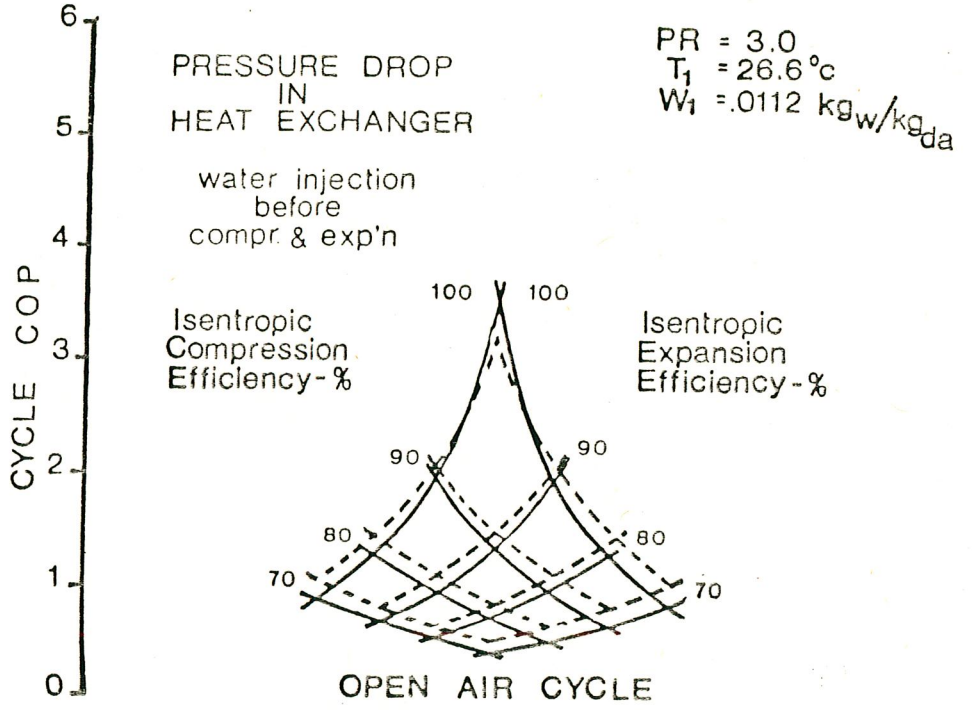

Fig.2.10. Effect of Pressure Drop in the Heat Exchanger to the C.O.P. of the Air Cycle

Another study was performed by Edwards (7) who used multi-component mixed phase fluid, a water air mixture, in his cycle. This cycle was called after his name, the Edwards Cycle. The simple configuration of this cycle is shown in Fig.2.11 . Edwards used a positive displacement device named as the circulator. It employs substantially, an eliptical stator cavity together with a rotating vane

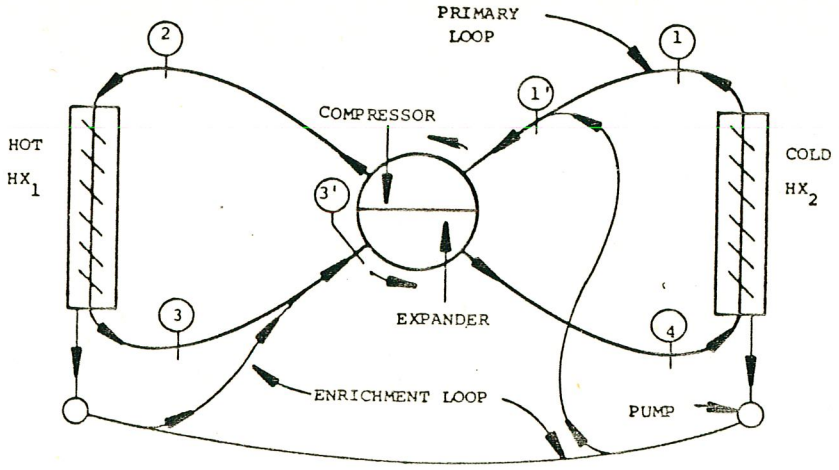

Fig.2.11. General Configuration of Edwards Cycle

assembly. When in motion, the rotor vane assembly simultaneously compress, provides for intercooling of air in the heat exchanger, expands and provides reheating of the circulating air. The refrigerant of this cycle has two components, namely the primary component which is air and the secondary component which is water. It was conceptualized as a synergistic union between the air cycle and the vapor compression cycle. In other words, the reverse Brayton and the reverse Rankine cycles are subcases of the new cycle. Further it was shown that this new cycle yields ideal C.O.P. greater than the C.O.P. of reverse Brayton and reverse Rankine cycles.

Edwards, concentrated his study in this work, primarily on qualitative and quantitative aspects of this cycle from the polytropic viewpoint.

Further study of Edwards Cycle was developed by Ecker, Edwards and Wark (6) . In this work they suggested the

optimization of pressure ratio and amount of system pressurization for the given external constraints to determine the effect of the above mentioned parameters on optimum C.O.P.

The coefficient of performance for a system comprising work recovery is a quantity that magnifies small difference in the work terms. Because the net work input, which is generally a small term, is the result of the difference of two substantialy larger terms. In other words, C.O.P. is sensitive to the variation in the work terms and the efficiencies of the compressor and the expander. Fig.2.8 shows the effect of compressor and expander isentropic efficiency on the cycle performance with comparison to a Freon-22 system.

In the existing literature that was surveyed, it is seen that, of all the components of reverse Brayton cycle system, the compressor and expancer are the most important ones . Therefore, prior to discussing the complete cycle and various sytem configurations, attention will be given to the two machinery; namely the compressor and the expander, which are most difficult to design for high efficiency.

So, the general description of the compressor and the expander will be given and the literature about the types and the developments of the compressor and the expander, is surveyed and presented in the following sections.

2.3. COMPRESSORS

The word 'compressor' is loosely defined in practice for many years , 'blower' meant ; any machine that compressed a gas 1.03 bar absolute pressure to 3 bar absolute pressure ; a machine which produced a pressure rise greater than 3 bar absolute pressure was called a 'compressor'. This definition is not valid for single stage centrifugal and axial machines. Today distinction between blowers and the compressors has vanished. A machine is now called a compressor if a pressure rise greater than 3 percent is achieved between the inlet and exit of the machine, on the other hand machinery producing a pressure rise under 3 percent, is called a fan (20) .

The compressors may be classified as the positive displacement and the turbo compressors. The main distinction between these above mentioned compressor types is in the energy transfer method. In positive displacement machinery the fluid is compressed by varying the volume of the fluid ; where as in the rotodynamic machines the pressure rise results from dynamic effects between the fluid and the rotor blades.

Depending on the practical direction of the gas flow

in turbocompressors, they may also be classified as the axial flow and the radial flow machines. Intermediate mixed flow types employ varying combinations of axial and radial flow.

Positive displacement compressors may be reciprocating machines such as piston and diaphram types and rotating machines of the vane, gear, screw and lobe types.

Operating characteristics of all types of compressors can be compared with each other by combined use of the two parameters namely the specific speed and the adiabatic head. The concept of specific speed was first developed for liquid pumps and later it was also used for the analysis of machinery handling compressible fluids.

$$N_s = N\ Q^{1/2} / h^{3/4} \qquad 2.1$$

For liquids, h is the total head developed by the machine, but, for machinery handling compressible fluids, h must be integrated for density change in the compression process. Using the thermodynamic description of a reversible adiabatic process, adiabatic head, H, maybe expressed as :

$$H = (R\ T / m)\ (k / k - 1)\ [(P_2 / P_1)^{\frac{k-1}{k}} - 1] \qquad 2.2$$

or $$H\ m / T = f[k , (P_2 / P_1)] \qquad 2.3$$

where ; T is inlet temperature in °K, R is the universal gas constant, m is the molecular weight of the gas, k is the ratio of specific heats, P_2 and P_1 are discharge and intake pressures respectively.

This relationship is presented graphically in the 'adiabatic head' curves shown in Fig.2.12 . It expresses the compressor performance in terms of : pressure ratio across the machine, fluid inlet temperature, molecular weight and the ratio of the specific heats of the fluid. This relationship can be used to determine the adiabatic head needed for a given application, or to select a specific compressor from the catalog performance cata (20) .

In a centrifugal or an axial flow compressor, H is determined by the speed, the impeller diameter and the vane

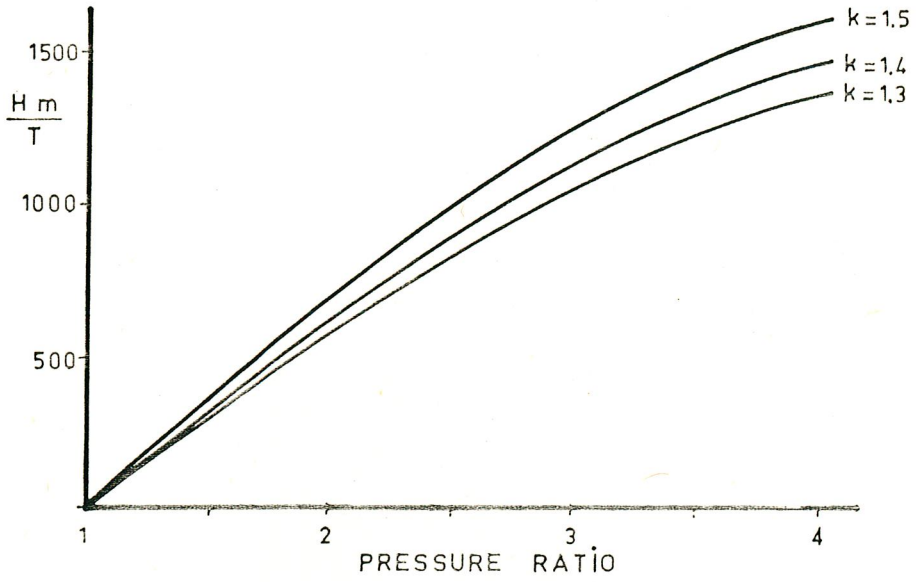

Fig.2.12. Adiabatic Head Curves

geometry.In a positive displacement machine, H is determined by the volume change in flow space during the compression stroke. Thus, this factor is a useful parameter in evaluating the capability of compression of any compressor under given operating conditions.

The adiabatic head concept helps to evaluate the effect of the fluid properties, inlet pressure and inlet temperature on compressor performance.

For a given machine :

* An increase in inlet temperature decreases the pressure ratio.

* Change in inlet pressure produces a proportional change in discharge pressure.

* Using a working fluid with higher molecular weight increases the pressure ratio.

Since this relationship applies to both positive displacement and turbo compressors, it offers a direct method of comparing the performance of different types of conventional compressors for a specific application. This is done by plotting relative efficiency against specific speed, Fig.2.13 (20).

As is shown in Fig.2.13 , centrifugal and axial flow machines have relatively high efficiency but at higher specific speeds. If the outer dimensions of the machine are limited, axial flow and centrifugal compressors must

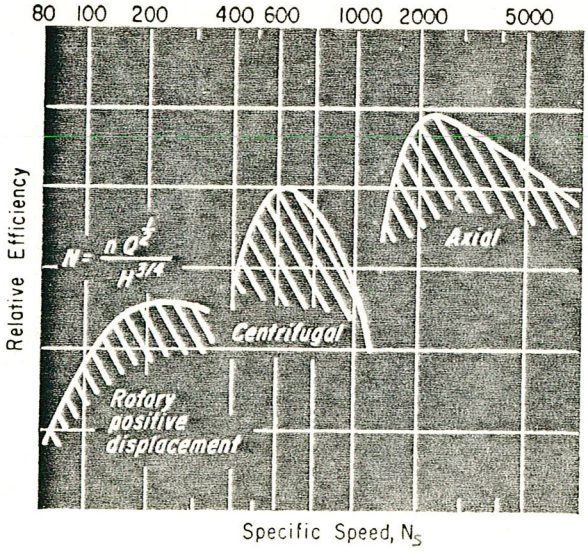

Fig.2.13. Specific Speed Chart of Conventional Types of Compressor

operate at relatively very high speeds for reasonable efficiencies. This high speed requirement imposes some design difficulties such as requirements of high speed, high efficiency gearbox production which increases the cost and weigth of the system. Turbocompressors can suffer from a phenomenon known as 'surge' and this is an important consideration with regard to the selection of the compressor operating point. The surging characteristics of a turbocompressor make the design of a specific compressor very difficult so that it operates at a wide speed range. As is seen from Fig.2.14 , a positive displacement machine gives almost constant efficiency for a wider operating speed range in comparison to axial flow and centrifugal compressors.

If the prime mover of the compressor is an internal

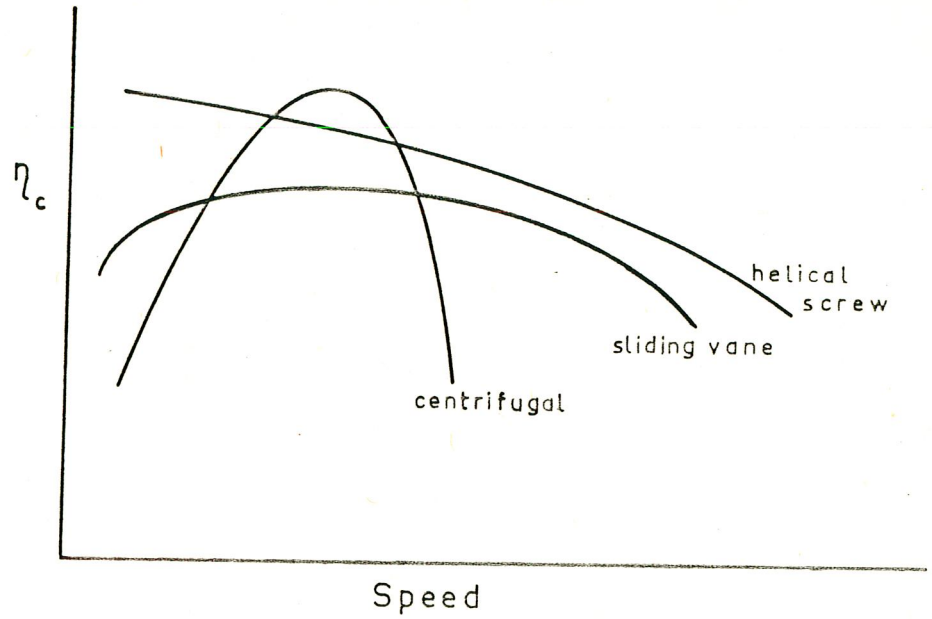

Fig.2.14. Relative Efficiencies of Convertional Types of Compressor

combustion engine operating on an automobile the selected compressor must operate at almost all speeds with a reasonable efficiency. Positive displacement machines have this special feature. So, the general information about the positive displacement compressor will be given here.

Basically, in a positive displacement machine, capacity is related to swept volume and rate of revolution. Thus for a given geometry, capacity is directly proportinal to speed. Therefore the capacity is constant for any given speed, neglecting the effect of internal leakage.

2.4. TYPES OF POSITIVE DISPLACEMENT COMPRESSORS

2.4.1. Reciprocating Piston Compressor

Piston-type reciprocating compressors are available in great variety , including special machines for unusual requirements. These are basically fixed-capacity positive displacement units which discharge a definite quantity of fluid per stroke. When the piston moves downward the gas is taken into the cylinder through a one-way valve. On the up-stroke piston discharges the air through the discharge valve. Maximum compression ratio of reciprocating compressors is 10 per stage. Two stage compressors are available for compression ratios greater than 8.

There are several cylinder arrangements for reciprocating piston type compressors , such as multicylinder 'V' or 'Y' type, four cylinder radial type, two cylinder angle compressors with one cylinder vertical and the other one horizontal.

A special type of reciprocating compressor shown in Fig.2.15 is an axial piston compressor which is utilized as refrigerant compressor in air-conditioning units of

automobiles. The rotating input motion is converted to a reciprocating axial piston motion by the cam plate or swash plate which is keyed to the shaft. This arrangement provides smoother operation thus eliminating the disadvantage of unsteady discharge of reciprocating compressors.

In our design, the reciprocating piston compressor does not satisfy the requirements of low cost for production and sufficient compactiness in size. However, the axial piston compressor used in the automotive refrigeration cycles, the relatively small displacement of such compressors does not satisfy our mass flow rate.

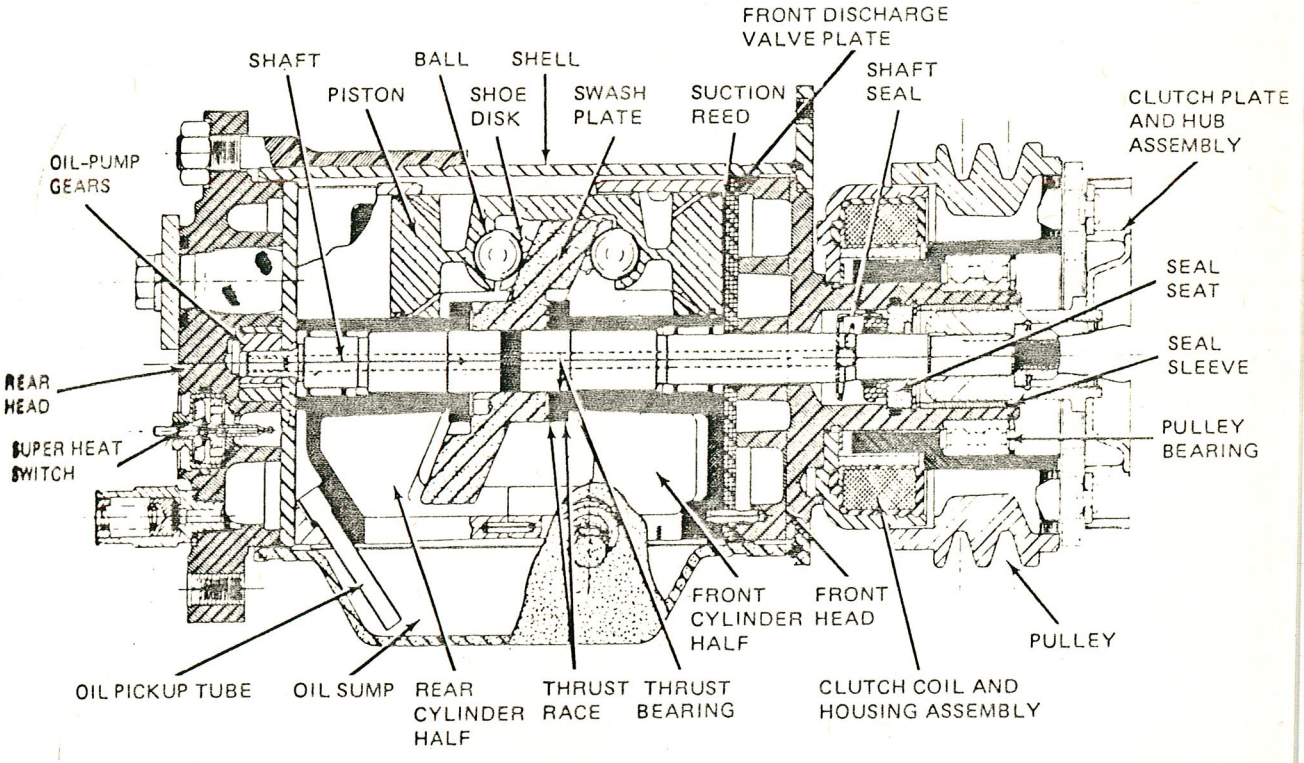

Fig.2.15. An Axial Piston Compressor

2.4.2. Screw Compressor

The commonest type of screw compressor is often called The Lyshlom compressor, after its Swedish inventor. The principle of operation is easy to follow in general terms, but becomes more complex if the details are examined. The description here is restricted to general principles.(13)

The compressor consist of two rotors running together within a sealing sleeve. The rotors are identified as 'male' and 'female'. The male rotor has a number of lobes on it (usually 4) which are semicircular in section and formed in a helix along the rotor body. The female rotor has a number of flutes and channels in it, formed in the opposite helix to the male as shown in Fig.2.16 and Fig.2.17 .

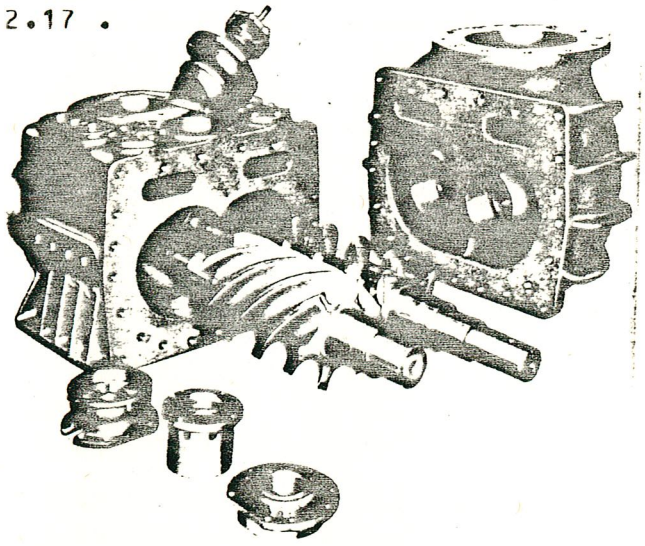

Fig.2.16. Exploded View of Helical Screw Compressor

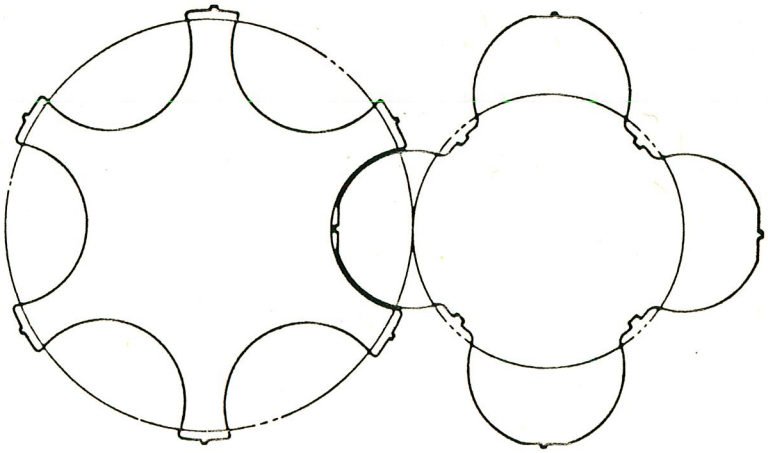

Fig.2.17. Rotor Profiles of Helical Screw Compressor

Compression is achived in a volume within one channel of the female rotor, sealed by the discharge end, peripheral face of the casing, and the interface between the male and female rotors. Discharge occurs through a port in the end of the casing, and all the gas or vapour is discharged, so there is no expansion loss during discharge.

When a screw compressor is designed to run dry, then it is an oil-free compressor offering high outputs at reasonable efficiencies, and high discharge temperatures. In these compressors, there are sealing problems, and compression pressures are relatively low. The oil-injected screw compressor is in comparison to the dry running compressor is more suited for many refrigeration and heat pump applications.

The principle of oil-injection is that oil is

continuously pumped into the suction volume of the compressor, to about 1 percent by volume. Because the ratio by weight of oil to refrigerant fluid is much greater, the oil seperation after discharge becomes a disadvantage. After the oil is injected into the compressor inlet, the oil and the refrigerant are mixed at high pressure, and oil dilution usually becomes a problem.

The principle disadvantages of screw compressors are the high cost relative to the other positive displacement machines and its high noise level.

2.4.3. Rotary Lobe Compressor

Lobe type compressor have specially shaped rotors. As shown in Fig.2.18 and Fig.2.19, the rotors may have two , three or even more lobes of specific form. The rotors of lobe type compressors are externally driven and are syncronously timed, so that instead of physical contact between them the lobes mesh with a small clearance at all times, thus eliminating need for internal lubrication as in the screw type compressors. These mating lobed impellers push the gas from inlet to discharge line. No internal compression takes place, but the impeller forces the gas through discharge openning against the back

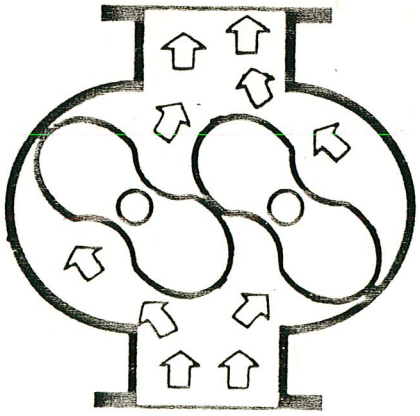

2.18. Two Lobe Compressor

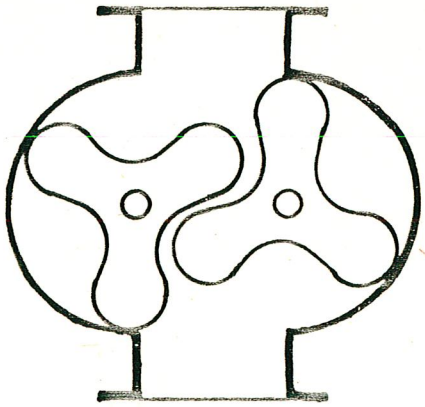

2.19. Three Lobe Compressor

pressure of the system.

Particular mechanical advantages are the absence of wear, no need for lubrication of the rotor faces, and absence of out of balance forces. Due to the latter, compressor can be operated at high speeds. The lobe rotor is suitable for manufacturing in larger sizes (12) .

The main disadvantages of lobe-type compressors are : (i), production difficulty of impeller profiles which are precision ground, (ii), unsteady flow output and torque input, (iii), high noise level, (iv) the maximum compression ratios are limited to about 1.7 in a single stage lobe compressor (20) .

2.4.4. Liquid Piston Compressor

As shown in Fig.2.20, liquid piston compressors employ water or other low viscosity liquid to compress gas

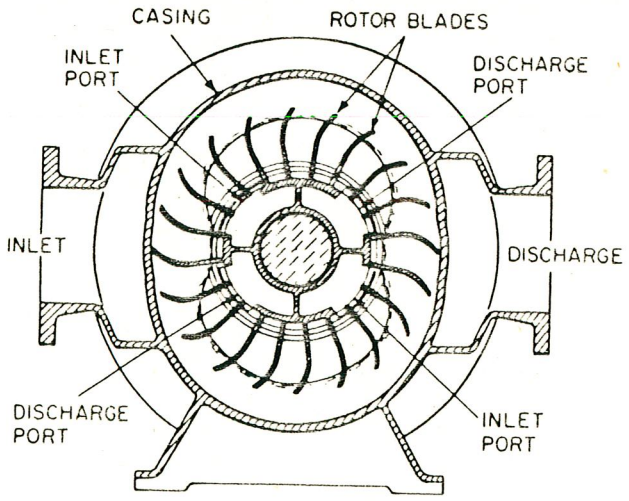

Fig.2.20. Liquid Piston Compressor

trapped between the blades and the liquid interface. The blades of the rotor form a series of buckets carrying the liquid around inside of an elliptical casing. Since the liquid following the contour of the insice of the casing, it surges back into the buckets at the narrow point of the ellipse, and the air in the buckets is compressed and discharged through properly located ports (16) .

There is no metal to metal contact between the blades and the casing wall; therefore there is no need for lubrication at these points. Single stage compressors have a wide range of flow capacities with compression ratios up to 4. Due to its low efficiency and liquid loss for long time of operation, the field of application of this type of compressor is very narrow.

Liquid piston compressors need an external cooling system for cooling the liquid, which means some extra cost.

2.4.5. Vane Type Compressor

Vane type compressor may be categorized uncer two basic types ;

A) Sliding vane type compressors, Fig.2.21 , where the vanes or the blades are housed in slots in the rotor and can extend in radial direction,

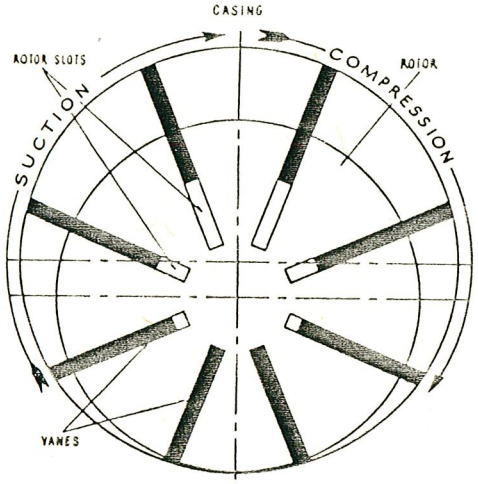

Fig.2.21. Sliding Vane Type Compressor

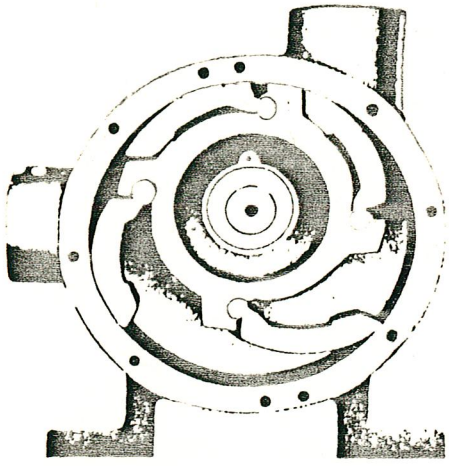

Fig.2.22. Swinging Vane Type Compressor

B) Swinging vane type compressors, shown in Fig.2.22 , where the vanes are hinged to the rotor and swings outwards under centrifugal forces.

Both compressors rely on the same basic mechanical action of producing a variable intervane volume during rotation, by mounting the rotor eccentric to the casing. This type of compressor instead of purely relying on a centrifugal force to throw the vanes outwards; vanes may be individualy backed by springs or push rods to ensure adequate sealing pressure at low speeds. Particular advantages offered include good sealing and thus low leakage without the necessity of extremely accurate manufacturing methods, and self compensation against the leakage due to wear on the tip of the impeller blades. The range of application of the conventional vane type rotary compressors can be seen in Fig.2.23 . In the swinging vane type compressors, the vanes occupy a considerably large space ; therefore the number of vanes are limited.

Sliding vane type compressors were extensively used before the development of the modern centrifugal compressors. Their valveless, simple, compact, light in weight and low cost construction enhanced their usage in the industry. However the discharge pressure is somewhat limited and seldom exceeds 3.5 atm.. At high blade tip speeds, the blade tip friction becomes a limiting factor

due to rapid increase of wear which causes the efficiency to decrease (3) .

If the friction on the tip of the vanes is reduced, the sliding vane type compressor can be operated at higher efficiencies. Sliding vane type rotary compressor have a great possibilty of improvements among the above mentioned and other types of positive displacement compressor. After the discussion of types of the expanders the most suitable compressor type will be selected for design and development purposes.

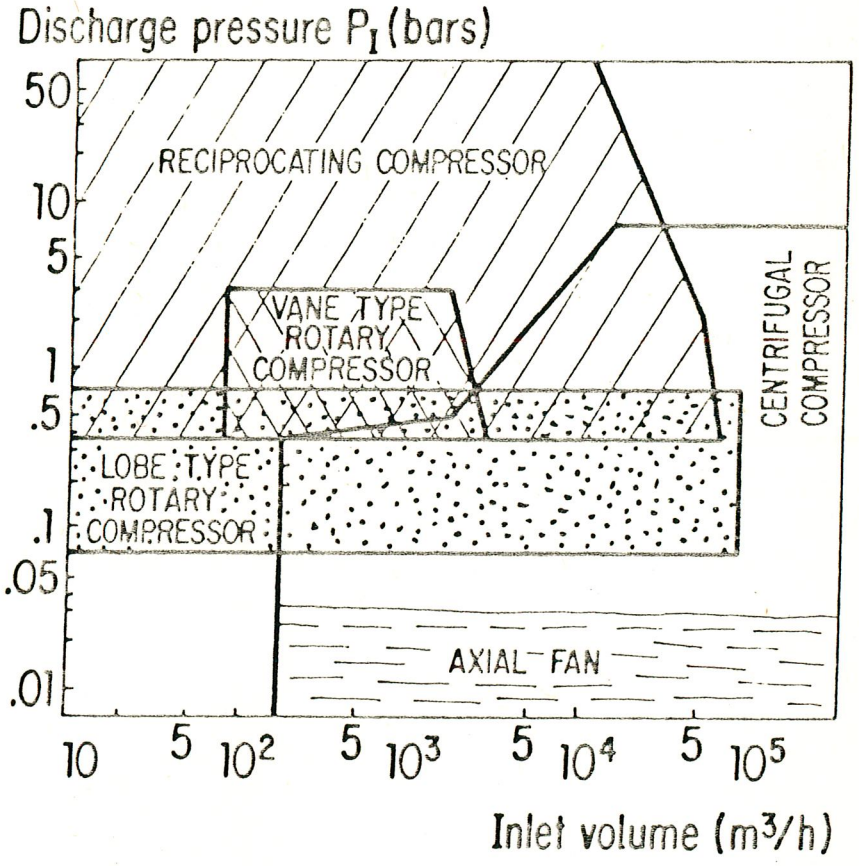

Fig.2.23. Duties of Various Compressors

2.5. EXPANDERS

Of all the components of the reverse Brayton cycle system, the expander, which is the most important unit of the system, is the most difficult to design for high efficiency.

An expander can be defined as a machine which is basically a compressor operating in reverse. In other words, if the sequence of operations in a compressor can be reversed and the valves are properly governed, a compressor can be operated as an expander or a mechanical energy recovering device ; namely a motor.

Vapor expanders of various types have received much attention in recent years and some impressive accomplishments have been achived (18). Development activity has been concentrated on both the turbine and the reciprocating piston expander. Although the vane type rotary expander is by no means a new concept its development for high flowrate and most efficient expansion is virtualy does not exist, except the case where it is used as a low temperature, low expansion, low efficiency air motor.

General Electric had developed a multi-vane rotary

expander for high temperatures and high pressures which has a measured isentropic efficiency of 80 % and brake horsepower of 40 HP (14). This work was done to improve the fuel economy of the long-haul trucks by increasing the output power of the diesel engine simply by coupling an expander to it. As is shown in Fig.2.24 the use of organic working fluids to recover the waste heat of diesel exhaust and adding a portion of this energy to the basic engine output ; had the potential to provide a peak fuel savings of up to 15 % . The results of the preliminary cycle analysis and the hardware of this study lead to the conclusion that the multi-vane rotary expander is an atractive alternate to high-speed turbine-gearbox

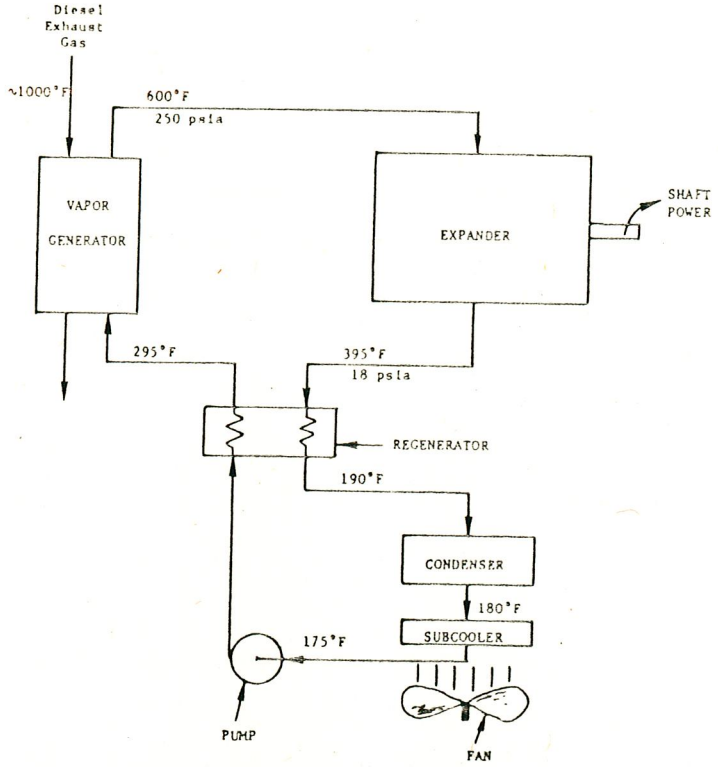

Fig.2.24. Reverse Rankine Cycle with an Expander

combination.

The vane-type rotary expander is basically a low speed device , possesing certain advantages over the charecteristics of the reciprocating expander ano also of the turbine, while remaining fairly simple in design and potentially low cost in production. Table 2.2 shows a comparison of the three potential expanders. Eecause of the combination of features embodied in the vane-type rotary expander, it is thought to be mcst preferable for our purpose.

TABLE 2.2

FEATURES OF EXPANDERS (14)

Expander requirements	Turbine	Piston	Rotary-Vane
Low profile geometry	yes	no	yes
Low noise and vibration	yes	no	yes
Low speed-High torque	no	no	yes
Wider speed range	no	yes	yes
Minumum of complexity	yes	yes	yes
Smooth torque output	yes	no	yes
Moderately high eff.	yes	yes	yes
Low cost	yes	no	yes

The detail of a vane-type rotary expander is shown in Fig.2.25 and 2.26 . A cylindirical rotor with sliding

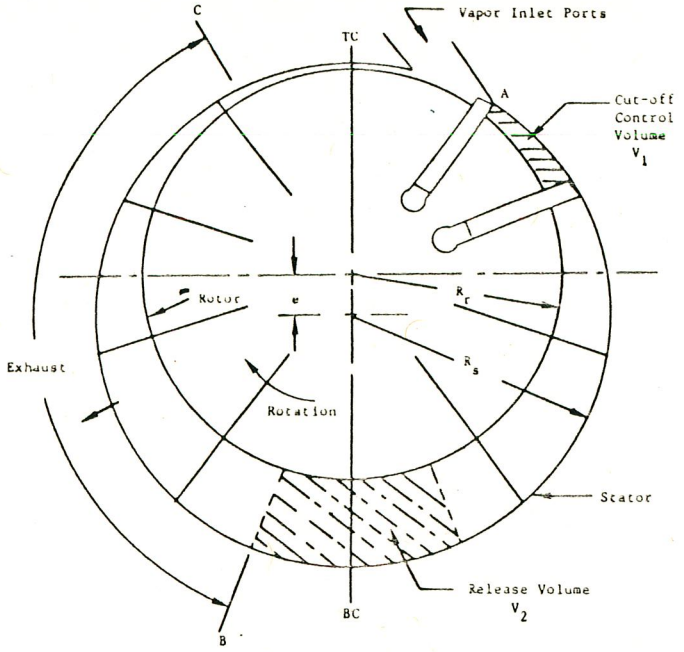

Fig.2.25. Basic Multi Vane Expander

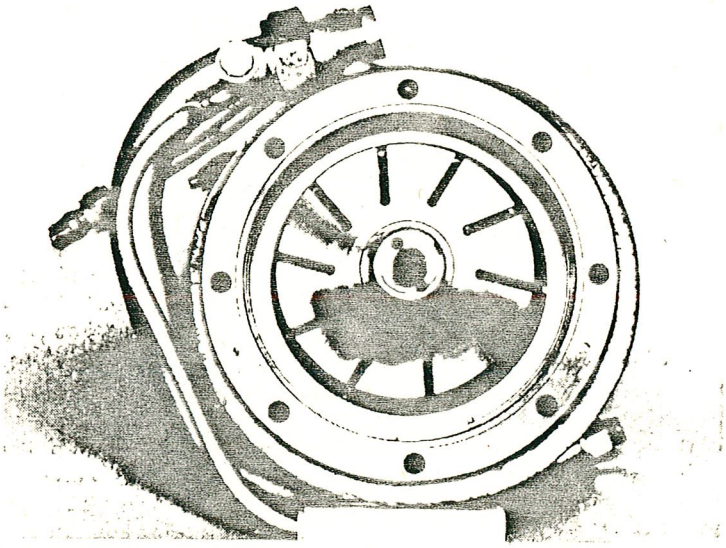

Fig.2.26. End View of Multi Vane Expander

vanes is set eccentrically in a cylidirical housing same as the vane-type rotary compressor. Compressed air is admitted trough the inlet ports and fills the cavity between two adjecent vanes. The rotor, the stator and the end plates forms a confined control volume, V_1 . Pressure unbalance acting on the vanes causes the rotor to rotate.

As the rotor continues to rotate the control volume increases as the gas expands doing work on the blades. As the control volume moves to position B, the fluid can no longer expand and is exhausted. The flow of a gas into the expander is continious provicing relatively smocth torque output. The amount of work done per unit mass of the gas generally depends on completeness of the expansion, internal leakage and internal friction of the machine. Fig.2.27 shows the effects of over or under expansion (14).

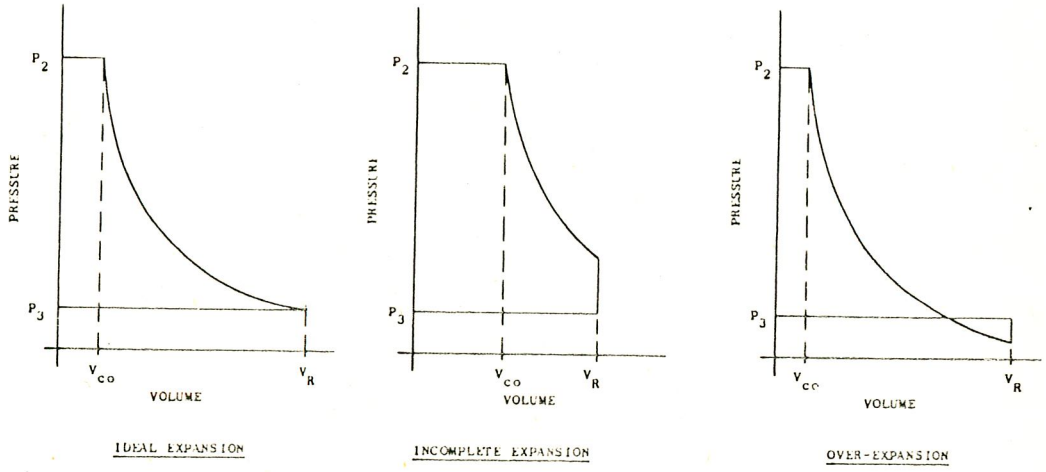

Fig.2.27. Effect of Mismatched Expansion

Expansion losses are due to a mismatch between actual ratio of inlet pressure to exit pressure, as imposed by the cycle pressure external to the expancer, and the pressure ratio which corresponds to the cesigned volume ratio of the expander. This condition may be due to off design operations or a deliberate mismatch at the design point. Fig.2.28 shows the efect on efficiency of off-design pressure ratios on a machine with a fixed

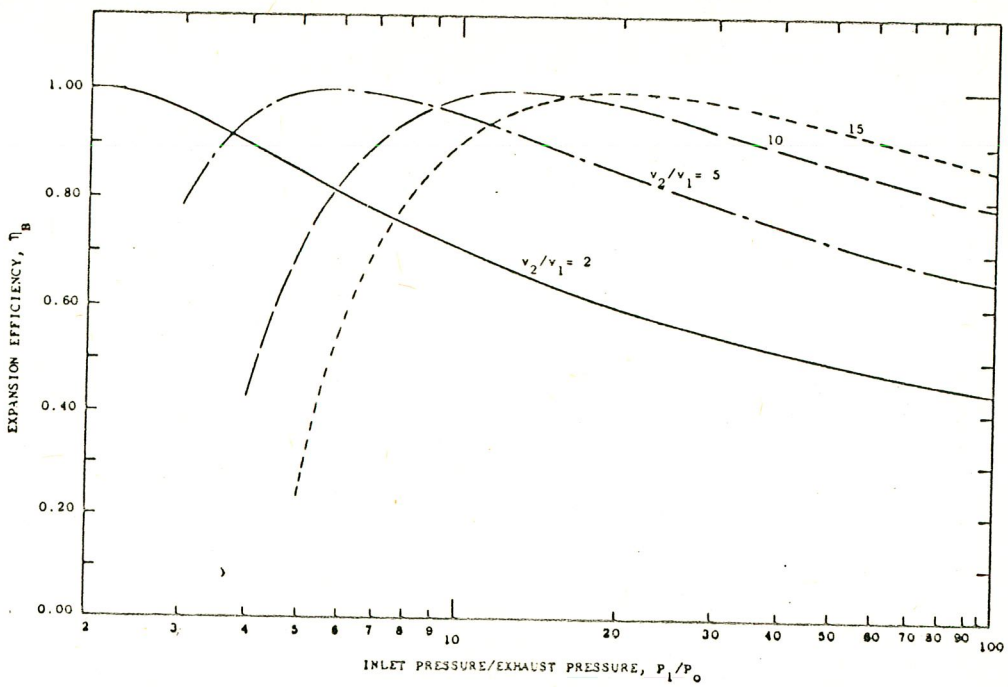

Fig.2.28. Effect of Presure Ratio Variation on Efficiency

volume expansion ratio. Note that the efficiency remains quite high over a wide range of pressure ratio mismacth, but eventually become zero for low pressure ratios.

In order to eliminate the disadvantages of pressure ratio mismacth, a variable expansion ratio device must be designed to obtain most efficient expansion, or in other words the device must be adapted according to variable cycle charecteristics for a wide range of requirements.

In the existing literature that was surveyed, it was not possible to locate a device which has a variable expansion and compression ratios, especially for use in air-cycle heat pumps.

2.6. ATTEMPTS TO DEVELOP VANE-TYPE MACHINARY

In vane-type rotary machines, the contact required between the casing and the vane is maintained by the centrifugal force as shown in Fig.2.29 . Since the centrifugal force is proportional to the radius, manufacturing of a vane type machinery in large dimensions is restricted. Because large radius results in higher peripheral speed and higher centrifugal force and thus greater friction. At high speeds, this friction becomes so high that the efficiency decreases to very low values. If this friction can be held within reasonable limits,

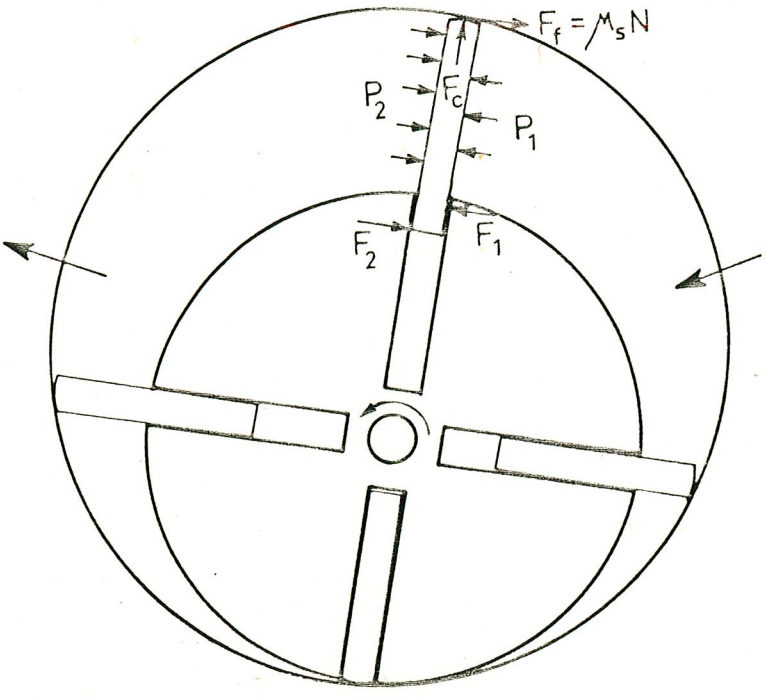

Fig.2.29. Forces Acting on a Vane

machines having high speeds or large dimensiors can be realized. These machines would be advantageus in cases where constant and high flows, and moderate pressures are needed and where other positive displacement types would be costly to apply.

As is shown in Fig.2.29 the line contact between the vane and the casing, and the line contact between the vane and its slot acts as a sealing between the high and low pressure regions of the vane type machinery. However, as the pressure head is increased the friction between the vane and the slot increases to a high level and efficiency falls. If this pressure difference is maintained at low values and coefficient of friction between the vane and its slot is reduced the friction resulting from the pressure difference may be overcome.

In order to eliminate the effect of centrifugal force on the vanes which causes high vane wear and high friction, Kozousek (3) suggested a system combining two opposite vanes into one unit. In Fig.2.30, the casing is denoted by a, the rotor by b and slots by c. In this system opposite vanes were combined into double-vanes, d. The outer sliding edges were enlarged and borne against the bars, f, which have a segment shaped cross section. These segments rotated concentrically with the cylinder at the same angular velocity as the rotor b. During rotation the

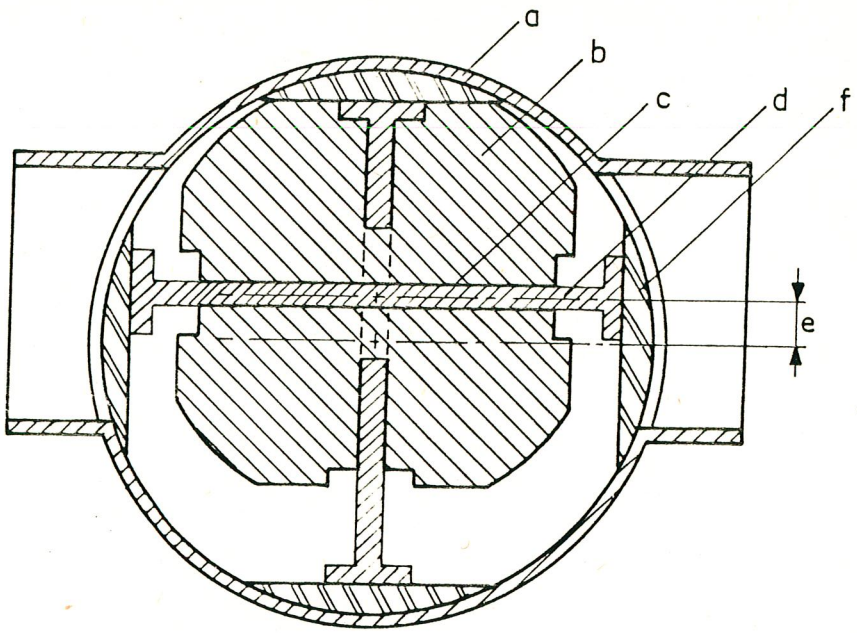

Fig.2.30. Kozousek's Compressor

double-vane slided in relation to its guide f, remaining perpendicular to it. This friction path for one revolution equal to four times the eccentricity e; consequently the friction path was very small. Vane pumps constructed in this way were balanced and thus were suitable for very high rotational speeds, but it needs an extremely accurate manufacturing and in addition, the segment shaped bars occupy a space thus reducing the useful volume.

Another attempt was made by Fenni and Gama Ltd (3) to decrease the mechanical losses and in particular the excessive friction caused by centrifugal forces in vane type machinery. As can be seen from Fig.2.31 , this design, comprised three main parts A, B, C, among which the part B was stationary. In contrary to the classical

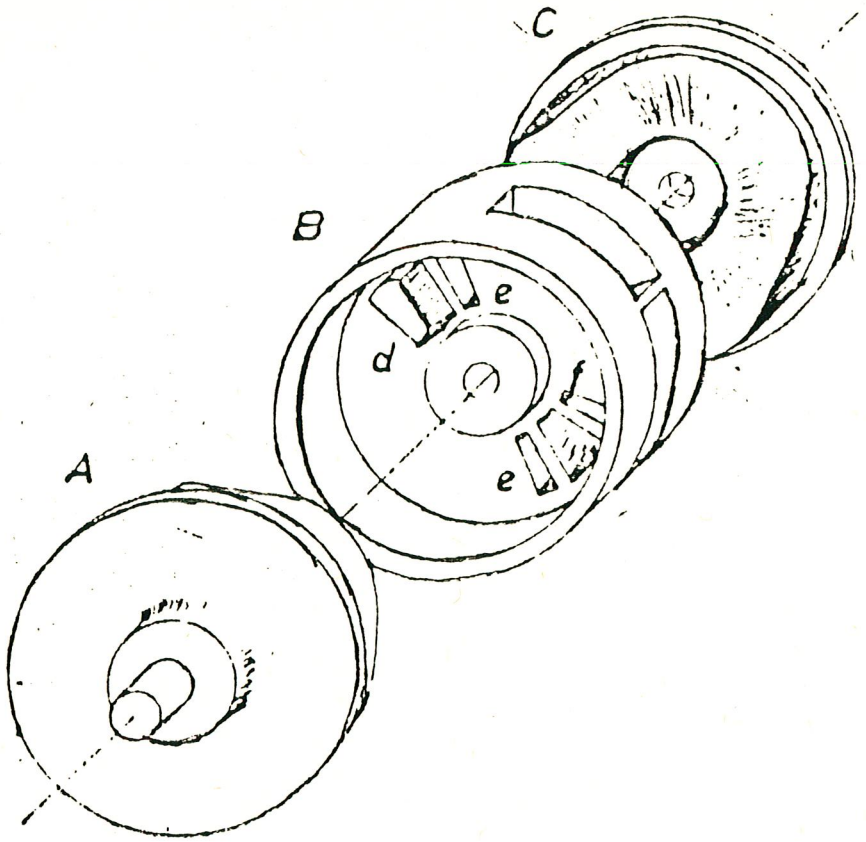

Fig.2.31. Compressor Developed by Fenni And Gama Ltd

designs the blades d were placed which sweep an axial volume. The suction and discharge canals are indicated by e and f respectively.

The conical surface on the rotors A and C which were mounted on either side of the part B formed, together with B, the pumping chambers. The blades d which were placed so as to cross the chambers formed between the rotors and the part B were designed in a way to sweep the conical surfaces of the rotors.

As the blades were made stationary they were not subjected to centrifugal forces. Thus the frictional energy

loss and wear caused by these forces were eliminated. When this pump was being tested, it was observed that the mechanical efficiency was 60 % . The discharge head under these condition was 2.5 m of w.c. . However, as the head was increased, the slip between the rotors and the part B increased. This resulted a decrease of efficiency at higher pressures. Furthermore high levels of vibration was also noticed. Due to these adverse effects this attempt was considered unsuccesful.

C H A P T E R T H R E E

DESIGN CRITERIA AND THEORETICAL ANALYSIS

3.1. INTRODUCTION

Before starting the design of the prototype, thermodynamics of the reverse- Brayton air cycle for air-conditioning purposes are discussed in this chapter. The theory and applications of the reverse Brayton air cycle showed that, to improve the cycle effectiveness it was necessary to improve the units which are the most important parts of the cycle. For this reason, the parameters effecting the performance of the positive displacement machinery are discussed. By using the defined performance coefficient, the evaluation of the performance characteristics of the compressor and the expander under different operating conditiors can be done.

Since the designed prototype in this study is considered for the operation in automotive vehicles, as a first approximation, the cooling capacity of an

automobile air conditioning system must be estimated. The pressure, capacity requirements and consequently the size and applicability of the system for the above mentioned purpose then can be determined.

3.2. CAPACITY DETERMINATION

When compared to the home, office, store or school, the automobile interior represents a unique environment. The interior of an automobile is confining and dynamic, and its thermal properties cannot be found in any other surrounding that is commonplace to most of us.

During the summer , its radiant heat loads are staggering at low vehicle speeds, while, at higher speeds convective heat loads takes a greater percent on total heat gain. At high cruising speeds the temperature of the roof of the automobile is reduced to nearly the outdoor air temperature due to the convective heat treansfer, thus reducing the radiant heat gain.

Its well known that thermal comfort is not simply the selection of a suitable air temperature with an upper and lower limits, but a psychological response to a complex combination of physical and possible psychological stimuli.

The major physical variables are cooling air temperature,its humidity and speed, and the radiation exchange between the passengers and their surroundings. However, providing the humidity of the cooling air and its

speed are kept within reasonable limits and that the mean radiant temperature of the bounding surfaces follows the cooling air temperature reasonably closely, the cooling air temperature can be used as an index of thermal comfort.

From 1973 to 1977 a series of laboratory tests involving almost 3000 people were conducted to determine the factors that contribute to the thermal comfort of automobile passengers while using air-conditioning under summer heat load (8) . This study concucted by Frederic H.R. and Stan B. Wallis, involves steady-state and transient air conditioning for the purpose of evaluating the effects of the register size, the air flow rate and the discharge air temperature on comfort. Air conditioning system in this work pertrains to the steady-state operation of the system . This justified by the fact that the settling time of the transients is small compared to the time periods that the system actually operates, and therefore, the effects of the transients can be neglected.

According to ASHRAE specifications (2) and tests carried out by Frederic and Stan (8) the average car temperature is about 24 °C- 27 °C for the summer comfort condition. This temperature is satisfied by 5 °C tc 15 °C of temperature of the out flowing air at the registers for a rate of air flow of 25 to 100 l/s . These values differ from car to car and depends on the size, color, insulation

etc.of the car. The cooling capacity of the air conditioning unit also varies with the speed of the engine.

For our purpose , small size cars which are manufactured in Turkey, (i.e. Murat 131, Renault 12, Anadol) are considered and the average speed of the engine is taken as 3000 rpm. Thus the design speed of the circulator was decided to be varied about 3000 rpm. The average speed of the circulator is adjusted by means of a suitable pulley of the V-belt drive connected to the engine.

Considering the size and the specifications of the car the cooling capacity was estimated as 2000 W approximately at an average engine speed of 3000 rpm. The cooling capacity is proportional to the engine speed hence for higher cooling requirements, the cooling capacity can be increased by increasing the circulator speed.

The dry -bulb temperature of outdoor air is taken as 40 °C . This is choosen from the charts which were prepared for refrigeration purposes. This peak temperature is valid for South-East Turkey and the most of the regions in the Middle-East as well. The prototype designed for such a temperature, can also satisfy the requirements for other regions of Turkey.

3.3. THERMODYNAMIC ANALYSIS OF AIR CYCLE

The air cycle choosen for study is shown in Fig.2.2 . This is an open air cycle; thus, air to be compressed is drawn from the conditioned space or from outdoor and the cool air from the expander is rejected directly to the conditioned space.

The pressures and temperature of a isentropic compression can be calculated by using the following equations :

$$(P_2 / P_1) = (V_1 / V_2)^k = r_c^k \qquad 3.1$$

$$(T_2 / T_1) = (V_1 / V_2)^{k-1} = r_c^{k-1} \qquad 3.2$$

where r_c is the compression ratio.

If the inlet conditions are known, for a given compression ratio the discharge temperature and enthalpy can be determined for isentropic compressicn. The isentropic compression work is the difference in enthalpy of air between inlet and discharge conditions of the system.

However, actual air compression follows a polytropic curve as shown in Fig.3.1 . work, W_c , required for this compression is given by the equation :

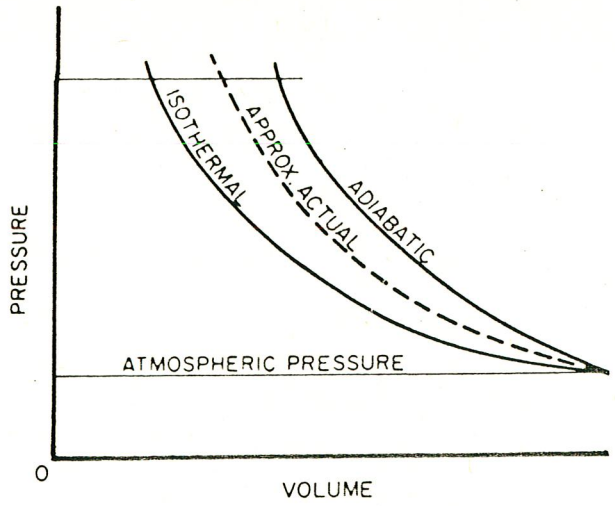

Fig.3. 1. Relationship of Isentropic to Isothermal Compression

$$W_c = (n/n-1)\ P_1 V_2 [(P_2/P_1)^{k-1}{}^{k} - 1] \qquad 3.3$$

where n is the polytropic constant.

If the compression were isothermal less work would have been needed and the difference between the isothermal and isentropic compression work increases with increasing pressure ratio. Therefore, when pressure ratios are higher then 7, compression is usually carried out in two or more stages with intercoolers between stages so that isothermal conditions are more nearly approximated. For a comparison, the theoretical power requirement for compression of 50 l/s of free air at approximately from 1 bar to 2 bar for isothermal, polytropic (n=1.30) and isentropic conditions are 3.7 hp, 4.7 hp, 5.0 hp respectively.

If the isentropic compressor efficiency is defined

as the ratio of isentropic compression work to actual work input to the compressor, the actual work is found by dividing the isentropic compression work by the isentropic compressor efficiency, η_c .

$$W_c' = W_c / \eta_c \qquad 3.4$$

where prime denotes the actual conditions.

The actual enthalpy leaving the compressor is equal to the entering enthalpy plus the actual compression work. The discharge temperature may be found by solving Eqn.3.5 for temperature, T_2' .

$$C_p (T_2' - T_1) = C_p T_1 (r_c^{k-1} - 1) / \eta_c \qquad 3.5$$

Since the temperature and pressure of air leaving the compressor now are known, the entering conditions of the heat exchanger are known . If the leaving dry - bulb temperature of the air from the heat exchanger is specified, the amount of heat rejection can be calculated.

The process in the expander is the reverse of that in the compressor. The isentropic exparsion work is the enthalpy difference between the air entering the expander and the air leaving the exparder. The actual expander work output is determined from the isentropic expansion work

multiplied by the isentropic expander efficiency, η_e .

$$W_e' = W_e \eta_e \qquad 3.6$$

The losses in the expander reduce the amount of net cooling capacity available since the air temperature entering the space will be increased because of losses. The difference between the isothermal and the isentropic expansion can be seen in Fig.3.2 . The temperature and pressure ratio of the isentropic expansion can be determined by the following equations :

$$(P_3/P_4) = (V_4/V_3)^k = r_e^k \qquad 3.7$$

$$(T_3/T_4) = (V_4/V_3)^{k-1} = r_e^{k-1} \qquad 3.8$$

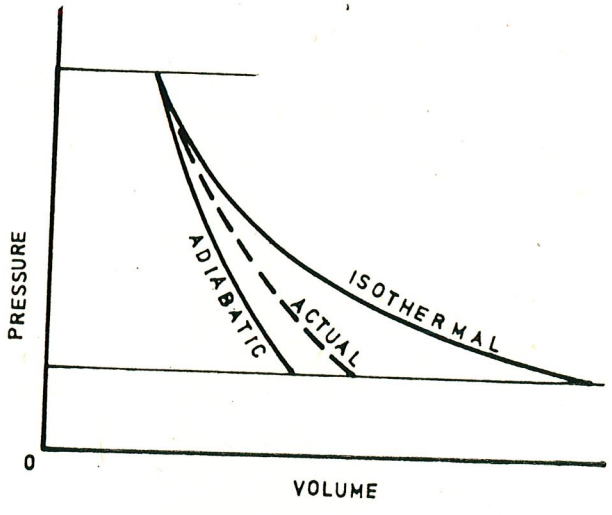

Fig.3. 2. Relationship of Isentropic to Isothermal Expansion

The net work of the cycle is the difference between actual compression work and actual expansion work. Net cooling capacity may be calculated as the difference between the enthalpy of the air entering the cyle at the compressor and enthalpy of air leaving the cycle from the expancer.

If it were possible to compress the air isothermally and expansion were isentropic the T-s anc P-v diagrams will be as shown in Fig.3.3 . For this case the coefficient of performance is given as:

$$C.O.P. = \frac{\text{cooling effect}}{\text{work input}} = \frac{C_p (T_1 - T_4)}{T_1 C_p \ln(T_1 / T_4) - C_p (T_1 - T_4)}$$

$$\frac{(T_1 / T_4) - 1}{(T_1 / T_4) \ln(T_1 / T_4) - (T_1 / T_4) + 1} \qquad 3.9$$

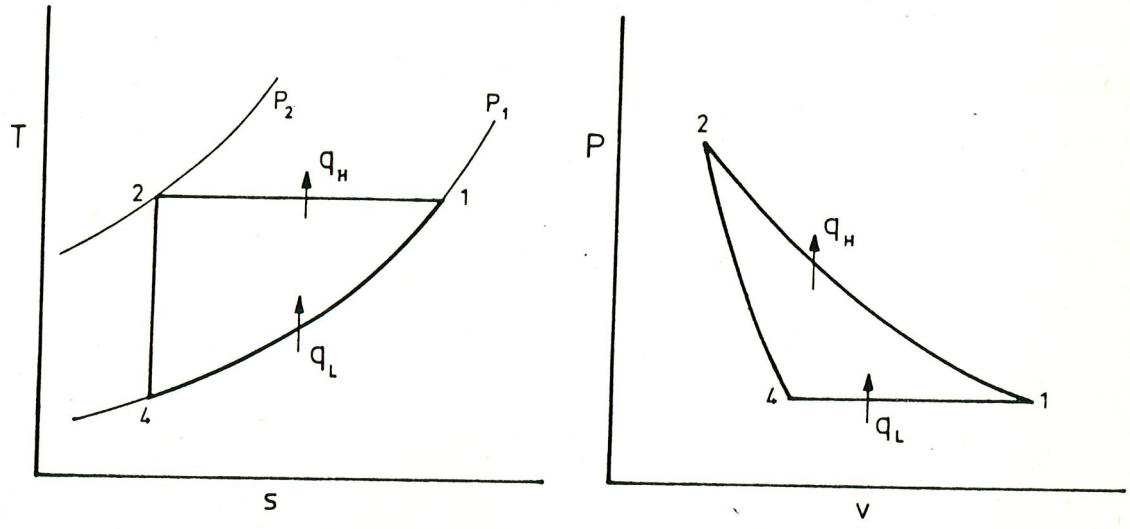

Fig.3. 3. T-s and P-v Diagrams of Cycle with Isothermal Compression and Isentropic Expansion

As is shown in Eqn.3.9 , COP is only a function of the (T_1 / T_4) ratio.

For a reversible adiabatic cycle, if the compression ratio of the compressor and expansion ratio of the expander were equal, and the temperature at the inlets of the compressor and the expander were assumed to be the same and equal to the ambient temperature, the theoretical coefficient of performance, C.O.P., is related only to the pressure ratio, as shown in Fig.3.4 and is given by Eqn.3.10 :

$$C.O.P. = \frac{q}{W} = \frac{C_p (T_1 - T_4)}{C_p (T_2 - T_1) + C_p (T_4 - T_3)} = \frac{1}{r^{k-1} - 1} \qquad 3.10$$

where ; $r = r_c = r_e$, $(T_2 / T_1) = (T_3 / T_4) = r^{k-1}$, $T_1 = T_3 = T_0$

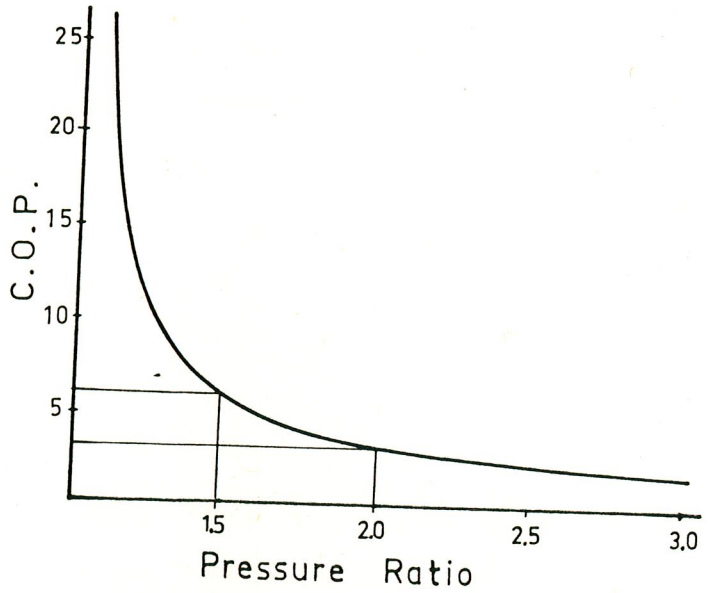

Fig.3. 4. C.O.P. Variation with Pressure Ratio

For a given (T_1 / T_4) ratio the C.O.P. of an air cycle with an isothermal compression can be compared with the C.O.P. of an air cycle with an isentropic compression. Table 3.1 shows the C.O.P. of air cycles with isothermal and isentropic compression for different T_1 / T_4 ratios.

TABLE 3.1

C.O.P. OF AIR CYCLES WITH ISOTHERMAL AND ISENTROPIC COMPRESSION

T_1 / T_4	C.O.P.(isothermal)	C.O.P.(isentropic)
1.1	20.6	10.0
1.2	10.6	5.0
1.3	7.3	3.3
1.4	5.6	2.5
1.5	4.6	2.0

But in reality the cycle is polytropic and irreversible. It may be concluded that, the C.O.P. of air cycle, with polytropic compression process increases as the polytropic compression approaches the isothermal process. It should be noted that, the expansion process is also polytropic in each case, and , in order to increase the C.O.P. of the cycle, the polytropic expansion process should be kept as close as possible to the isentropic expansion. So the expander side should be insulated to

approximate an adiabatic process, and the compressor side should be cooled to approximate an isothermal process.

As is seen from Eqn.3.10 , when the pressure ratio decreases, the C.O.P. of isentropic cycle increase somewhat; however, the compressor will be larger for the same cooling capacity and speed. It can be seen from Fig.3.4 that, by reducing the sytem pressure ratio from 2:1 to 1.5:1 , an increase in performance over 80 % occurs, accompanied by a 25 % reduction of cooling capacity per unit mass of air. This reduction in cooling capacity can be eliminated by increasing the mass flow rate at a lower pressure ratio system. Increasing the mass flow rate of air causes an increase in the pressure drop due to the fluid friction losses in pipes and the heat exchanger. In a lower pressure ratio system the pressure drop due to frictional effects become relatively high when compared to the pressure on the high pressure side of the cycle. So the system must be designed to operate at low pressure, while the losses are kept as low as possible by designing the ports on the units as wide as possible and by selecting a large size heat exchanger.

Along with the the pressure losses, the efficiency of compression , the efficiency of exparsion and effectiveness of the heat exchanger must be taken into account for determining the actual operation cycle. As are

shown in Fig's 3.5 anc 3.6 the actual cycle deviates from the ideal cycle. The cashed lines in these figures show the isentropic cycle.

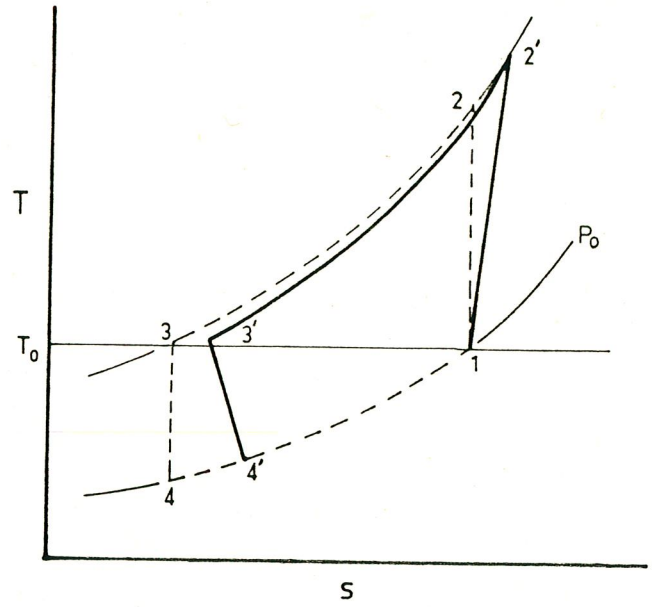

Fig.3. 5. Difference Between the Actual and Ideal T-s Diagrams of Air Cycle

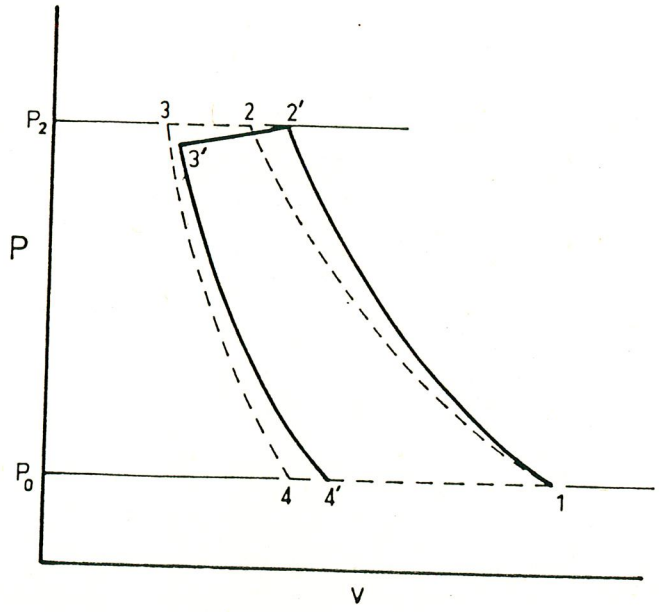

Fig.3. 6. Difference Between the Actual and Ideal P-v Diagrams of Air Cycle

In order to obtain a 2000 W cooling capacity, for a specified temperature difference, air flow capacity of the circulator must be determined. As was explained in the previous chapter, the flow capacity is limited by the speed and the geometry of the positive displacement units. But in Chapter 4 , it will be shown that ideal flow rate of 60 l/s is possible at 3000 rpm with minumum outer dimensions. However outer dimensions of the circulator is strongly effected by the dimensions of the space available in an automobile engine compartment. Flowrate through the circulator can be increased by design improvements.

In order to determine the pressure ratio of the system, the states labelled as $2'$,$3'$,$4'$ on Fig's 3.5 and 3.6 should be determined for an actual cycle by assuming the efficiencies of the units. For simplifying the following analysis, the pressure drop in the heat exchanger may be neglected, ($P_3' = P_3$) without introducing significant error in the analysis.

Referring to Fig.3.6 and Eqn.3.4 for the compressor one can write,

$$T_2' - T_1 = (T_2 - T_1)/\eta_c \qquad 3.11$$

and for the expander, from Eqn.3.6 ,

$$T_3 - T_4' = (T_3 - T_4)\,\eta_e \qquad 3.12$$

and if the heat exchanger effectivenes is defined as,

$$E = \frac{T_3 - T_1}{T_3' - T_1} \qquad 3.13$$

and , from Eqn's 3.2 and 3.8 ;

$$T_2 = T_1 \; r_c^{k-1} \quad \text{and} \quad T_4 = T_3 \; / \; r_e^{k-1}$$

and assuming $r = r_c = r_e$, $r^{k-1} = \sigma$, T_4 becomes:

$$T_4 = T_1 \, (1 - \eta_e (\sigma - 1) / \sigma \,) [(1-E)(\sigma-1) / \eta_c + 1] \qquad 3.14$$

and $$q = \dot{m} \; C_p \, (T_1 - T_4) \qquad 3.15$$

In accordance with the existing literature the isentropic efficiency of the compressor, isentropic efficiency of the expander and the effectiveness of the heat exchanger were assumed as 85 %, 80 % and 95 % respectively. Using the above assumed efficiencies r is determined as 1.36 at 50 l/s flow rate. But in order to have a variable capacity system , and satisfy the requirements of the experimental set-up which can be changed, maximum compression ratio of 1.6 and minumum compression ratio of 1.3 is selected. Expansion ratios can also be taken within the same range (1.6 -1.3). These compression and expansion ratios correspond to pressure ratios of (2.0 -1.4). In order to eliminate the adverse

effect of incorrect assumptions which was made during the theoretical analysis, the pressure ratios are taken as variables. This variable pressure ratio also permits us to adjust the pressure of the system and to investigate the effects of the system pressure change. Therefore a unit which has a variable compression and expansion ratios, were designed. Since, over expansion, over compression and incomplete expansion have a great effect on efficiency of the units, the pressures in the ports and pressures within the units must be matched by pressure adjustment. This can be done by changing the compression and expansion ratios. The adjusment of the pressure in the system , by adjusting the pressure ratios, reduce the losses in the ports ,thus most efficient expansion and compression may take place.

3.4. THEORY AND SIGNIFICANCE OF PERFORMANCE COEFFICIENTS OF POSITIVE - DISPLACEMENT MACHINERY

3.4.1. Steacy-State Analysis

Torque and speed, as well as flow and pressure difference across the machine, are the variables which are of most concern in the operation of positive displacement machinery. Actual characteristics of any machine deviates from the ideal case. If these deviations can be explained by some apropriate theory, the actual characteristics of any machine can be determined. However, the determination of the actual characteristics is very difficult without using some empirical inputs which are named as performance coefficients . These performance coefficients were determined from a series of experimental results. By using the experimentally determined performance coefficients the efficiencies and the overall performance of the units can then be predicted under the operating corditions that were not obtained by the experimental investigations.

This section presents a general analysis of the steady-state charecteristics that is applicable to all

types of positive displacement machines. Here, the parameters effecting the performance of the rotary-vane type compressors and expanders are discussed.

In this section, the losses are defined and the effect of these losses on the performance of the machinery are discussed by the inclusion of some coefficients.

The losses can be investigated in two main headings; the aerodynamic losses and the mechanical losses. For a compressor, aerodynamic losses can be defined by the proper definition of the compression efficiency. A similar definition was used for the expander, namely the expansion efficiency. These compression and expansion efficiencies must be multiplied by the mechanical efficiencies to obtain the overall efficiency of the machines.

For a compressor the compression efficiency can be defined as :

$$\eta_{cc} = \frac{\text{Ideal (isentropic) compression work}}{\text{Actual compression work}} \qquad 3.16$$

and the overall efficiency of the compressor defined as :

$$\eta_{c} = \frac{\text{Isentropic compression work}}{\text{Work input from the shaft}} = \eta_{cc}\,\eta_{mc} \qquad 3.17$$

where η_{mc} is the mechanical efficiency of the compressor.

For the expander the expansion efficiency is

$$\eta_{ee} = \frac{\text{Actual expansion work}}{\text{Isentropic exparsicn work}} \qquad 3.18$$

and the overall efficiency of the expander becames

$$\eta_{e} = \frac{\text{Work output from shaft}}{\text{Isentropic exparsicn work}} = \eta_{ee}\,\eta_{me} \qquad 3.19$$

where η_{me} is the mechanical efficiency of the expander.

In the next two sections the process efficiencies, which are the compression and the exparsion efficiencies, and the mechanical efficiencies are derived. After these derivation the performance of the machinery can be predicted.

3.4.2. Aerodynamic Losses

The aim of this section is the investigation of the three aerodynamic losses which occur in the rotary displacement type machinery.

The first loss occurs during charging and exhausting through the ports which increases the necessary

compression and decreases the available expansion ratios. The second loss results due to the leakage between the moving parts relative to each other and between the rotating parts and the casing. The third loss is the thermal burden caused by intake warm up in the compressor.

The port charging losses are considered to be a function of the rotor tip speed. The gas must follow the wake of the vanes as the gas continuously enter through the inlet port. It is necessary to expend a certain amount of velocity head in the process of accelerating the gas to a speed match the rotor speed.

Table 3.2 shows the pressure differential that must be sacrificed to attain a velocity equivalent to the rotor tip speed for a compression process. The sonic velocity of the air considered here is 340 m/s at the suction temperature of 20 °C . These velocity head losses are applied to Eqn.3.20 to produce the 'B' correction factor mentioned below. This modifies the apparent line pressure ratio to the more realistic intrinsic pressure differential for a compressor.

$$B_c = (1.0 + PD_2 / P_2) / (1.0 - PD_1 / P_1) \qquad 3.20$$

By using the value of B_c determined from the above equation the dynamic breathing efficiency can be written

as ;

$$\eta_{bc} = \frac{\text{Ideal compression head}}{\text{Actual compression head}} \qquad 3.21$$

$$\eta_{bc} = (r_c^{k-1} - 1) / ((B_c r_c)^{k-1} - 1) \qquad 3.22$$

TABLE 3.2

CHARGING AND EXHAUSTING PRESSURE LOSSES FOR ROTARY TYPE COMPRESSORS

Tip Speed		Velocity Head	Differential Pressure		
Mach	m/s	$U^2/2g$	PD_1	PD_2	$(P_2/P_1 = 2)$
0.05	17	15	0.002	0.003	bar
0.10	34	59	0.007	0.012	"
0.20	68	236	0.028	0.046	"
0.30	102	530	0.064	0.104	"
0.50	170	1473	0.177	0.290	"
0.70	238	2887	0.347	0.572	"

If K_{ic} is defined as the resistance coefficient of flow at intake side of the compressor, the total velocity head loss for charging operation is K_{ic} times velocity head that is consumed in overcoming the resistance of the intake port, and stagnation of flow in the rotor pocket. The absolute velocity of the air must also match that of rotor speed. This totals to the (K_{ic} + 1) times the velocity

head for the charging operation. This loss is expressed as a decimal fraction of the suction pressure of the compressor and can be expressed by the following simplified equations as follows :

$$\theta_{ic} = PD_1 / P_1 = (K_{ic} + 1) (U^2 / 2g) \gamma_1 / P_1 \qquad 3.23$$

where γ_1 is the specific weight of the air and equals to ;

$$\gamma_1 = 0.03414 \; P_1 (Pa) / T_1 (^\circ K) \qquad 3.24$$

$$\text{Thus} \quad \theta_{ic} = 1.74 \times 10^{-3} (K_{ic} + 1) U^2 / T_1 \qquad 3.25$$

where U is the tip speed in m/s and T_1 is the temperature at inlet in °K.

It is further presumed that the rotating chambers relases the trapped air at or very close to the discharge chamber pressure; so that no overcharging or undercharging exists in the exhaust pocket. The absolute velocity of gas leaving the rotor and entering the discharge chamber represents another velocity head expenditure. The analytical difference between the suction and discharge velocity head is the change in the gas specific volume.

$$v_d = v_i / r_c \qquad 3.26$$

then, the exhaust loss of the flow at the discharge side can be written by the equation below which includes the resistance coefficient, K_{dc};

$$PD_2 = K_{dc} / (K_{ic} + 1) PD_1 r_c \qquad 3.27$$

and $$\theta_{dc} = PD_2 / P_2 = K_{dc} / (K_{ic} + 1) \theta_{ic} r_c^{1-k} \qquad 3.28$$

The two dimensionless pressure loss ratios θ_{ic} and θ_{dc} are used to evaluate the intrinsic pressure correction factor 'B_c', by introducing them into equation 3.20 .

$$B_c = (1.0 + \theta_{dc}) / (1.0 - \theta_{ic}) \qquad 3.29$$

As is seen in Table 3.3 B_c is approximately equal to unity below Mach number 0.1 , and increases up to 1.77 for Mach number 0.5 accompanied by a sharp decrease of dynamic breathing efficiency.

In the same manner, the dynamic breathing efficiency of an expander can be defined as :

$$\eta_{be} = \frac{\text{Actual expansion head}}{\text{Ideal expansion head}} \qquad 3.30$$

$$\eta_{be} = (1 - 1 / (B_e r_e)^k) / (1 + 1 / r_e^k) \qquad 3.31$$

where $$B_e = (1.0 - \theta_{de}) / (1.0 + \theta_{ie}) \qquad 3.32$$

TABLE 3.3

VARIATION OF DYNAMIC EFFICIENCY OF A COMPRESSOR DUE TO BREATHING LOSSES

Tip Velocity (Mach)	B_c	η_{bc} % ($r_c = 2$)
0.05	1.005	99
0.10	1.020	97
0.20	1.084	89
0.30	1.206	77
0.50	1.772	50
0.70	4.203	26

As was mentioned above the dynamic breathing efficiency of the positive displacement machinery is very high below the 30 m/s tip speed. By designing a machine which operates below this speed, the breathing losses can be significantly reduced.

The next step is the formulation of the leakage losses. In the rotary vane type machinery it is possible to group the leakages under three headings. The first path of the leakage is at the addendum of the rotor and the casing . The second path of leakage is through the clearance between the vane and the casing, and the third one passes between the vanes and the rotor. These leakage paths have different dimensions but basically similar characteristics . Therefore , all these paths can be

combined into one composite or equivalent path without deviating from the generality of the discussion.

The deviation between the ideal and the actual flowrate of any positive displacement unit can be expressed by the inclusion of the slip coefficient , C_s Thus , the difference between the ideal and actual flowrates can be named as slip flow and expressed as ;

$$Q_s = C_s V_d \Delta P^{1/2} \qquad 3.33$$

where V_d is the displacement per revolution. Detailed analysis for Q_s and the derivation of Eqn.3.33 is presented at Appendix A.

The slip flow consists of two similar flows. One of them is the internal leakage and the other is the loss from the sealings to the outer space. Although the leakage to the outer space is usually negligible when compared to the internal leakage , these two leakage flow have the same characteristics. They are combined and called as slip flow.

Thus the slip efficiency of the compressor can be defined as:

$$\eta_{sc} = \frac{\text{Actual flow}}{\text{Ideal flow}} = \frac{Q_{tc} - Q_{sc}}{Q_{tc}} \qquad 3.34$$

and for the expander:

$$\eta_{se} = \frac{\text{Ideal flow}}{\text{Actually supplied fluid flow}} = \frac{Q_{te}}{Q_{te} + Q_{se}} \qquad 3.35$$

where Q_{tc} and Q_{te} are the ideal flowrates and are equal to the swept volume times the revolution per second. It is apparent that the ideal flow will be ;

$$Q_t = V_d \; N \; / \; 60 \qquad 3.36$$

By using Eqn's 3.34, 3.35 and 3.36, and referring to Appendix A, it is seen that these slip efficiencies can be expressed for the compressor and expander respectively, as :

$$\eta_{sc} = 1 - C_s \; \Delta P_c^{0.5} / \; (\; N \; / \; 60 \;) \qquad 3.37$$

$$\eta_{se} = \frac{1}{1 + C_s \; \Delta P_e^{0.5} / \; (\; N \; / \; 60 \;)} \qquad 3.38$$

As was mentioned in Section 3.3 the actual compression follows a polytropic process and the stage after compression can be determined by the usage of polytropic compression constant , n , which is less than 'k' and greater than unity. However, the discharge

temperature of a rotary positive displacement compressor rises above the normal adiabatic temperature. This results in an increase of the value of 'n' above the value of 'k' which is equal to 1.4 for air. This high temperature is a result of internal bypass leakage from the discharge side to the intake side. The mixing of intake gas with the compressed gas warms the suction gas which increases the temperature of gas before the compression process and consequently the discharge temperature. This leakage causes a thermal burden and also increases the necessary adiabatic head and consequently the input power. The percent of power loss is directly proportional to the percent increase in the inlet temperature in Kelvin.

The effect of suction warm-up at the compressor may be taken into account by defining the thermal efficiency ;

$$\eta_{tc} = \frac{\text{Inlet temperature}}{\text{Increased temperature before compression}} = \frac{T_1}{T_1'} \qquad 3.40$$

where T_1' results from isothermal mixing of intake and discharge gas, and is given by ;

$$T_1' = T_1 \eta_{sc} + T_2' (1-\eta_{sc}) \qquad 3.41$$

where η_{sc} is the slip efficiency and $T_2' = T_1' r_c^{k-1}$

So, the thermal efficiency of the compressor becomes :

$$\eta_{tc} = \frac{1 - r_c^{k-1}(1-\eta_{sc})}{\eta_{sc}} \qquad 3.42$$

The thermal efficiency of the compressor should be used for evaluating the performance of the machine. Thus the effect of internal leakage on the inlet condition before the compression process is coverec by the usage of the thermal efficiency term. But in the expander , the internal leakage does not affect the inlet condition of the exparsion process. The effect of internal leakage in the expander on the temperature of the discharge air is included in the slip efficiency, . Therefore, a similar concept for the thermal efficiency of the expander, as was encountered for the compressor, is not necessary.

For a compressor, compression efficiency was defined as ;

$$\eta_{cc} = \frac{\text{Ideal (isentropic) compression work}}{\text{Actual compression work}}$$

Thus the compression efficiency can be expressed as :

$$\eta_{cc} = \eta_{sc}\ \eta_{tc}\ \eta_{bc} \qquad 3.43$$

By using Eqn's 3.22 , 3.37 and 3.42 the compression efficiency becomes ,

$$\eta_{cc} = \frac{r_c^{k-1} - 1}{(B_c\, r_c)^{k-1} - 1} \cdot \frac{1 - r_c^{k-1}(1-\eta_{sc})}{\eta_{sc}} \cdot \eta_{sc} \qquad 3.44$$

If the tip velocity is less than 30 m/s the breathing efficiency can be assumed as 1.00 and the compression efficiency becomes

$$\eta_{cc} = 1 - r_c^{k-1}(1-\eta_{sc}) = 1 - C_s\, r_c^{k-1} \Delta P_c^{0.5} / (N / 60) \qquad 3.45$$

If this expression is compared with the equation 3.37 , the only difference is in the r_c^{k-1} term which increases the sensitivity of η_{cc} to the pressure ratio variation.

For a certain pressure range Eqn.3.45 can be modified into the following form :

$$\eta_{cc} = 1 - C_s\, \Delta P^{x} / (N / 60) \qquad 3.46$$

For the expander, the expansion efficiency was defined as :

$$\eta_{ee} = \frac{\text{Actual expansion work}}{\text{Isentropic expansion work}}$$

Thus the expansion efficiency can be expressed as :

$$\eta_{ee} = \eta_{se}\ \eta_{be} \qquad 3.47$$

If the breathing losses are neglected the expansion efficiency becomes ,

$$\eta_{ee} = \frac{1}{1 + C_s\ \Delta P_e^{0.5} / (N / 60)} \qquad 3.48$$

The capacity of the machine depends upon the charging pressure and temperature. Equation 3.25 has established the percent of the suction pressure that is lost in the charging operation. The rise in temperature which caused by internal bypass increases the specific volume thus reduces the amount of fresh charge. The percent of volume decrease is directly proportional to the percent increase in inlet temperature in Kelvin . Thus the volumetric efficiency of the compressor becomes ;

$$\eta_{vc} = \eta_{sc} (1 - \theta_{ic}) (T_1 / T_1') \qquad 3.49$$

If the dynamic breathing losses are neglected and (T_1 / T_1') ratio, which is equal to the thermal efficiency as shown previously , the volumetric efficiency of the

compressor becomes ;

$$\eta_{vc} = 1 - r_c^{k-1}(1 - \eta_s) = 1 - C_s r_c^{k-1} \Delta P_c^{0.5} / (N / 60) \qquad 3.50$$

η_{vc} is equal to the compression efficiency, and the same modification applied in the evaluation of the compression efficiency can be used here. Thus the volumetric efficiency of the compressor can be expressed as :

$$\eta_{vc} = 1 - C_s \Delta P_c^{x} / (N / 60) \qquad 3.51$$

Instead of the compression efficiency, the volumetric efficiency of the compressor can be used for simplicity of experimental investigations.

The volumetric efficiency of an expander can be written in a similar way,

$$\eta_{ve} = \eta_{se} (1 - \theta_{ie}) \qquad 3.52$$

and by neglecting the breathing losses η_{ve} becomes ;

$$\eta_{ve} = \frac{1}{1 + C_s \Delta P_e^{0.5} / (N / 60)} \qquad 3.53$$

η_{ve} is also equal to the expansion efficiency.

The volumetric efficiency is used to determine the capacity of the machinery .

The variation of η_{vc} with the pressure difference across the ports for various speeds can be seen in Fig.3.7 in a non-dimensional form. The variation of η_{vc} with speed for various pressure differences is shown in Fig.3.8 . The shape of these curves gives us a general idea about the variation of volumetric efficiency with speed and pressure difference, and assist the understanding of the operation of the positive displacement machinery.

The variation of η_{ve} with pressure difference for various speeds and variation of η_{ve} with speed for various pressure differences can be seen in Fig's 3.9 and 3.10 on a non dimensional basis.

3.4.3. Mechanical Losses

The torque required to drive the positive displacement compressor at constant speed can be divided into four components :

$$M_{ac} = M_{tc} + M_{fc} + M_{rc} + M_{cc} \qquad 3.54$$

where M_{ac} :Actual torque required to drive the compressor,

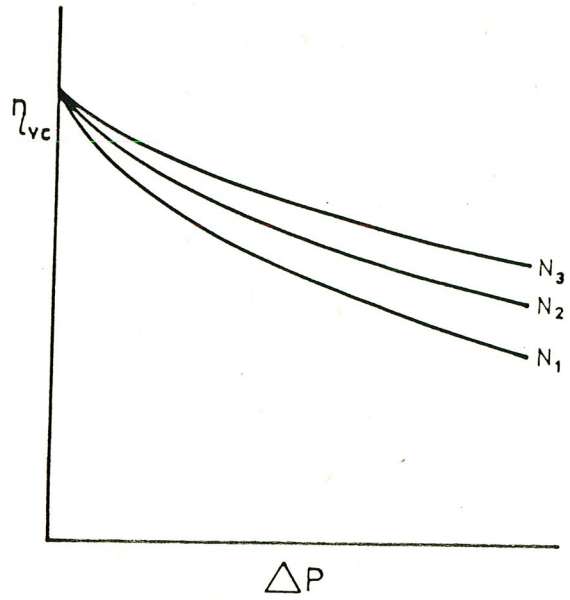

3. 7. Variation of Volumetric Efficiency of the Compressor with the Pressure Difference

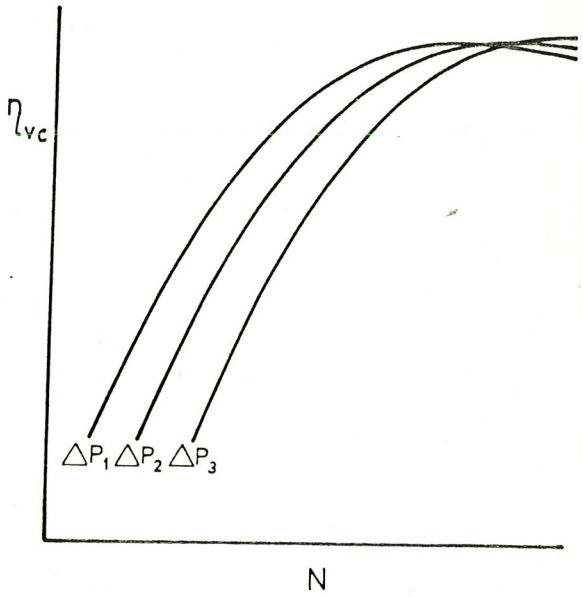

3. 8. Variation of Volumetric Efficiency of the Compressor with the Rotaticnal Speed

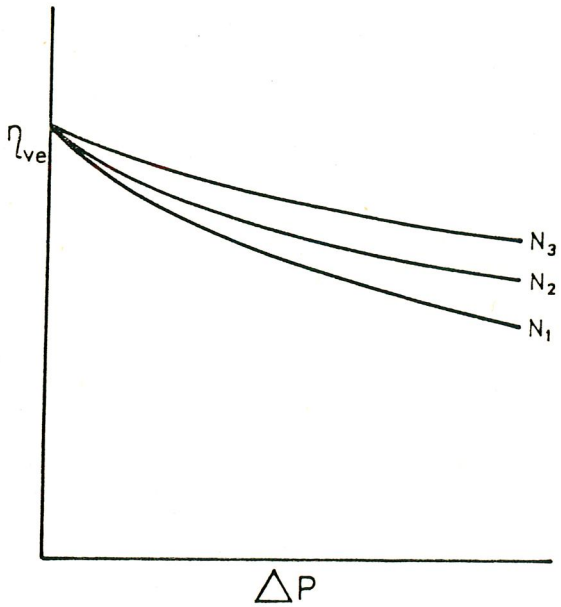

3. 9. Variation of Volumetric Efficiency of the Expander with the Pressure Difference

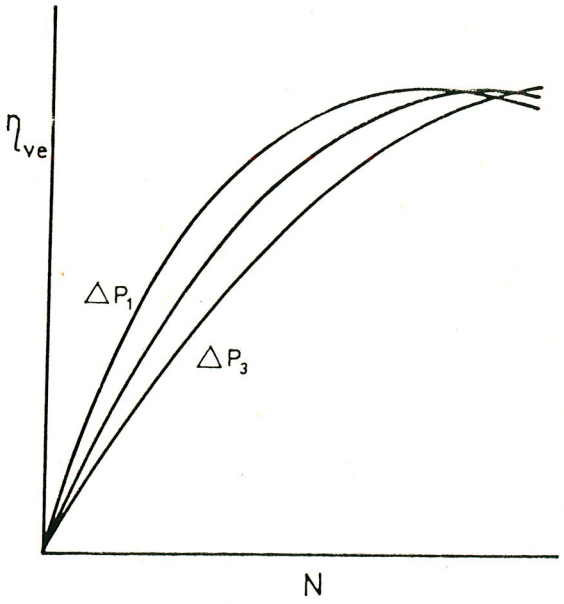

3.10. Variation of Volumetric Efficiency of the Expander with the Rotaticnal Speed

M_{tc} : Ideal torque due to pressure difference accross the ports, and size of the compressor.

M_{fc} : Friction torque due to mechanical friction which is directly proportional to the pressure difference across the ports.

M_{rc} : Friction torque due to mechanical friction which is related to the rotational speed.

M_{cc} : Constant friction torque that is independent of the pressure difference across the ports and the speed of the compressor.

The torque delivered by the expander at constant speed is given similarly by :

$$M_{ae} = M_{te} - M_{fe} - M_{re} - M_{ce} \qquad 3.55$$

where M_{ae} : Actual torque delivered by the expander

M_{te} : Ideal torque due to the pressure differenceacross the ports and physical dimensions of the expander

M_{fe} : Friction torque due to mechanical friction which is directly proportional to the pressure difference across the ports .

M_{re} : Friction torque due to mechanical friction which is related to the rotational speed.

M_{ce} : Constant friction torque that is independent of

pressure difference across the ports and speed of the expander.

The first terms on the right-hand side of equations 3.54 and 3.55 are the ideal torques. As was mentioned in section 3.3 the work required for an isentropic compression was given by the equation :

$$W_c = (k/k-1) P_1 V_1 (P_2 / P_1)^{\frac{k-1}{k}} - 1$$

With the aid of adiabatic head concept which is explained in Section 2.3 , the power required for adiabatic compression is ,

$$\text{Adiabatic power} = \text{Adiabatic head} \times \text{Mass flow-rate}$$

$$= H Q \rho_1 g \qquad 3.56$$

where g is the gravitational acceleration, ρ_1 is the density of air at inlet, Q is the volume flowrate in m / s. If the volume flowrate is expressed as the displacement per revolution times the angular speed in revolutions per second, the ideal power becomes ;

$$\text{Adiabatic power} = H \rho_1 g V_d N / 60 \qquad 3.57$$

where N is the rotational speed in rpm.

The adiabatic power can also be expressed as ;

$$\text{Adiabatic power} = M_t \; N \; 2\pi / 60 \qquad 3.58$$

and, thus the ideal torque can now be expressed as :

$$M_t = H \rho_1 g V_d / 2\pi \qquad 3.59$$

The term $H \rho_1 g$ can be expressed as $\Delta P'$ for simplicity;

$$M_t = \Delta P' V_d / 2\pi \qquad 3.60$$

$\Delta P'$ in this equation is less than ΔP_c that is equal to the pressure difference accross the ports of the compressor.

Eqn.3.60 is also valid in evaluation of the ideal torque of the expander. It should be noted that, the adiabatic head across the expander is different from the compressor's adiabatic head, and can be given as ;

$$H = (R T / m) (k/k-1) [1 - (P_3 / P_4)^{\frac{k-1}{k}}] \qquad 3.61$$

The existence of sealing elements , which exert retarding torques that are related to the working pressure, makes necessary the inclusion of a pressure dependent friction torque term. The friction force between the rotor

and the vane in a vane type machinery is an example to this type of friction. By selecting a parameter C_f, the pressure dependent drag torque may be written as ;

$$M_f = C_f \Delta P \quad V_d \qquad 3.62$$

where C_f is a dimensionless coefficient, related to the friction coefficient, μ_s, of materials in contact and, equals to :

$$C_f = k \mu_s \qquad 3.63$$

where k is an empirical constant.

This definition permit us to relate the friction torque to the ideal torque.

The normal forces acting on the vanes are related to the diameter and the square of the rotational speed. Thus, the frictional torque, M_r, is proportional to the cube of the rotational speed in case of positive contact between the vanes and the casing. The speed dependent drag torque then can be written as :

$$M_r = C_r V_d (N/60)^3 \qquad 3.64$$

where C_r is a dimensionless constant.

If the positive contact of the vanes and casing are eliminated the M_r becomes linearly proportional with the rotational speed. For this case speed depencent drag torque can be expressed as :

$$M_r = C_r \; V_d \; N/60 \qquad 3.65$$

Constant friction term, M_c , includes the friction torque not related to pressure and speed.

Now the resultant expression for the torque required in the compressor and torque delivered in the expander may be written as ;

$$M_{ac} = \Delta P_c \; V_{dc}/2\pi + C_f \; P_c \; V_{dc} + C_r \; V_{dc} N/60 + M_{cc} \qquad 3.66$$

$$M_{ae} = \Delta P_e \; V_{de}/2\pi - C_f \; P_e \; V_{de} - C_r \; V_{de} N/60 - M_{ce} \qquad 3.67$$

Since these expressions are also based on the assumption that clearances remain fixed , the same reservations apply as were encountered in the leakage analysis. It is also assumed that the viscosity of the working fluid remains constant.

The mechanical efficiency of the compressor and the mechanical efficiency of the expander respectively can be defined as :

$$\eta_{mc} = \frac{\text{ideal torque required}}{\text{actual torque required}} = \frac{M_{tc}}{M_{ac}} \qquad 3.68$$

$$\eta_{me} = \frac{\text{actual torque delivered}}{\text{ideal torque delivered}} = \frac{M_{ae}}{M_{te}} \qquad 3.69$$

Now the efficiencies can be derived with the aid of the pertinent dimensionless coefficients.

If we substitude the M_{ac} from Eqn.3.66 in Eqn.3.68 and for the simplicity of the following analysis, $\Delta P'$ in the ideal torque term can be assumed to be equal to the ΔP_c in the friction torque term, mechanical efficiency of the compressor becomes ;

$$\eta_{mc} = \frac{1}{1 + 2\pi C_f + 2\pi M_{cc} / \Delta P_c V_{dc} + 2\pi C_r N / \Delta P_c 60} \qquad 3.70$$

The mechanical efficiency of the expander can be written in the same way as ;

$$\eta_{me} = 1 - 2\pi C_f - 2\pi M_{ce} / \Delta P_e V_{de} - 2\pi C_r N / \Delta P_e 60 \qquad 3.71$$

Since the performance parameters derived in the same way, the same comments as in the compressor are valid here.

The variation of the mechanical efficiencies of the

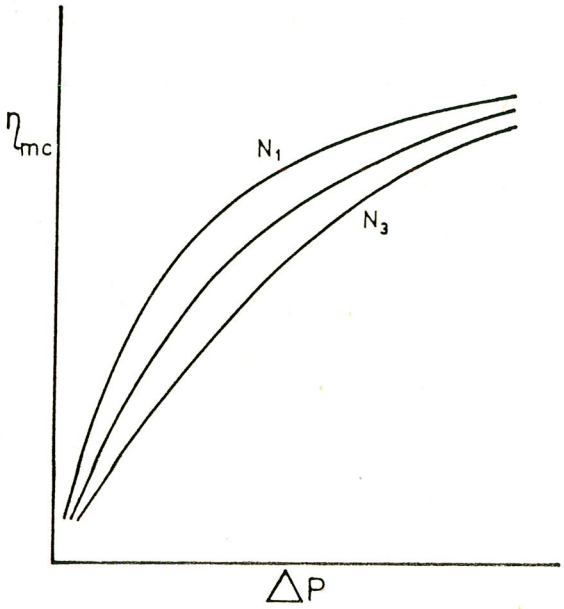

3.11. Variation of Mechanical Efficiency of the Compressor with the Pressure Difference

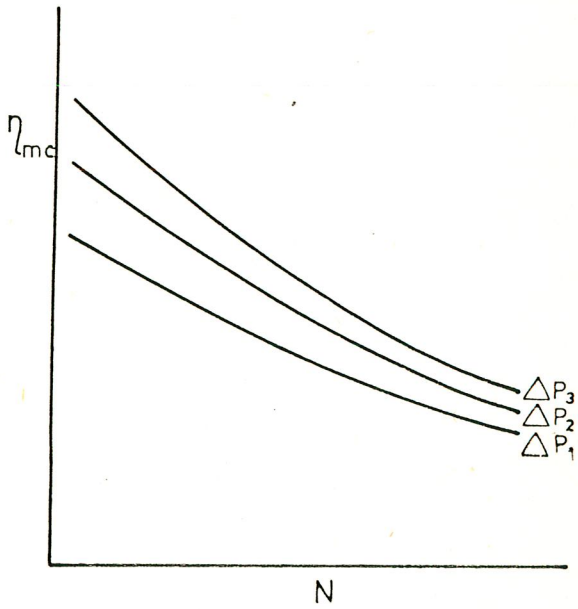

3.12. Variation of Mechanical Efficiency of the Compressor with the Rotaticnal Speed

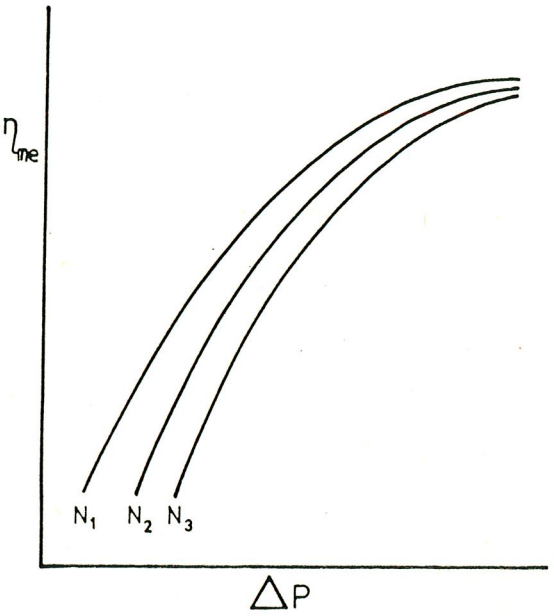

3.13. Variation of Mechanical Efficiency of the Expander with the Pressure Difference

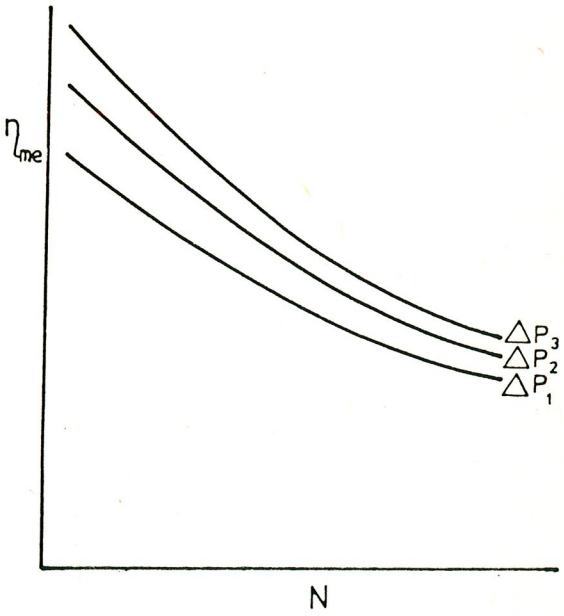

3.14. Variation of Mechanical Efficiency of the Expander with the Rotational Speed

Thus the efficiencies of a series of geometricaly similar units are largely determined by four parameters ; C_s , C_f , C_r and M_c . If the expander and compressor are manufactured from the same material, and have a similar construction, we can assume that the coefficients of the compressor are equal to the coefficients of the expander. If the operating pressure differences across the unit are the same, we can also assume that, $\Delta P_c = \Delta P_e$.

According to the above analysis we can predict the characteristics and the variation of the efficiencies for different operating conditions.

The trend of the overall efficiency variation as a function of speed for various pressure differences and the trend of the overall efficiency variation as a function of pressure difference for various speeds are shown in Fig's 3.15, 3.16 for the compressor and in Fig's 3.17, 3.18 for the expander on a non-dimensional basis.

3.4.5. Experimental Determination of the Performance Coefficients

In a compressor, output flow can be measured as a function of pressure difference while holding the speed and viscosity constant. The theoretical delivery curve for

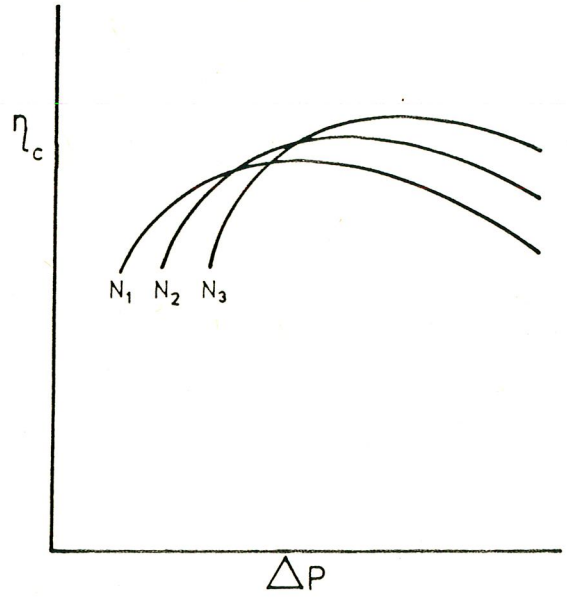

3.15. Variation of Overall Efficiency of the Compressor with the Pressure Difference

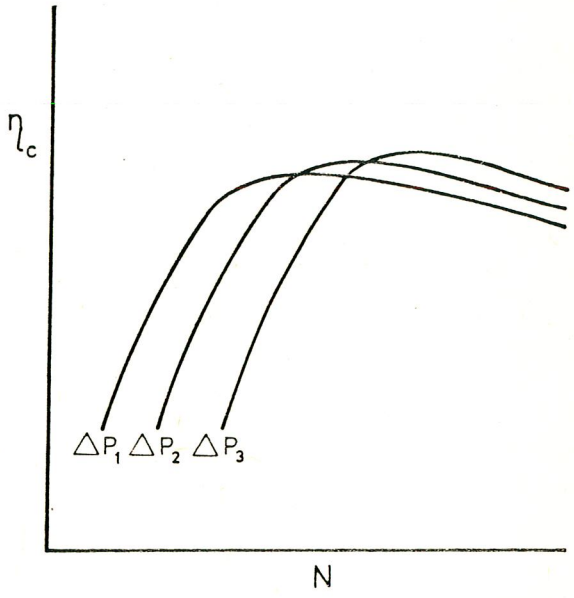

3.16. Variation of Overall Efficiency of the Compressor with the Rotational Speed

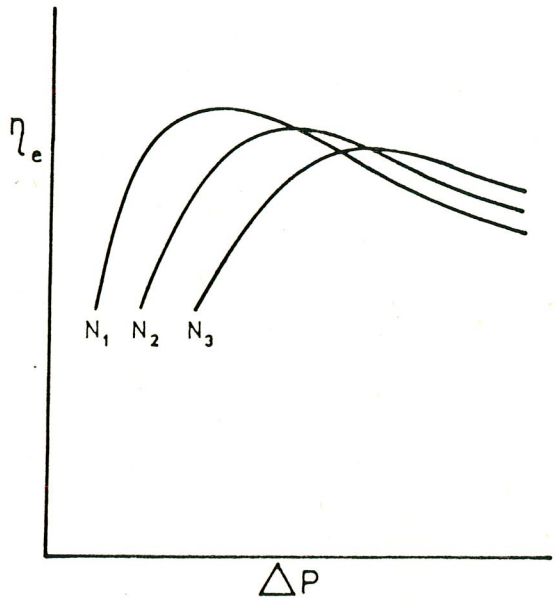

3.17. Variation of Overall Efficiency of the Expander with the Pressure Difference

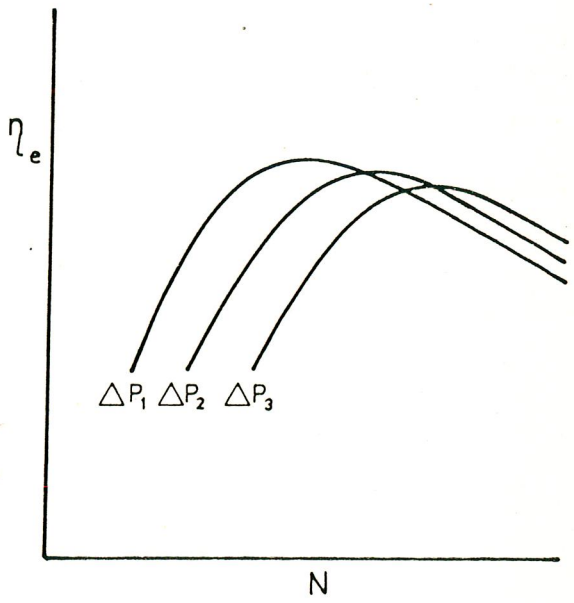

3.18. Variation of Overall Efficiency of the Expander with the Rotational Speed

a series of runs at different speeds are plotted as shown in Fig.3.19 where the dashed lines indicates the ideal flow. The differences between ideal and actual discharge is equal to the slip flow.

If the delivery of the compressor is plotted as a function of speed, for various pressure differences, it will be as shown in Fig.3.20 . If the constant pressure difference curves in Fig.3.20 are extended to zero-speed ordinate, the deviation from the ideal delivery must be the slip flow due to the cappilary passages. This zero-speed slip flow can be plotted against the pressure difference as shown in Fig.3.21 . The plot of this curve on logaritmic scale gives a line which has an intercept of ln ($C_s V_{dc}$), and a slope of about 0.5 as is shown in Fig.3.22.

On the other hand , if there is a significant difference between inlet and outlet flow rate, the plot of this difference on a logaritmic scale gives us a line which has an intercept of ln ($C_l V_{dc}$) as is shown in Fig.3.23.

Thus C_i can be obtained by subtracting C_l from C_s .

By the same procedure, similar curves can be plotted for the expander as shown in Fig.3.24 the suppliec flowrate at various pressure differences as a function of speed .

By referring to Eqn.3.66 the torque required to drive the compressor for various pressure differences can be plotted as a function of speed. This is shown in Fig.3.25 .

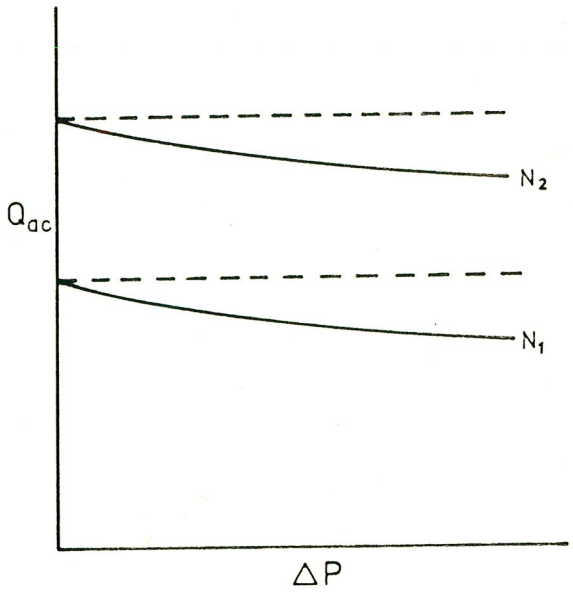

3.19. Plot of Delivery of the Compressor against Pressure Difference

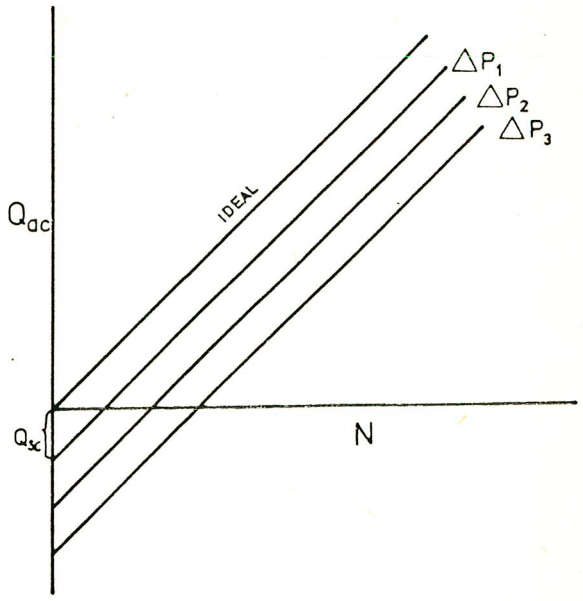

3.20. Plot of Delivery of the Compressor against Rotational Speed

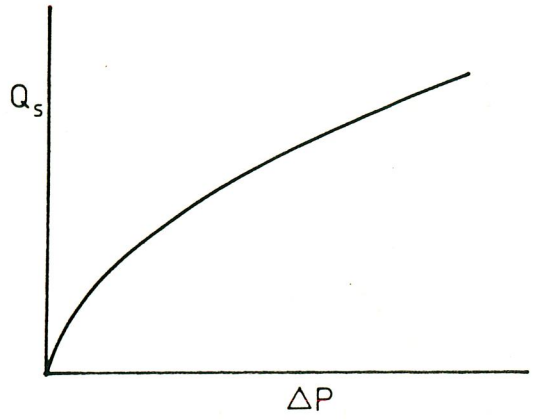

3.21. Plot of Slip Flow Variation against Pressure Difference

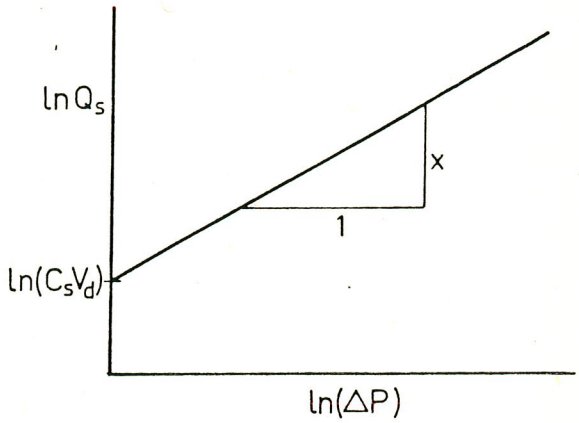

3.22. Plot of Slip Flow Variation against Pressure Difference on Logaritmic Scale

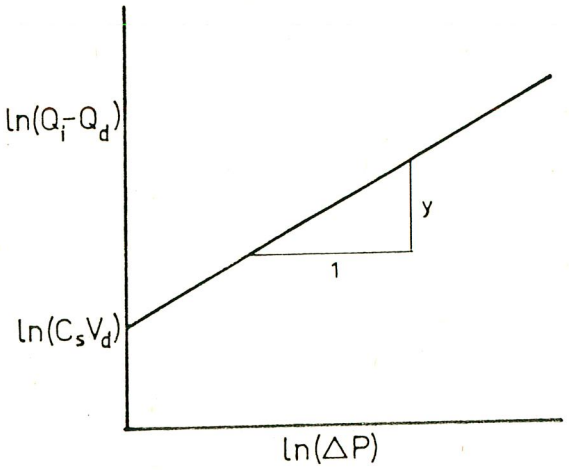

3.23. Plot of Difference of Discharge and Intake Flowrates on Logaritmic Scale

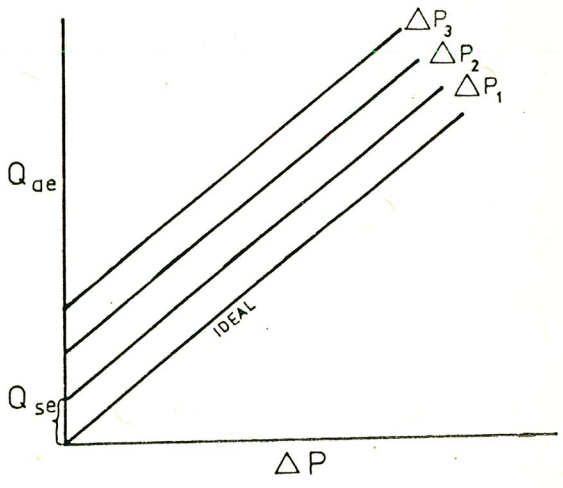

3.24. Variation of Required Flowrate of the Expander with the Rotational Speed

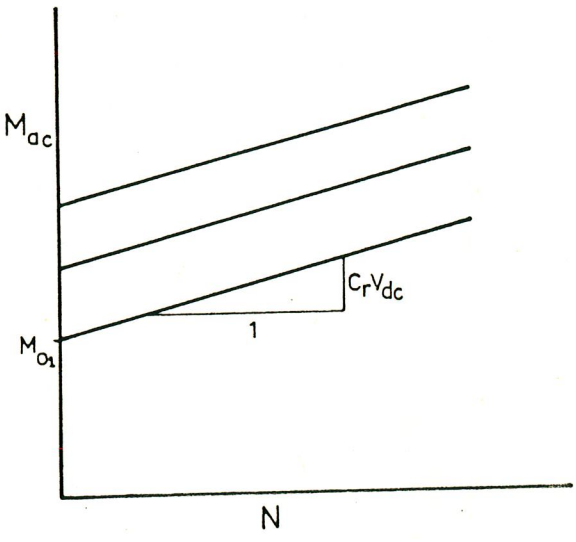

3.25. Variation of actual Torque of the Compressor with Rotational Speec

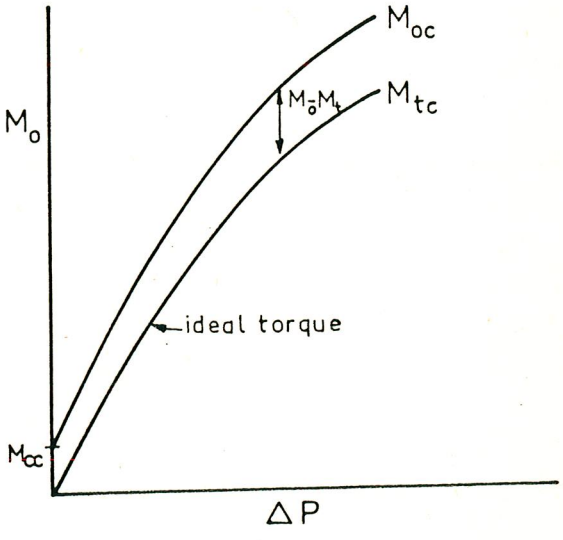

3.26. Plot of Zero - Speed Torque of the Compressor against Pressure Difference

The slope of these lines gives us C_r times V_d. Thus C_r is determined. If the lines for constant pressure difference are extrapolated to zero speed ordinate the zero-speed torques for each pressure difference are obtained. Fig.3.26 shows the zero-speed torques against pressure difference with the ideal zero-speed torque. If the difference between these two curves are plotted, a line which has a slope of $C_f V_{dc}$ and an intercept of M_{cc} can be obtained as shown in Fig.3.27 .

The same procedure can be followed for the determination of the performance coefficients of the expander, as shown in Fig's 3.28, 3.29 and 3.30 .

All the pertinent coefficients can thus be evaluated and it becomes possible to predict the actual characteristics of the units under the other operating conditions.

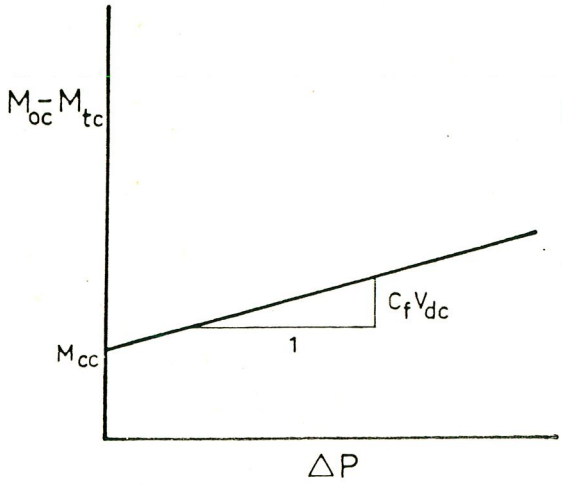

3.27. Plot of Difference of Zero-Speed Torque and Ideal Torque against Pressure Difference for the Compressor

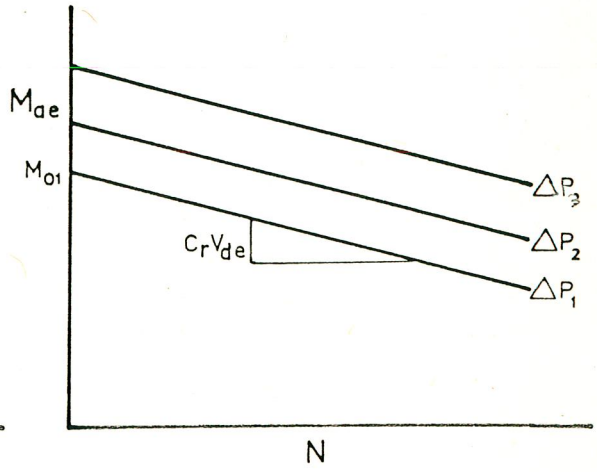

3.28. Variation of actual Torque of the Expander with Rotational Speed

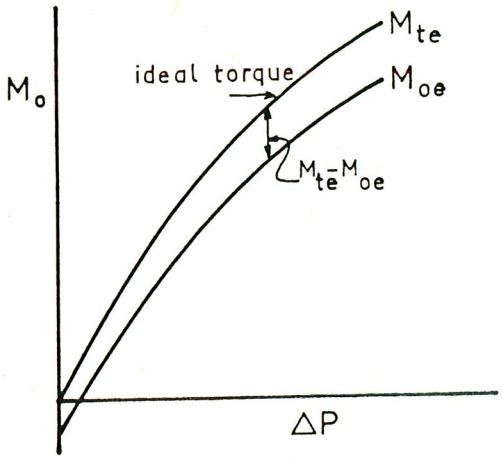

3.29. Plot of Zero-Speed Torque against Pressure Difference for the Expander

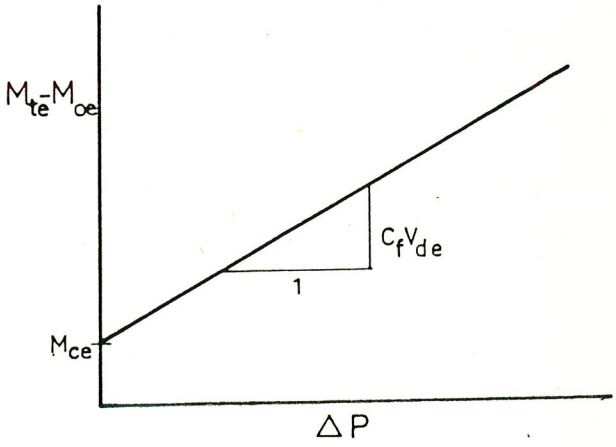

3.30. Plot of Difference of Zero-Speed Torque and Ideal Torque against Pressure Difference for the Expander

C H A P T E R F O U R

DESIGN

4.1. INTRODUCTION

In design of a satisfactory compressor - expander couple which is named as circulator, the specifications of the operating conditions should be determined.

As was mentioned in the in the previous chapters, the rotary vane type compressor and expander will be designed which operate at low pressures with high flowrates.

Since the circulator which will be designed in this chapter, is considered for the operation in the automobiles, it must operate in a wide range of rotational speeds. Therefore an average design speed of 3000 RPM and a maximum operating speed of 4500 RPM were taken. The size of the circulator is determined by the dimensions of the available space in the engine compartment.The cooling capacity of an automobile air conditioning unit was

determined in the third chapter. As was mentioned in the third chapter, to satisfy the cooling requirements; the volumetric flowrate of the units should be 50 l/s, the pressure ratio across the units should be varied from 1.4 to 2.0 while the overall efficiencies of the compressor and the expander are maintained at 85 % and 80 % respectively.

Thus, the specifications were completed. After the comparision of the conceptual designs the decision of the alternative type, which will be designed and constructed, are done in the next section.

The effect of geometry on the flowrate and on the volume change is presented, and the dimensions are determined in Section 4.3.

In design of a positive displacement machinery , the selection of the materials has a great importance. Therefore the evaluation of materials is presented in Section 4.4.

The circulator which consist of two seperate units are designed, and the design of the parts which build up the units are presented in Section 4.5. The assembling procedure is described in the Section 4.6.

4.2. CONCEPTUAL DESIGNS

Several conceptual designs for a vane-type expander and compressor were made. All matched the air cycle conditions described previously.

Even though the mass flowrate is the same in the expander and the compressor; due to the temperature change in the heat exchanger the volume flowrate in the expander is smaller than that in the compressor. In addition to the above mentioned volume flowrate difference, one must also keep in mind the leakage losses occuring in the compressor and the expander. Therefore the compressor must have a different swept volume from the expander. This could be achived by changing the rotational speed, the diameter and the length of either the expander or the compressor in the vane-type machinery.

In the beginning, design of the expander and the compressor were consicered seperately and was planned to be matched with each other by means of a clucth or a gear mechanism. But, in order to have a simple and a compact unit the number of alternative designs were reduced to two. First of these two basic designs has an eliptical housing and single rotor, and the second has similar two

units that matched with each other on a single shaft. The simple configurations of the first and second design alternatives are shown in Fig. 4.1 and Fig. 4.2 respectively.

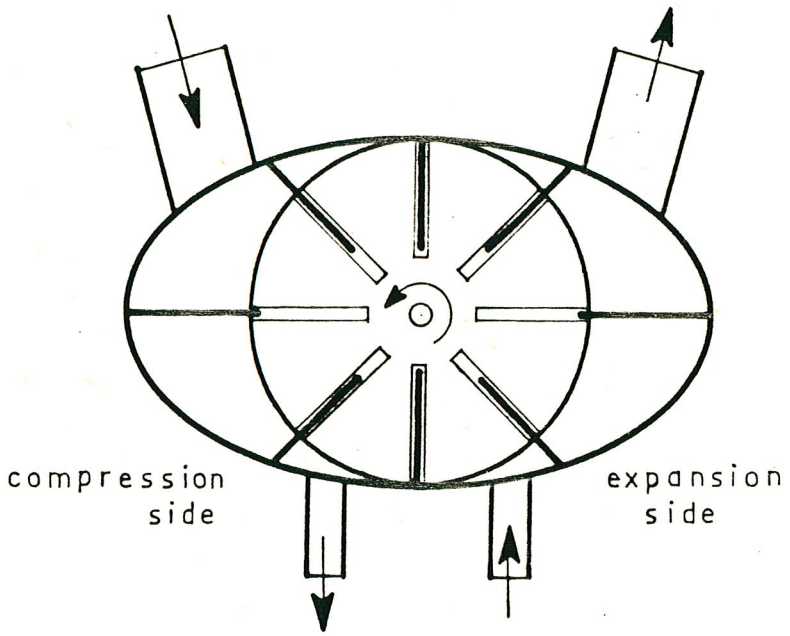

Fig.4. 1. Circulator with Eliptical Casing

In the rotary vane-type machinery, especially at high speeds, the vane tip friction due to centrifugal force strongly effects the performance of the machinery. But as is shown in the previous chapter if the speed of the machine is increased, overall efficiency will increase up to a certain speed. In both of these alternative designs this friction is reduced by adding roller bearings at the roots of the vanes. The bearings must be housed in a cam, which is produced according to the track of the tip of the vanes, or the track of the tip of vanes must be

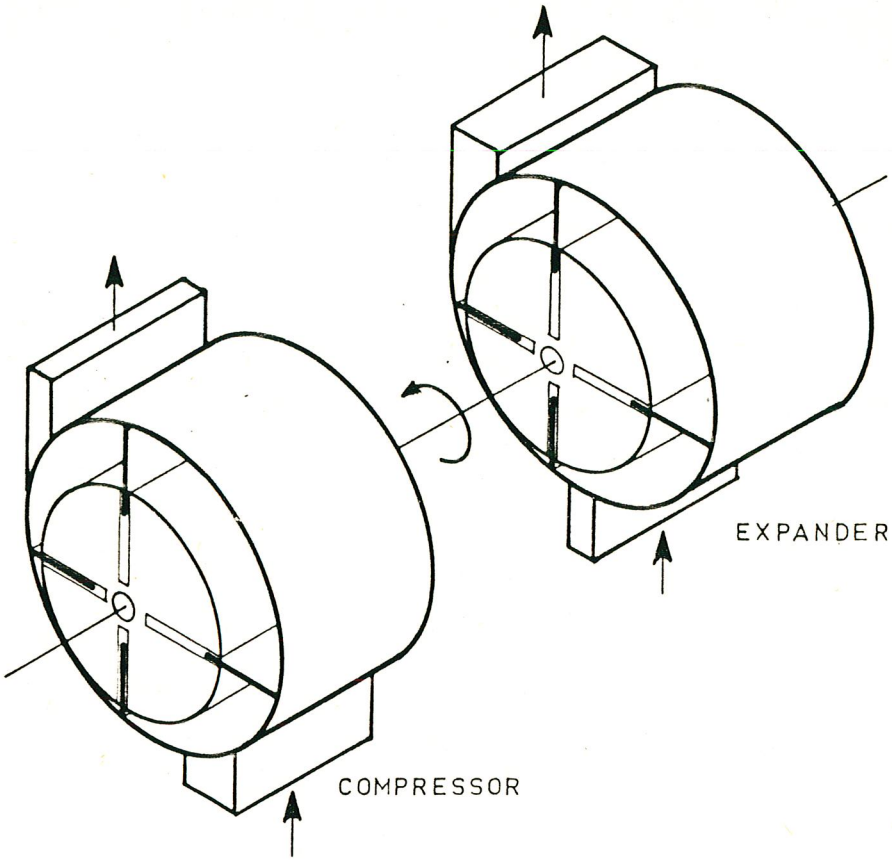

Fig.4. 2. Circulator with Seperate Units

determined according to the cam. The bearings in the roots of the vanes are referred as followers. Due to the addition of a cam and a follower system, the production of the housing and the cam, which were carved on inside of the front and the rear cover, had to be considered together.

In the first alternative, which has an elliptical housing, the cam can be produced by simple and ordinary manufacturing methods, but the housing must be generated according to this cam by using special production methods, such as, using a copy unit on a lathe. But in this case, the production of the master model, which were to be

duplicated, needed some special apparatus and attachments.

The second design alternative, which is composed of two similar machines, has a cylindirical housing, and the cam must be generated from the inner surface of the housing. The generation of the cam was possible by using a copy unit on a milling machine. In the second design alternative the number of cams on the end covers is four. Whereas in the first alternative two cams would have been manufactured, the marufacturing of the casing is simple and does not need any special methods.

One of the advantages of the second alternative is the material requirement. The cylindirical casing can be produced from a pipe, but the eliptical casing of the first alternative should be cast and manufactured. Another advantage of the cylindirical housing is the possibility of producing a better surface finish by grinding. In the cylindirical housing, the position of the outlet port can be changed by predetermined rotation of the casing. Thus the variation of the compression or expansion ratio is possible. The swept volume of the units in the second design alternative can be changed by some machining operations . But in the first alternative once the circulator was manufactured, neither the position of inlet and outlet ports nor the swept volume can be changed. These are the most important advantages of the second

design alternative which provide versatility in experimental investigations.

For the elliptical case, there is no closed formed exact mathematical solution for some design and optimization calculations, but in the second alternative there exists mathematical solutions for the aforementioned calculations.

In the first alternative, as the vanes are rotating, they behave as a regenerator, thus heat transfer between the compression and the expansion chambers occur due to the thermal storage of vanes. On the other hand the isothermal compression on the compressor and the isentropic expansion on the expander can be approximated if the compressor is cooled and the expander is insulated. This is possible by operating these two units seperately.

From the above mentioned comparisons, the second alternative which comprise two seperate cylindirical units, seemed to be the best solution and was easier to manufacture.

4.3. DETERMINATION OF THE SIZE OF UNITS AND THE NUMBER OF VANES

As was menticned in the previous chapter, the pressure ratio of tne system should be reducec and the mass flow rate shoulc be increased, tc obtain a higher C.O.P. for the same cooling capacity.

Since the higher C.O.P. means less work input for the same cooling capacity, the cooling of a space with a smaller amount of work input could be possible with a device having a greater C.O.P..

If the system could have a capability of delivering high flow rates, the pressure ratio of the system may be reduced to increase the C.O.P. of the system, or, for a reasonable pressure ratio, flow capacity of unit should be increased to achieve adequate cooling capacity. Reasonable pressure ratio means, a pressure ratio low enough to obtain a reasonably high C.O.P. for a given capacity, but high enough so that the pressure losses have an insignifciant effect on the cycle performance. So a device must be designed capable of operating at a reasonable pressure ratio and high flow rate. In a theoretical

refrigeration cycle, pressure ratio can be determined for a required cooling capacity at a given temperature and mass flow rate, but to predict the parameters in the actual cycle, the losses must be known. The losses in the whole cycle can only be predicted by reasonable assumptions, but there may be differences between the assumed and the actual losses. In order to eliminate the effect of this undetermined losses the units shculd be adopted to new pressures in the system. For this reason a variable pressure ratio system should be designec. In the vane-type compressor the compression ratio can be changed by changing the position of the discharge port; However, in the vane-type expander, variable exparsion ratio can be obtained by changing the position of the intake port by the same way. Thus , variation in system parameters could be compensated by designing a unit which has a variable pressure ratio.

Now , the flow capacity of the units should be increased to increase the cooling capacity. Since the flow rate of the unit depends on the geometry and the rotational speed; the capacity must be maximized for a given speed and size by simply maximizing the swept volume in the unit.

For an autumobile air-conditioning unit, providing the mechanical restrictions in design of the unit are eliminated, the outer dimensions of the unit is limited by

the available space in the engine compartment. The heat exchanger may be placed in front of the radiator in a car, as in other types of automobile air conditioning units. The placing and the method of mounting of the circulator in the engine compartment should be determined. In the automobiles manufactured in Turkey, the dimensions of the available space is found to be approximately equal to the volume of a 30 cm long cyclinder having a diameter of 20 cm.

In order to increase the volume flow rate for a given speed and outer dimensions of the unit, the swept volume should be increased. The swept volume is strongly effected by the eccentricty. The eccentricty is defined as the distance between the centers of the rotor and the casing, and is denoted by e. The swept volume in the compressor, V_d, is defined as the volume trapped between two adjacent vanes, V_i, when the trailing vane covers the inlet port, times the vane number, Z, thus;

$$V_d = V_i \times Z = 2\ D\ e\ b\ Z\ \mathrm{Sin}(\pi / Z) \qquad 4.1$$

where D is the casing diameter and b is the length of the rotor. Since the crossection of the unit remains constant along the length of the rotor, the volume trapped between the vanes, V_i, is the length b times the crossection area

of the chamber, A_i.

The equation of the eccentric casing in polar coordinates can be written as ;

$$r = R (e \cos \phi + (1 - e^2 \sin^2 \phi)^{1/2}) \qquad 4.2$$

where ϕ is the angular position and R is the radius of the casing .

The distance between the casing and the rotor can be expressed as :

$$l(\phi) = r - r_r = R(e \cos \phi + (1 - e^2 \sin^2 \phi)^{1/2} + e - 1) \qquad 4.3$$

where r_r is the rotor radius.

If Eqn.4.3 is integrated with respect to ϕ ,the variation of the area swept by the vane can be obtained as a function of R, ϵ and angular position , ϕ.

$$A(\phi) = R^2 / 2 \; (\epsilon/2 * \sin 2\phi + \sin\phi \; (1 - \epsilon^2 \sin^2 \phi)^{1/2} + \pi/180 * ((2-\epsilon)\epsilon \phi + \arcsin(\epsilon \sin\phi)) \qquad 4.4$$

where $\epsilon = e / R$.

A non-dimensional graph of the accumlated area swept by the vanes of a vane type machinery is shown in Fig.4.3 (20) for different eccentricty values The area

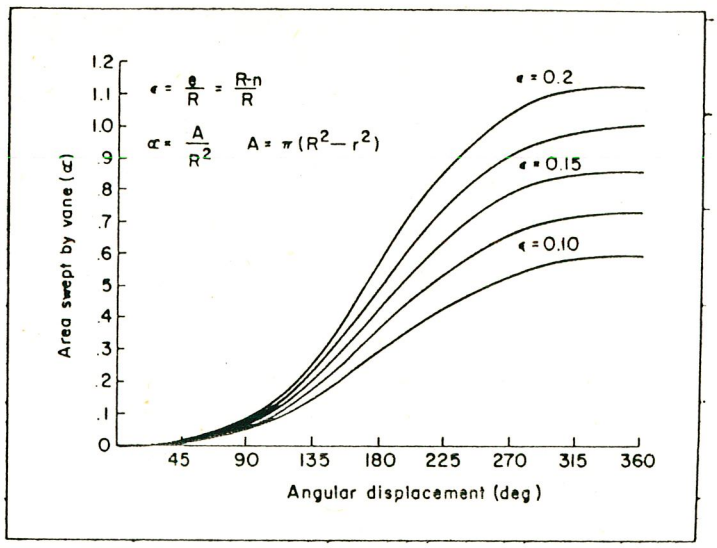

Fig.4. 3. Non-Dimensional Plot of Swept Area

swept by a vane is plotted as a function of the angular position of the vane.

Since the angular displacement between two successive vanes is $2\pi/Z$ the volume bounded by two successive vanes, casing and rotor, named as the chamber volume can be expressed as :

$$V(\emptyset) = b\,(A(\emptyset) - A(\emptyset - 2\pi/Z)) \qquad 4.5$$

If the vane thickness, w, is taken account; then the space covered by the vane must be subtracted from $V(\emptyset)$. The volume occupied by the vane at $\emptyset$ can be calculated from the following equation.

$$a(\emptyset) = R^2 w/2(\epsilon\cos\emptyset + (1-\epsilon^2\sin^2\emptyset)^{1/2} - (1-\epsilon)) \qquad 4.6$$

and the net chamber volume, $V(\emptyset)$, becomes:

$$V(\phi) = b(A(\phi) - A(\phi - 2\pi/Z) - (a(\phi) + a(\phi - 2\pi/Z))) \qquad 4.7$$

The compression ratio $r_c = V_{ic} / V_{dc}$, in the compressor side and the expansion ratio, $r_e = V_{de} / V_{ie}$, in the exparder side are determined by the location of the entrance and the discharge ports, and the number of vanes. The maximum value of $V(\phi)$ occurs when the vanes straddle the common centerline and $\phi = \pi / Z$. V_{ic} is the maximum volume of $V(\phi)$ which corresponds to the volume at the beginning of the compression process in the compressor, and V_{de} is the maximum volume of $V(\phi)$, which corresponds the volume at the end of the expansion process in the expander. The values of $V(\phi)$ and the corresponding compression or expansion ratios were calculated and plotted by using a Fortran VS program. The output of this program for different number of vanes is given in Appendix D.

The ideal swept volume is also effected by the number of vanes. The Table 4.1 shows the variation of the swept volume, based on the swept volume of a unit having 4 vanes with the number of vanes.

In this table, the volume occupied by the vanes is ignored. The actual values of the swept volume for a given vane thickness is less than those given in Table 4.1 and are shown on the Figures D.1 to D.6 in Appendix D. The volume ratio in the compressor is defined as the

TABLE 4.1

EFFECT OF VANE NUMBER ON SWEPT VOLUME

Number of Vanes	% Swept Volume
4	100
5	104
6	106
8	108
10	109
12	110

compression ratio in the compressor and as the expansion ratio in the expander. The maximum volume ratios achieved in the unit are determined by the number of vanes and tabulated in Table 4.2 .

TABLE 4.2

VARIATION OF MAXIMUM VOLUME RATIO

Number of Vanes	Maximum Volume Ratio
4	2.25
5	3.53
6	5.17
8	9.51
10	15.3
12	22.6

From the view point of manufacturing simplicity less vanes are preferable if adecuate volume change could be achieved. In a vane type machinery, which has 4 vanes, maximum volume change, r_c , or r_e , is 2.25 and this is enough for our purpose. Therefore the number of vanes is taken as 4. This decision also permited a lower manufacturing cost.

As is seen in Fig.4.3 and Eqn.4.1 , the value of eccentricity determines the swept volume and consequently the flow rate of the unit. Increasing the eccentricity increases the swept volume, but the eccentricity value is limited by the physical restrictions. From Fig.4.4 , the stroke of the vanes is seen to be equal to two times the eccentricty. Thus the depth of the slots in the rotor must be greater than the stroke of the vanes. If the distance t ,

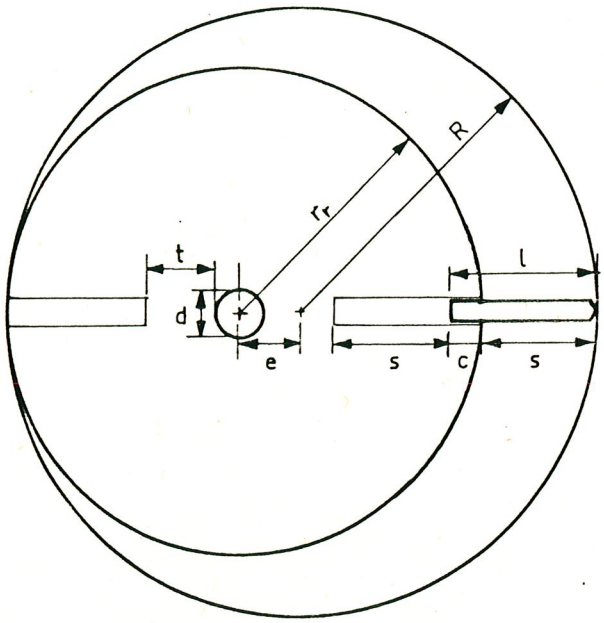

Fig.4. 4. Dimensions of a Sliding Vane Type Machinery

which is the safety thickness against loading, and c , which is the necessary distance for sealing against leakage and supporting the vane, are added to the stroke of the vane, the radius of the rotor can be written as;

$$r_r = 2\,e + c + t + d/2 \qquad 4.8$$

where d is the rotor shaft diameter.

By a reasonable approximation , the summation (c + t + d/2) was reduced to 30 mm. This was achieved by reducing the thickness, t . The thickness was reduced by adding the rotor drivers, which are shown in Drawing No 6 .

These were used for transmitting the torque to each part of the rotor seperately and to eliminate the stress concentration due to keyways. In this appoximation, the space necessary for the ball bearings at the roots of the vanes was taken into account. The radius of the casing is given as ;

$$R = r_r + e \qquad 4.9$$

where $r_r = 2\,e + 30$ mm 4.10

thus, $R = 3\,e + 30$ mm 4.11

Therefore, the maximum eccentiricity can be determined from Eqn.4.12 ;

$$e = (R - 30) / 3 \qquad 4.12$$

It should be noted that, the eccentricty is proportional to the radius of the casing, and for a given value of R, e can be determined from Eqn.4.12 . For the proposed casing diameters of 120, 132 and 150 mm the eccentiricities in terms of R, were found to be 0.16R, 0.18R and 0.20R respectively.

4.4. MATERIALS EVALUATION

Pressure rise in such machines, using gas as a working fluid, requires small clearances plus acequate lubrication. However, then, the gas may be subjected to contamination by the lubricant and also addition of the lubricants increases the viscous drag which occurs between moving parts. Some special reciprocating or vane-type compressors with carbon piston rings or carbon vanes were designed to run without lubricating oil. On the other hand, the commercial availability of such materials in Turkey, especially in the workshop of our department was scarce. Therefore the number of alternatives for the selection of the vane and the rotor materials were few. The available materials for the vane/rotor combination were : Fiber/Steel, Fiber/Brass, Brass/Steel, Teflon/Steel and Steel/Delrin.

The reduction of the friction losses has a major importance in the material selection ; therefore in selecting the materials for the vane and the rotor the following factors must be considered ;

* Selection of materials with appropriate coefficients of thermal expansion to maintain a minumum clearance over

the operating temperature range.

* Maintaining positive vane contact against the casing at all times but avoid excessive vane contact force.

Furthermore the reduction of the noise level and the weight of the units must also be considered to increase its applicability on commercial vehicles.

To a first approximation, frictional power losses are proportinal to the coefficient of frictions of the vane, rotor and the casing, the vane mass, mean racial position of the vanes, and the cube of the rotational speed in case of positive contact between the vanes and the casing. By consicering each of these quantities one at a time or in combination, frictional losses can be reduced to acceptable values for a vane-type compressor or expander.

By selecting ball bearings as centrifugal force transmitting elements and by designing for relatively low speed (3000 RPM) operation, frictional power losses can be maintained at low values. Since the friction is reduced significiantly between the vanes and casing, by preventing the physical contact between them, the mechanical friction between the vane and the rotor should be reduced.

In conventional types of sliding vane machinery, the vanes are often made of phenolic resin laminates, which is named as Fiber,using various bases such as asbestos cloth.

They are supposed to be strong , light weight , and non - scoring . Unfortunately they also warp , swell , delaminate, wear and suffer fatigue failures. Seeking greater reliability, some manufacturers turned to metallic vanes in recent decade. Hardness, resistance to wear and corrosion, and low thermal expansion made the metallic alloy vanes an excellent choice and brought relief from the problems associated with the plastic vanes.

Because of their low friction ccefficient, machinability for the required surface quality, lower weight and cost, design simplicity, reliabilty for long life operation, and their availability in the workshop of our department, Steel and Delrin 570X are selected as the vane and the rotor materials respectively. The casing was manufactured from a steel pipe and the front and rear covers were manufactured from steel plate with brass bushings.

Frictional losses have also been signifiiciartly reduced ;

i) By injecting a small amount of liquid lubricant into the compressor and the expander prior to their operation.

ii) By reducing the weight of the vanes by removing as much material as possible from the inside of the vanes without signifiiciantly effecting their mechanical strength.

4.5. DESIGN OF INDIVIDUAL PARTS

4.5.1. General

After the selection of material as was explained in the previous section, the design of the prototype unit named as the circulator was started.

The circulator comprises the compressor and the expander having similar designs were manufactured similarly. Therefore the discussion in this section is generally valid for both the compressor and the expander.

The circulator may be studied under two main headings; a) The stationary parts, b) The moving parts.

The stationary parts form the frame on which the side forces are to be transferred. As shown in the assembly drawing Drw.no 1 in Appendix H , stationary parts consist of two casings, two front covers, and two rear covers.

The position of these parts with respect to each other are very important because these are the parts which house the moving parts and determine the centering of the circulator assembly. As it is obvious, a slight deviation in the centering would effect the clearance at the vane

tips and the clearances between the rotor and the side covers all of which have a major significiance in the performance of the whole system.

The moving parts are ; the shaft, the rotors, the vanes, and the rotor drivers which transmit the torque from the shaft to the rotors or vice versa.

The circulator receives the power from a prime mover. The shaft transfers the torque received from the prime mover and the expander to the compressor. Torque transferred to and from the rotors is done by the rotor drivers, which are coupled by keys to the shaft.

The ball bearings on each side of the vanes travel around the contour of the cam which is carved on to the inner side of the front and rear covers and help the vanes follow the specified track.

4.5.2. The Vanes

To reduce the friction torque, the vanes were provided with a cam and follower system. In order to transmit the centrifugal force to the followers, small ball bearings were attached to the root of the vanes, which transformed the sliding friction at the tip of the vanes to the rolling friction at the root of the vanes. In

addition to the reduction of this friction force, transfering it from the tip of the vanes to the root of vanes also reduces the contact force between the rotor and the vane. In cases where the vanes are stuck in the slots of the rotor due to the contamination of slots by foreign materials, this cam and follower system maintains the radial movement of the vanes.

The method of production of the cam is described at Appendix B . The centrifugal force is directly proportional to the mass of the vanes and the followers. This force was reduced by decreasing the weight of the vanes by drilling 5 mm diameter and 42 mm deep holes on the root of the vanes. Thus the weight of each vane was reduced by 40 % , which resulted in vane weigths of about 150 gr in the compressor and 100 gr in the expander. Because of eccentricity of the casing and the rotor, the contact angle between the casing and the vanes vary and the point of contact moves around the tip of vanes as shown in Fig.4.5 . In conventional sliding vane machinery this is not a problem because they may have a circular tip or may be manufactured from material which has a higher coefficient of wear for self-compensation.

However, in this protoype, due to the necessity of having a constant distance between the casing and the root of the vane, the tip of the vane was designed as a wedge.

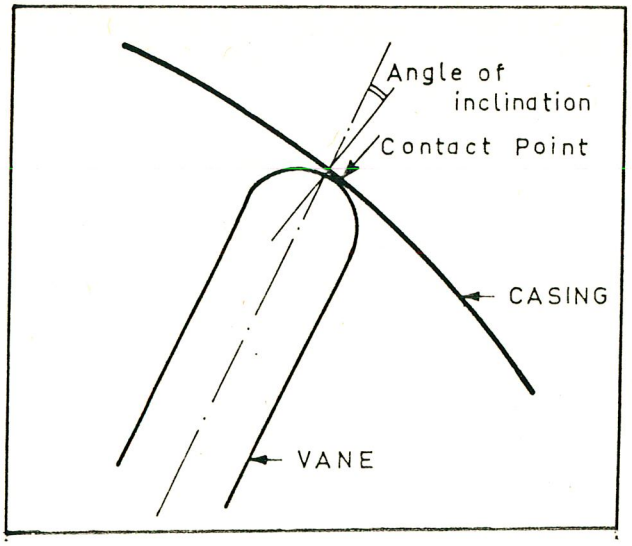

Fig.4. 5. Contact Point on the Vane Tip

The angle of the wedge was determined to be 11° 45' and was taken as 12°. This angle was found by calculating the maximum angle of incidence of the vane which occured at the points where the vanes were perpendicular to the line joining the centers of the rotor and the casing. The drawing of vane is shown in Drw.no 5 .

4.5.3. The Rotor

The rotor which is shown in Drw.no 6 , is the main element in regulating the vane motion.

As is done in machinery employing the sliding vane principle, the vanes should be housed completely within the rotor at the minimum stroke position. Therefore, slots were machined into the rotor to house the vanes. On the

other hand large rotor slots that will envelope the vane at the bottom dead center, weaken the rotor. As shown in Fig.4.4 , rotor radius was formed of the following parameters.

$$r_r = s + c + t + d/2$$

where r_r : Radius of rotor

s : Stroke, which is equal to twice the eccentricity

c : Necessary distance for sealing against leakage

t : The safety thickness which will resist loading

d : Shaft diameter

The rotor is to be subjected to rotational forces and pressure forces, as shown in Fig.2.29 . Delrin 570X was selected as the rotor material and its properties are given in Appendix E .

Since the smaller rotor means higher capacity for the same outer diameter of the casing, the rotor is designed as small as possible for a given casing diameter. In conventional vane type machinery the useful volume, which is the volume between the rotor and the casing, is about 22 % of the total volume within the casing. To reduce the radius of the rotor, the thickness, t, was reduced. If the strength of the rotor was disregarded the diameter of the ball bearings at the root of the vanes determines the minimum value of the thickness, t . Therefore, the smallest diameter ball bearing which stands

on the operating conditions was selected, FAG 624.2Z . In conventional type sliding vane machinery, the rotor is directly keyed to the shaft so that rotor has tc have an available space for the torque transmition via keyway. The rotor drivers are designed for this purpose . They have a keyway and four arms intruded to quarters of the rotor at each side for transmitting torque. The rotor drivers also maintain the axial movement so that no axial loading occur, and self alignment of the rotor during assembly is achieved.

By improving the design with the above mentioned way the useful volume is increased to 38 % of the total volume within the casing.

4.5.4. The Front Cover

The front cover was made to contain the brass bushing for the drive shaft, the bearing housing for the tapered roller bearing of the drive shaft, and the cam. It also contains a port for air passages. The bearing cap in the expander side allows the drive shaft to pass through the circulator. To reduce the leakage from circulator to the outer space, labyrinths were machined in the shaft seal. The seal was manufactured out from the brass.

As the material of the front cover, steel plate C1020 was selected which had a thickness of 20 mm. A photograph and the drawing of the front cover is shown on Fig.4.6 and Drw.no 3 respectively . The inlet ard exhaust ports are idendical in the expander and the compressor. The port on the front cover of the compressor is the intake port, and the port on the front cover of the expander is the exhaust port.

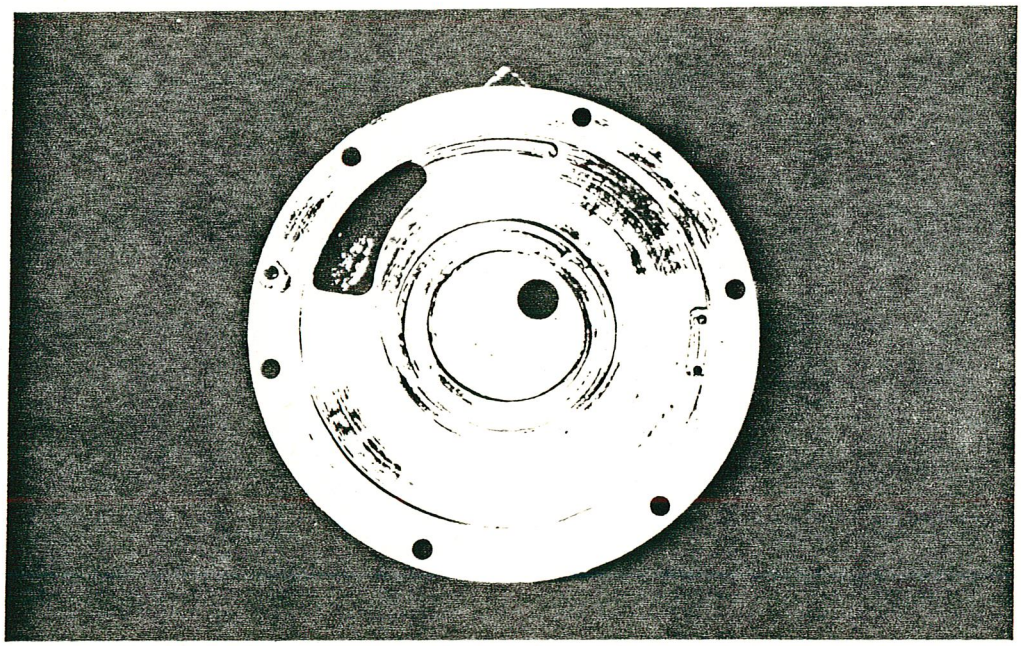

Fig.4. 6. Front Cover

In the compressor, the position of the intake port is determined so that, the air intake starts just after the chamber volume begins to increase. This effectively reduces the work done for the expansion of the residual gas, and allows the air to fill the compressor. The intake port in the compressor is enced at the point that is just

before the maximum chamber volume is achieved.

The outlet port of the expander is opened just after the chamber volume becomes maximum and stays open until the minumum chamber volume is reached. These ports is designed as wide as possible to reduce the breathing losses.

In order to avoid over compression after the vanes pass the outlet port of the compressor and the undesirable expansion of the resicual gases before the vanes reach the inlet port of the expander, a scavenging groove was made on the front covers . The variable compression and expansion ratio can be attained by changing the position of the ports which are on the casing. On the outer surface of the front cover there are line marks to identify the angular position of the ports on the casing.

The holes that were drilled on the circumference of the front covers enable the assembling and supporting of the unit by long bolts and nuts. The bearing caps reduce the leakage and satisfy dust proof working condition and lubrication for the tapered roller bearing. The ball bearings of the vanes in the grooved cam are lubricated by injecting oil through a small hole drilled on the front cover.

4.5.5. The Rear Cover

The rear covers are similar to the front covers except that they have no ports on them. The rear covers of the compressor and the expander is joined together by means of six M6 bolts. The rear covers also house the self alignment ball bearing, FAG 1203.

The rear covers have metal to metal contact to maintain the structure of the unit but this contact area was done as small as possible to prevent the heat flow from the compressor to the expander. A poly-sytrene foam is placed between the rear covers of the compressor and the expander for the above mentioned reason. The rear covers also carry a capillary copper tube to provide enough lubrication of the ball bearings of the vanes through a drilled hole on the cam groove.

4.5.6. The Shaft

The circulator takes the power through a coupling at one end. The torque received from the coupling is transmitted through a 2.5 mm diameter pin, to the shaft at the expander side.

The shaft, which is shown in Drw.no 4 was supported

by three bearings. Therefore it has three main steps on it. The 17 mm diameter portion at the mid point of the shaft is for self alignment ball bearing. The 16 mm diameter portions are for the rotors and pass through bushings. These parts have two keyways for 4X4X10 mm keys at each side that are used for securing the rotors. As is shown in Drw.no 4 , the shaft has threads on each end. The two nuts placed on each ends of the shaft were tightened enough in order to allign the axial position of the shaft and to secure the tapered roller bearings. Keeping in mind the direction of rotation, the threads at the ends of the shaft are made such that the thread at one end of the shaft is right hand threaded and the other one at the other end of the shaft is left hand threaded.

The shaft has also a 9 mm diameter portion at one end which is inserted into the coupling . This portion may be designed in various ways depending upon the type of the power transmission, such as by means of a coupling, a pulley or a clutch ...etc. In our design a small coupling takes the power from an electric motor via a torque transducer which measures the torque input to the circulator.

4.5.7. The Casing

The outer cover of the circulator, the casing, served to form the air chambers between the vanes and the rotor. The tecnical drawing of the casing is shown in Drw.no 7 .

The casings were made out of steel pipes which had a thickness of 8 mm and outer diameter of 175 mm. these pipes were machined to their final dimensions by turning them on a magnetic chuck, after the port holes were opened and the ports were welded on them. The inner casing surface that is swept by the vanes were finished to a surface of good quality and grinding of the surface was not necessary.

As can be seen from Drw.no 7 , a groove was machined on the inner surface of the casing so that the air can enter and leave the chambers. Since the inner surface of the casing is circular, the angular position of the above mentioned groove can be varied.

To reduce the pressure drop in the ports, these grooves are produced longitucinally and the width of the grooves is determined by taking into account of the maximum and the minumum compression and expansion ratios.

4.6. Assembling

The parts described in the previous section are assembled in the following way :

First, the bearing FAG 1203 (self aligning bearing) is fitted on the center part of the shaft and was provided with 1 mm gaskets to ensure sealing on both sices. Then, this bearing is inserted intc the housing on one of the rear covers. The 10 mm thick poly-sytrene foam is placed between the rear covers. After placing the long bolts on the circumference of both rear covers, the covers are secured in place by means of six M6 bolts and nuts (See Fig.4.7). After these, the assembling of the compressor and the expancer on each side of the rear covers are made in the same way. The small rollers are insertec on both

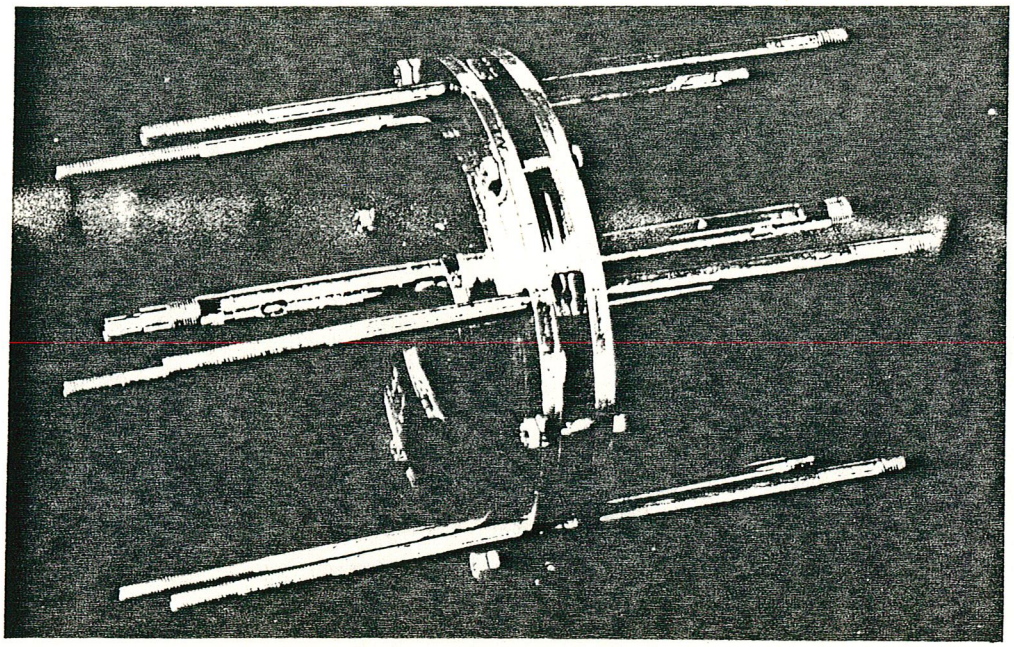

Fig.4. 7. Assembling Step 1

sides of each vane and the vanes are placed in the rotors, thus forming the rotor vane assembly. This is shown in Fig.4.8 .

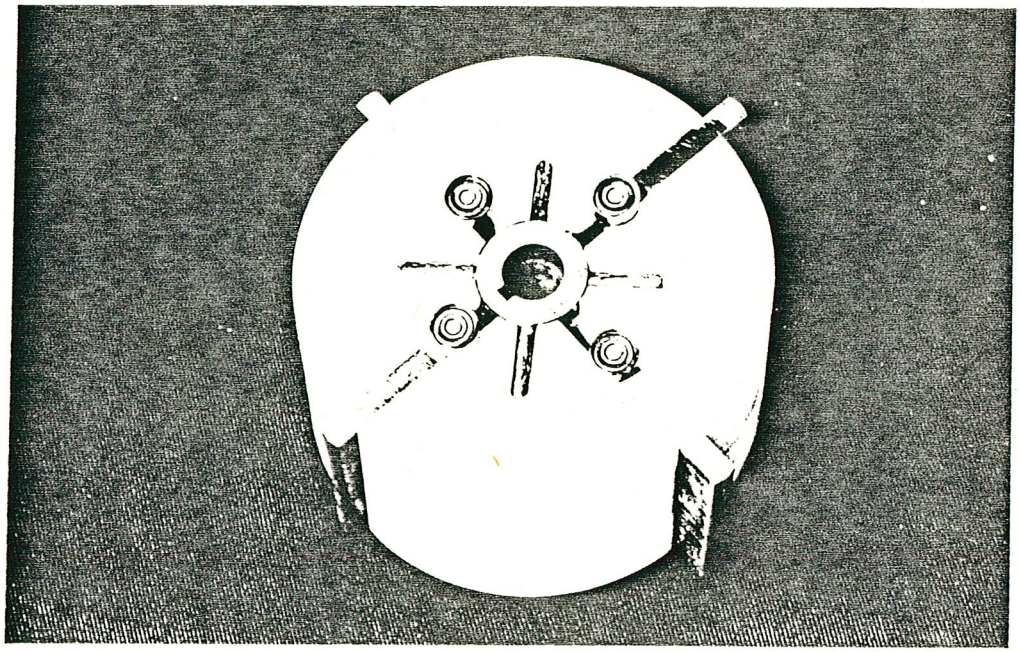

Fig.4. 8. Assembling Step 2

After the placing of the key on the shaft, one of the torque transmitting pieces is fitted, and then, the

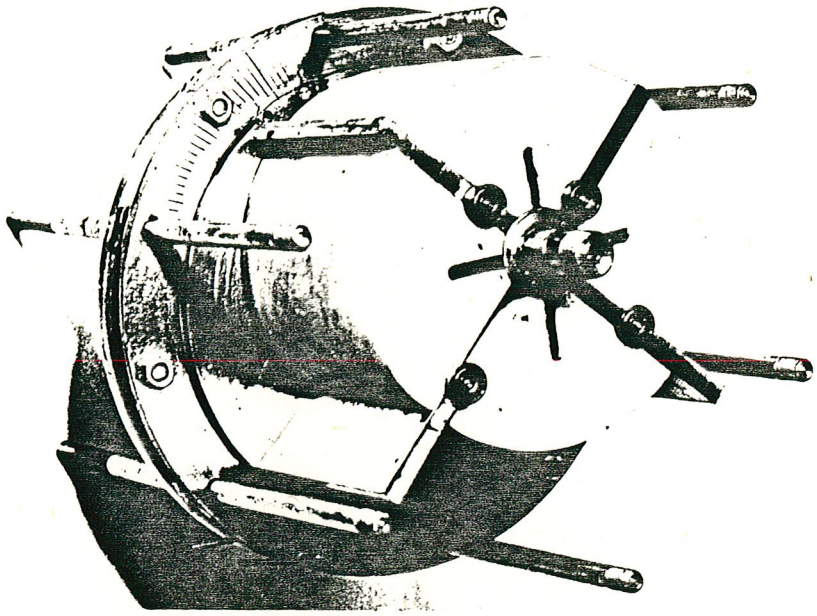

Fig.4. 9. Assembling Step 3

rotor-vane assembly is put into its place. Care must be given so that the followers of the vanes are positioned correctly (See Fig.4.9). This was followed by inserting the second key and second torque transmitting piece on the other side.

The casing, equipped with 0.10 - 0.15 mm craft paper gaskets on each end, is placed around the rotor. By using the linemarks on the rear cover, the angular position of casing is adjusted (See Fig.4.10). The adapter for

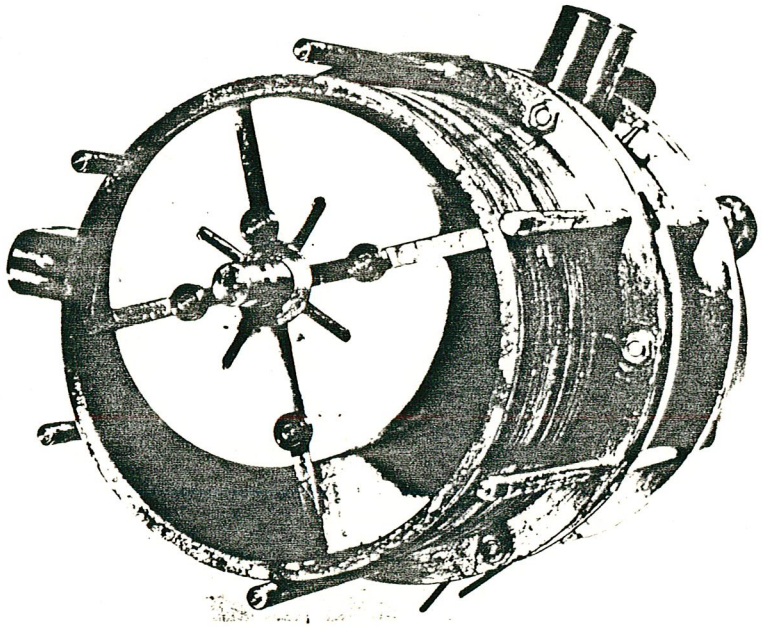

Fig.4.10. Assembling Step 4

fitting the inlet and outlet pipes to the ports on the front covers must be screwed before assembly of the front cover. After inserting the cup of the tapered roller bearing into the front cover; the front cover is placed on the asembly again paying attention to the position of the followers. Then, the cone of the tapered roller bearing is

inserted , followed by securing it with specially manufactured nuts. During this assembly procedure the angular position of the front cover with respect to the rear cover must be controlled. The long cover bolts are fastened by six M8 nuts to exert sufficient pressure on the packing. Thus the assembly of the unit is completed after placing the gaskets and the bearing caps, as shown in Fig.4.11 .

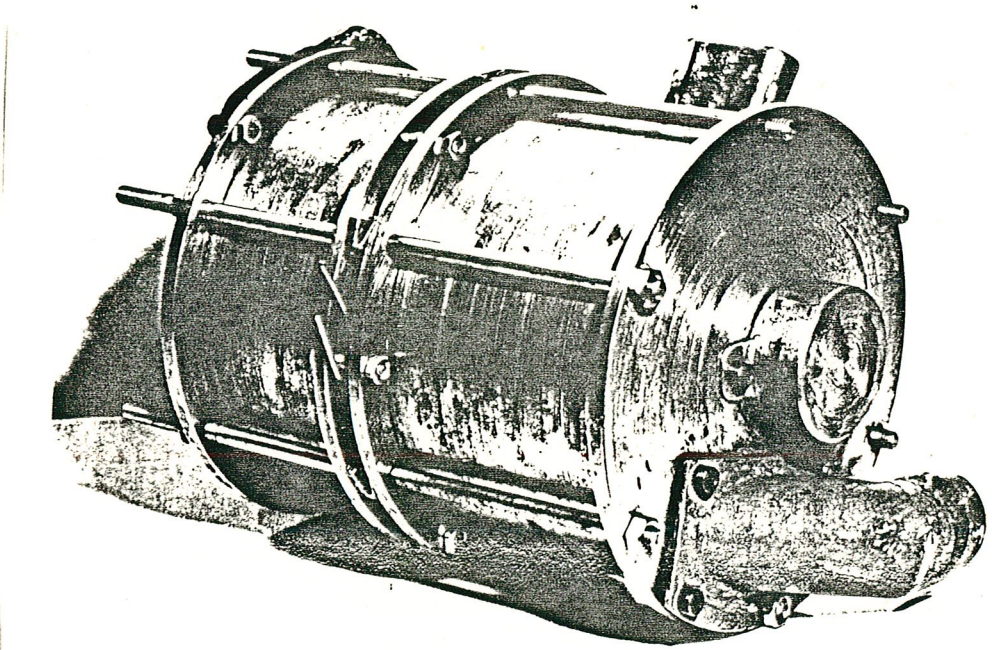

Fig.4.11. Assembling Step 5

C H A P T E R F I V E

EXPERIMENTAL STUDY

5.1. DESCRIPTION OF THE TEST RIG

5.1.1. General

In order to determine the characteristics of the prototype, a test set up was constructed. By this set up it was made possible to take the measurements of flow, power input, temperatures and pressures at different stations while running the circulator at different speeds, and at different pressure ratios. General view of the test set up is shown in Fig.5.1 .

In testing the device, a drive system which was designed and produced by A.Rıza Özyaman for his purposes was used. This drive system whose components are shown in Fig.5.2 was designed to obtain different operation speeds.

During the tests 3 kW (4 hp) electric motor was used as prime mover. Rotational motion was transmitted to a drive shaft parallel to the motor shaft by means of a

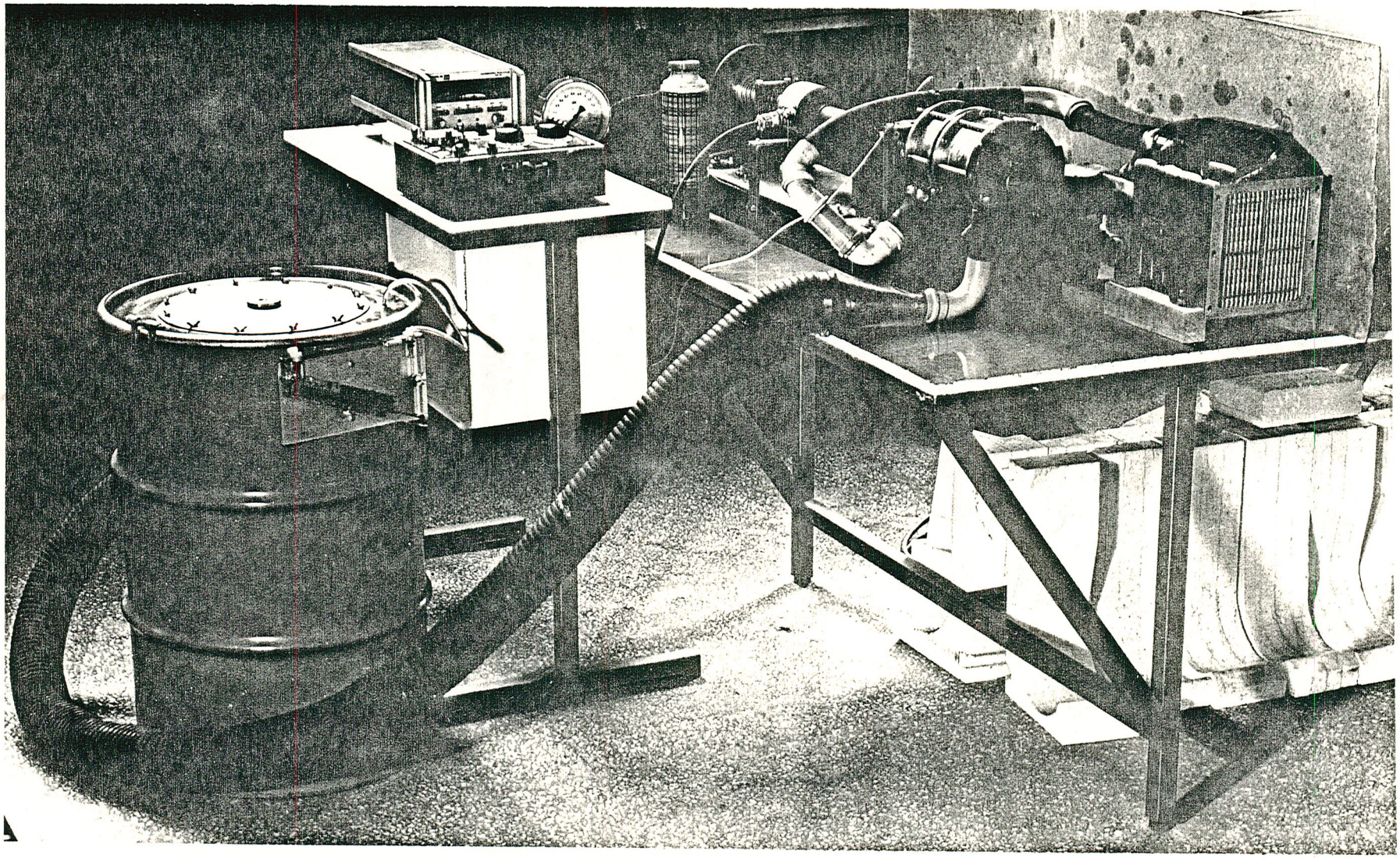

Fig.5. 1. General View of the Test Rig

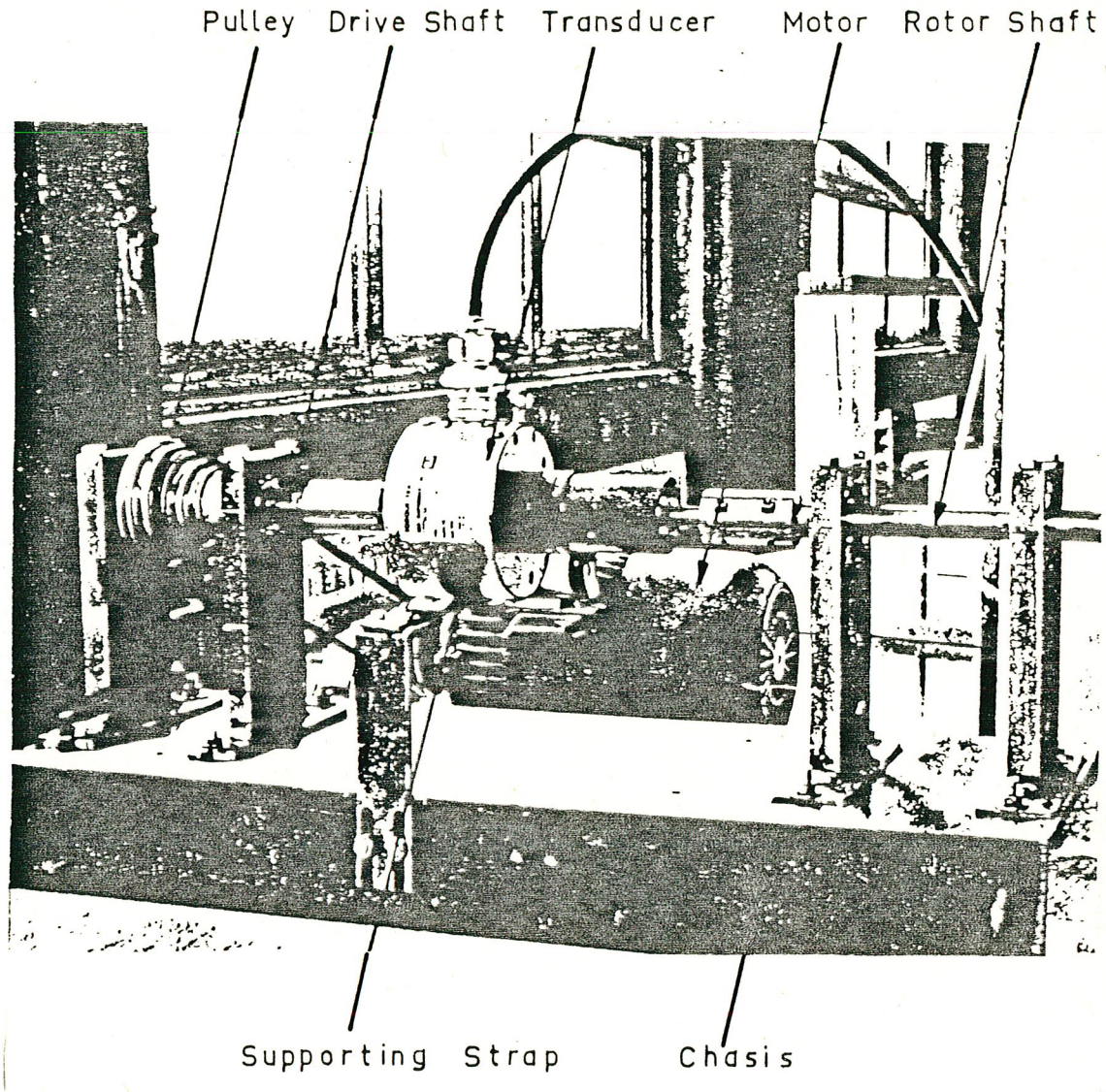

Fig.5. 2. Drive System

multi stepped V belt-pulley system. Drive shaft was supported by two ball bearings and was coupled to a torque transducer. The torque transducer is coupled to another shaft, which transmits the torque via a coupling to the shaft of the circulator. The torque transducer is used for measuring the torque at the circulator shaft by connecting it to digital strain indicator. The shafts on each sides

of the torque transducer were supported by ball bearings and bearing supports were mounted on a chasis. The circulator was carried on an another chasis which was simply produced by bending a sheet iron.

The heat exchanger used for cooling the compressed air is connected to the circulator by rubber and PVC pipes. This heat exchanger is a counterflow, four pass, air to air heat exchanger which was specially manufactured for aircraft applications, and it was cooled by a centrifugal fan running at 6000 rpm. During the tests carried out with this unit, the temperature of the pressurized air leaving the heat exchanger is found at nearly the ambient temperature (1 - 2 °C above the room temperature).

5.1.2. Measurement of the Torque

A torque transducer, whose specifications given in Appendix F , was used to measure the circulator input torque. It was supported by a strap for balancing the weight of its non-rotating part. This is shown in Fig.5.2.

For calibration purposes a 380 ohm test resistor is supplied with the torque transducer. This resistor simulates a torque output of 80 in-lbs (9.032 N-m) when

connected to the terminals of the transducer. The digital strain indicator, initially calibrated for zero output was used to determine the torque input. Digital strain indicator can take the reading in every 0.3 to 2.0 sec. This time can be adjusted by a variable resistor in it, and it is generally setted to 2.0 sec. for recucing the fluctuation of the display by longer integration time of analog signal output of the transducer.

The calibration of the torque transducer and the strain indicator combination was performed as follows :

When there was no torque on the transducer shaft, strain indicator was brought to zero by adjusting the bridge zero resistor. Ther, the test resistor of the transducer was connected to the input terminals of the indicator and the reading was found to be 6400 . Since the digital output, Ω , is linearly proportional with the applied torque, M , the relation between the torque and the digital output is found to be :

$$M / \Omega = 9.032 / 6400$$

or $$M = 0.001413\ \Omega \text{ N-m}$$

where Ω is the digital reading.

The shaft of the torque transducer was connected to the drive shafts by two couplings. These couplings were

designed to provide alignment of the coupled shaft within ± 0.02 mm.

5.1.3. Measurement of the Rotational Speed

During the experimental investigation, rotational speed was measured by a hand tachometer, and it was seen that even at maximum speed, the speed variation was found to be within ± 1 %.

5.1.4. Pressure Measurement

For measuring pressures a Bourdon-type pressure gage and U tube manometers were used. Since the magnitude of the dynamic head of flow was so small when compared to the static pressure at the high pressure side, the effect of dynamic head was not considered. Therefore only static pressure measurements were made at the exit of the compressor and at the inlet of the expander.

5.1.5. Temperature Measurement

The temperatures at different points of the system were measured by thermocouples. To record the voltage developed by Cu - Constantan thermocouple junctions a potentiometer was used . The measured voltages are transferred to °C in an accuracy of ± 0.5 °C. Temperature measurements are taken at four different points; namely at the inlet and the outlet of the compressor and at the inlet and the outlet of the expander. The potentiometer used had an accuracy of ± 0.01 mV .

5.1.6. Measurements of Flow Rate

Air-flow is measured for inlet and outlet flow rates respectively. For measuring the flow rate, a precision long radius flow nozzle was used. The inlet air-flow is measured by drawing the compressor air trough the nozzle into a pulse damping drum, and then out trough a flexible hose to the inlet port of compressor. All the air which enters the cycle must be drawn in trough the nozzle. By measuring the total pressure difference across the flow nozzle the air-flow rate can be measured to an accuracy of

± 1 % . The pressure difference accross the nozzle is measured in inches of water by ar inclined manometer which is shown on Fig.5.1 . The air flow charts supplied for each nozzle is used to determine the air-flow rate by taking the pressure difference across the nozzle from the inclined manometer. The calibration charts those are supplied by the manufacturer is presentec in Apperdix G .

To measure the outlet flow rate the flexible hose is connected to the outlet port and the direction of nozzle is reversed by simply reversing the plate on the drum.

5.2. TEST CARRIED OUT WITH THE PROTOTYPE

In accordance with the object of this work, first set of experiments was carried cut with the compressor. For testing the compressor seperately, the rotor-vane assembly of the expander was taken out, and the self alignment ball bearing is placed between the expander and the compressor.

For the best performance, the assembling have been made carefully since the positions of the parts with respect to each other were very important. Clearances between the side covers and the rotor-vane assembly is adjusted by changing the thickness of the gaskets.If these clearances were small,after a period of testing an abrupt change in the characteristics of the compressor was noticed. This resulted in a moderate increase of the volume flowrate followed by a significiant increase of the drive shaft torque. The change of the performance might have been caused by the change in the length of the parts due to temperature change. The temperature rise in the compressor causes the thermal expansion of the relavent parts. This expansion increases the dimensions of the rotor and the vanes. A small increase in the lengths of the vanes and the rotor decrease the clearance between them and the side covers. In fact the

length of the casing is increased due to thermal expansion, and the clearances should remain unchanged. But due to the difference in the thermal expansion coefficients of the rotor and the casing this clearance is reduced by the temperature rise. The change in clearance can be written as ;

$$\text{Change in clearance} = \text{Temperature rise} \times \text{Length} \times (\alpha_{\text{delrin}} - \alpha_{\text{steel}}) \quad 5.1$$

where α is the thermal expansion coefficient and α values for Delrin and steel are ; 36 μm/m°C and 12 μm/m°C respectively. The clearances at the sides of the rotor were adjusted by putting gaskets having proper thicknesses. The maximum tmperature rise reached during the experiments was 50°C and this temperature rise causes a change in the clearance of about 0.12 mm. It seemed that the clearance of about 0.15 mm is enough to prevent the touching of the surface of the rotor to the side covers. Thus the side cover gaskets thickness was taken as 0.15 mm.

The temperature of the casing is less than the temperature of the inner parts. The change in clearances is greater than the above mentioned value which causes the parts to rub one another. The rubbing of the parts increases the friction and causes a temperature rise in the parts

above the gas temperature. Thus the increase in the input torque and the increase in the flowrate can be explained by the above mentioned reasons.

At the beginning of the experiments, due to an error in the cam profile, one of the vanes touched to the edge of the groove at the discharge port of the compressor . The touching of the vane to this edge at a high speed resulted in the breaking of a part of the rotor. This broken part of the rotor was joined to the shaft by two M5 bolts and experiments were continued. The placing two brass strips in the groove of the discharge port prevented the touching of the vanes to the edge of the groove.

The experiments were started with the testing of the compressor at 715 rpm. At this speed the effect of internal compression ratio variation was investigated by changing the position of the outlet port. The data and other calculated results of this tests are tabulated at Table 5.1. For different compression ratio settings, the variation of the overall efficiency of the compressor with the various throtling conditions is shown in Fig.5.3 .

The throtling of the discharge side of the compressor produces a pressure difference across the exhaust and intake ports of the compressor. In the text of this thesis by the 'pressure difference' it is meant that the pressure difference across the intake and exhaust ports of the units.

TABLE 5.1

RESULTS OF THE COMPRESSOR TEST AT 715 RPM

	r_c = 1.3				r_c = 1.4			
ΔP Pa	Q l/s	η_{vc} %	M N-m	η_c %	Q l/s	η_{vc} %	M N-m	η_c %
10	12.4	79	3.5	45	11.6	74	3.6	41
20	11.1	71	5.5	50	10.6	68	5.7	46
30	9.5	60	7.4	46	9.1	58	5.7	43
40	7.9	50	9.2	40	7.8	49	9.4	39
50	6.7	43	10.8	35	6.2	40	11.0	32
	r_c = 1.5				r_c = 1.6			
ΔP Pa	Q l/s	η_{vc} %	M N-m	η_c %	Q l/s	η_{vc} %	M N-m	η_c %
10	9.6	61	3.8	32	7.8	50	4.1	24
20	8.9	57	5.8	38	7.7	49	6.1	31
30	8.4	53	7.7	39	7.6	48	7.8	35
40	7.1	45	9.7	34	6.9	43	10.0	32
50	5.9	38	11.5	29	5.4	35	11.7	26

The tests were continued by incresing the comressor speed to 1450 rpm. But just after starting to the run the compressor, it failed and came to a stop. When the compressor was disassembled it was noticed that all of the roller followers of the vanes at the rear cover side were broken. After this failure the vanes were changed. The vanes

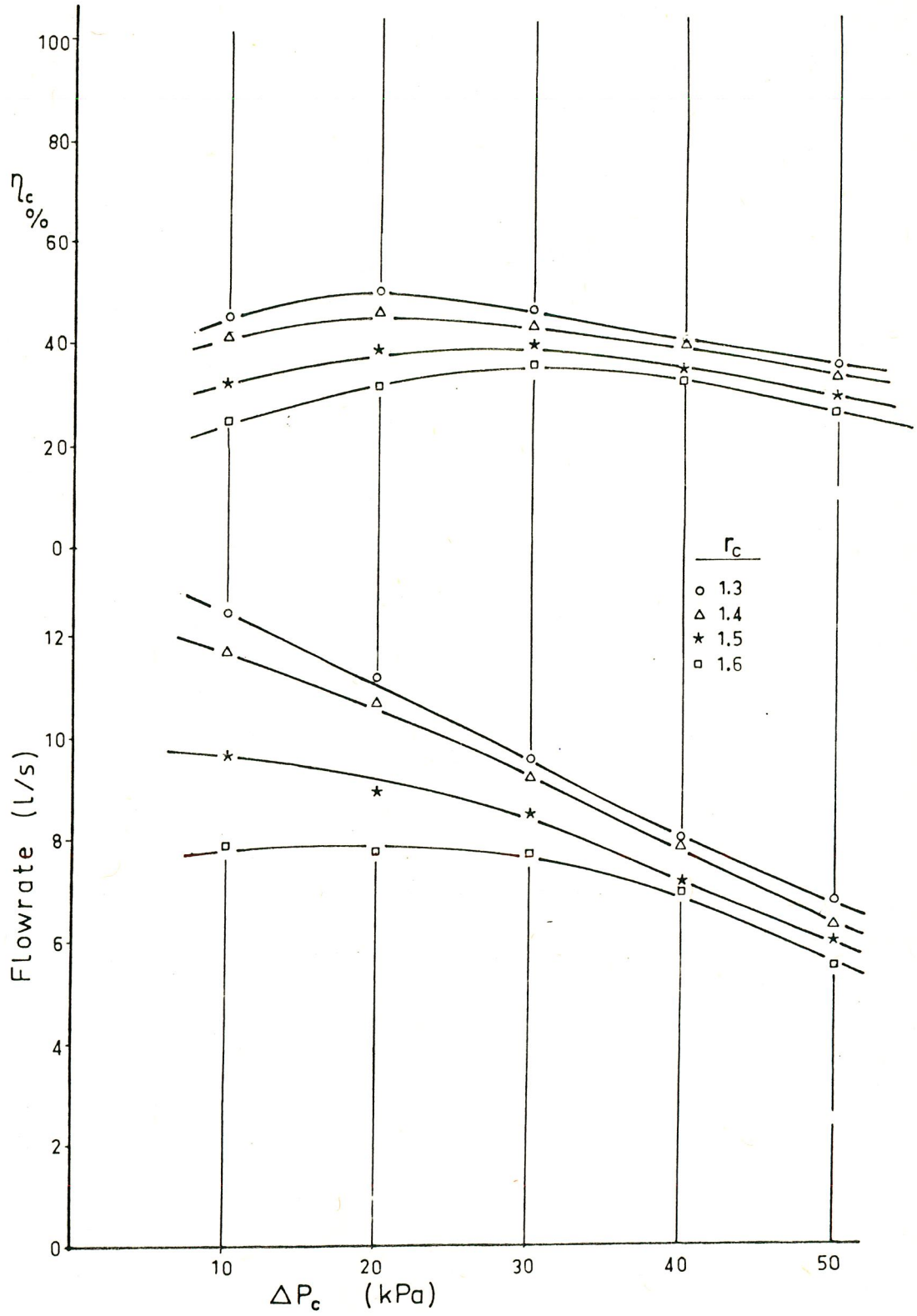

Fig.5. 3. Performance Graph of the Compressor at 715 rpm

maufactured from Delrin 570X were used. These Delrin vanes had no bearing at the roots of them. Although the performance of the compressor showed a relative increase with the Delrin vanes, after a prolonged time of operation under high pressure the sudden change in the operation characteristics of the compressor was noticed. The compressor was then disassembled and it was noticed that two of the vanes were stuck to the slots of the rotor.

Following the cleaning of the rotor slots, the cams on the covers were modified. During this modification, the ripples on the cam surface were filled with welding and smoothed by sand paper. This smoothing operation was done by the use of a crescent shaped tool in the milling machine.

After the modification of the cams, the tests were conducted with the steel vanes at six different speeds. These were 715, 860, 1005, 1320, 1750 and 1960 rpm. The higher speeds were avoided to prevent the failure of the roller followers at the root of the vanes.

At each speed setting, the discharge pressure is adjusted by throtling the discharge side of the compressor. Then, the gage pressure at the discharge sice of the compressor, the air-nozzle manometer reading, and the digital reading of the input torque were recorded. The barometric pressure and the ambient temperature were recorded before each run.

In order to determine the magnitude of the leakage flow to the outer space, the intake and discharge flowrates were measured for many times. It was observed that there was not a significiant difference between the intake and discharge flowrates. Therefore, during the experimental investigation only the intake flowrate was measured.

The parameters which are relavent in the determination of the performance characteristics of the compressor were calculated from the experimental data. Calculation procedure and sample calculations are shown in Appendix C. The results of these calculations are tabulated at Table 5.2 .In Fig.5.4 the flowrates were plotted against the pressure difference for each speed setting.

After the completion of the experimental investigation with the compressor, the expander was planned to be tested. For testing the expander, a high capacity pressurized air supply was needed. Since such a high capacity air supply was not available in our department the performance data of the expander could not be obtained. After the determination of the performance coefficients of the compressor, the performance coefficients of the expander were assumed to be the same of those for the compressor.

TABLE 5.2

ΔP Pa	715 RPM Q l/s	η_{vc} %	M N-m	η_c %	860 RPM Q l/s	η_{vc} %	M N-m	η_c %
10	12.4	79	3.5	45	15.3	81	3.6	45
20	11.1	71	5.5	50	13.8	73	5.8	49
30	9.5	60	7.4	46	12.5	66	7.7	48
40	7.9	50	9.2	40	10.9	58	9.3	45
50	6.7	43	10.8	35	9.2	49	11.1	39
ΔP Pa	1005 RPM Q l/s	η_{vc} %	M N-m	η_c %	1320 RPM Q l/s	η_{vc} %	M N-m	η_c %
10	18.1	81	3.7	45	25.1	86	4.0	44
20	16.8	76	5.8	51	23.5	81	6.2	51
30	15.3	69	7.8	50	21.7	75	8.1	52
40	13.6	62	9.7	46	19.8	68	10.1	49
50	12.4	56	11.3	44	18.5	64	11.6	49
ΔP Pa	1750 RPM Q l/s	η_{vc} %	M N-m	η_c %	1960 RPM Q l/s	η_{vc} %	M N-m	η_c %
10	34.4	89	4.8	38	39.5	92	5.1	36
20	32.5	84	6.8	48	37.3	87	7.2	47
30	30.5	79	8.6	52	35.4	82	9.0	52
40	28.7	75	10.6	51	33.5	78	11.0	52
50	27.0	70	12.3	51	31.4	73	12.6	51

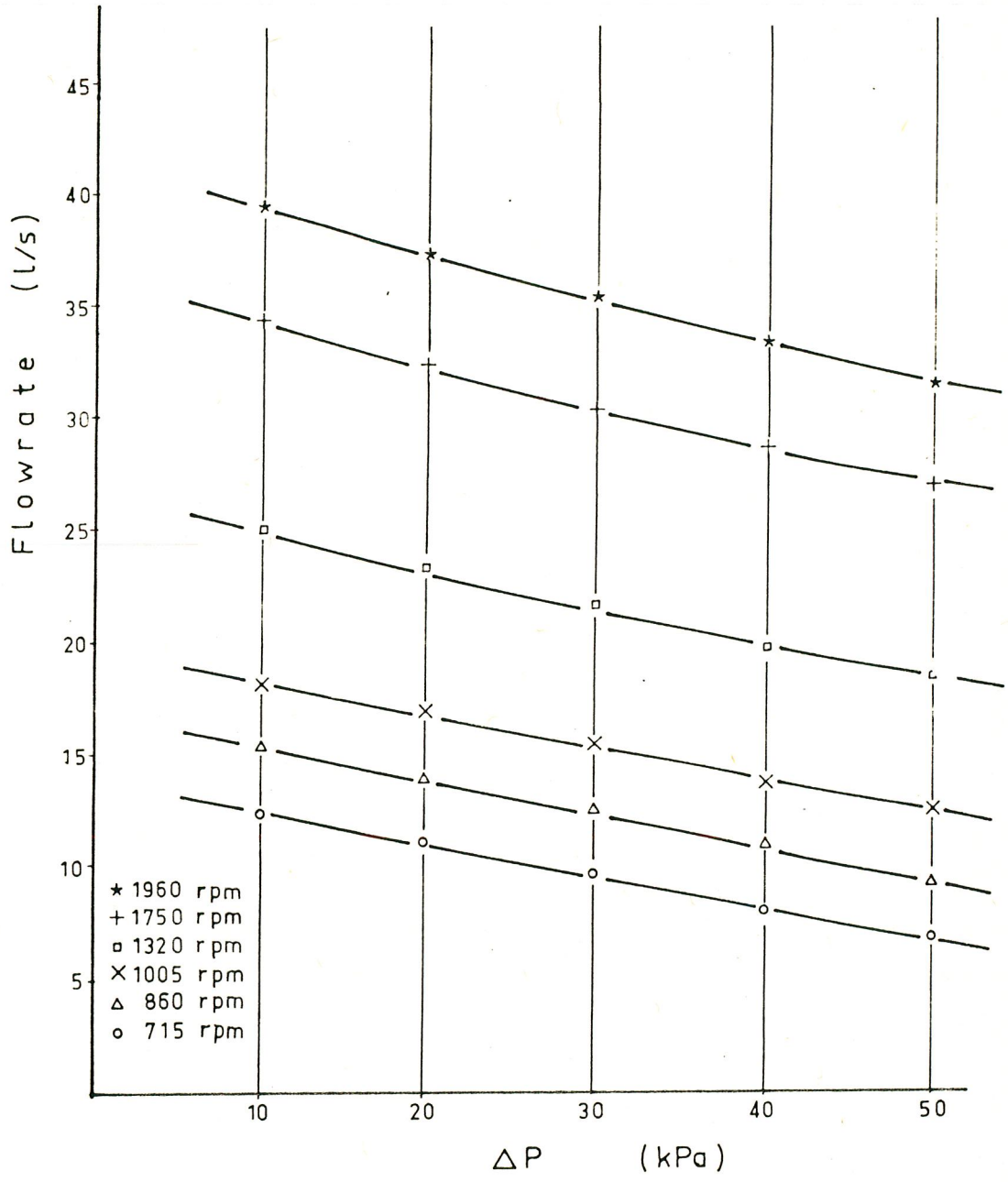

Fig.5. 4. Plot of Flowrate against Pressure Difference

Experimental investigations of the circulatior as an air-conditioning unit were performed as the next study. During these tests the pressure drop across the heat exchanger , compressor discharge pressure , temperature difference across the compressor and the expander, the flowrate and the input torque were measured. The effect of the pressure ratio on the system performance was investigated by changing the compression and expansion ratios of the units.

Initially the swept volume of the expander was designed as 90 % of the compressor's swept volume. With this swept volume ; it was observed that the pressure at the high pressure side could not be sufficiently increased for efficient operation of the expancer. Therefore, in order to increase the pressure at the inlet of the expander, the swept volume of the expander was reduced to 66 % of the compressor's swept volume. The swept volume of the expander was reduced by reducing the total length of the expancer.

5.3. DISCUSSION OF EXPERIMENTAL RESULTS

The displacement volumes of the compresssor and the expander were calculated from their geometry and dimensions, and they were determined as 1.32 l and 0.87 l respectively.

As was mentioned in the previous section the first set of experiments were carried out with the compressor at 715 rpm. In these tests the effect of internal compression ratio was investigated. The results of the first set of experiment were given in Table 5.1 . As is shown in Fig.5.3 the overall efficiency curves were plotted for each setting of the compression ratio against the pressure difference across the inlet and outlet ports of the compressor. In this figure, it was observed that ; the peak of the efficiency curves were shifted to the right side and they showed a significiant decreaseas the compression ratios were increased. It was noticed that the compressor gives the best performance at 1.3 compression ratio setting for all throttling conditions. Since the angular displacement between the inlet and outlet port of the compressor is increased to increase the compression ratio, the time for the compression process is increased. The longer time for compression means, the duration of time for leakage is

increased. In addition, when the pressure insice the compressor is increased, the internal leakage across the vanes also increases.

If the compression is carried above the discharge pressure the losses in the ports cue to the mismatch between the pressure in the exhaust port and the pressure in between successive two vanes which has opened to the exhaust port, is increased. The reduction of efficiency seen on the left hand side of Fig.5.3 may originate from the above mentioned reason. Since the 1.3 compression ratio gives the best performance for all throttling conditions, the compression ratio was set to 1.3 for the rest of the experimental investigations of the compressor.

The results of the tests carried out by the compressor at differeent speeds were tabulated in Table 5.2 . Now, the determination of the performance coefficients can be made by using graphical methods. The procedure for determination of the performance coefficients was described in Section 3.4.5 .

As shown in Fig.5.5 , the flowrates were plotted against compressor speed for varicus pressure differences. Each of the straight lines is for a pressure cifference. These lines should be parallel to the ideal delivery line according to the theoretical analysis made in Section 3.4 . However, as is seen in Fig.5.5 these straight lines have

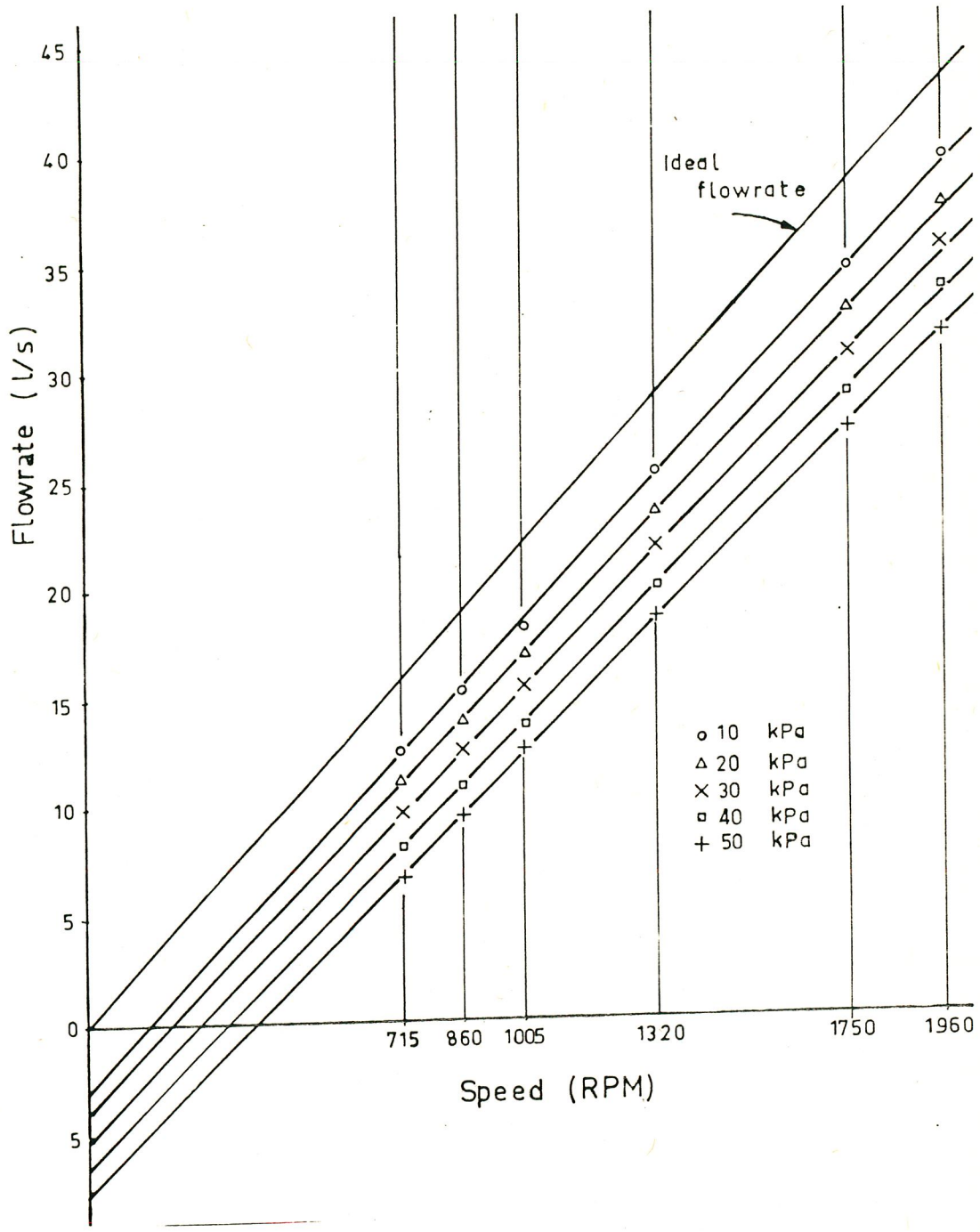

Fig.5. 5. Plot of Flowrate against Speed

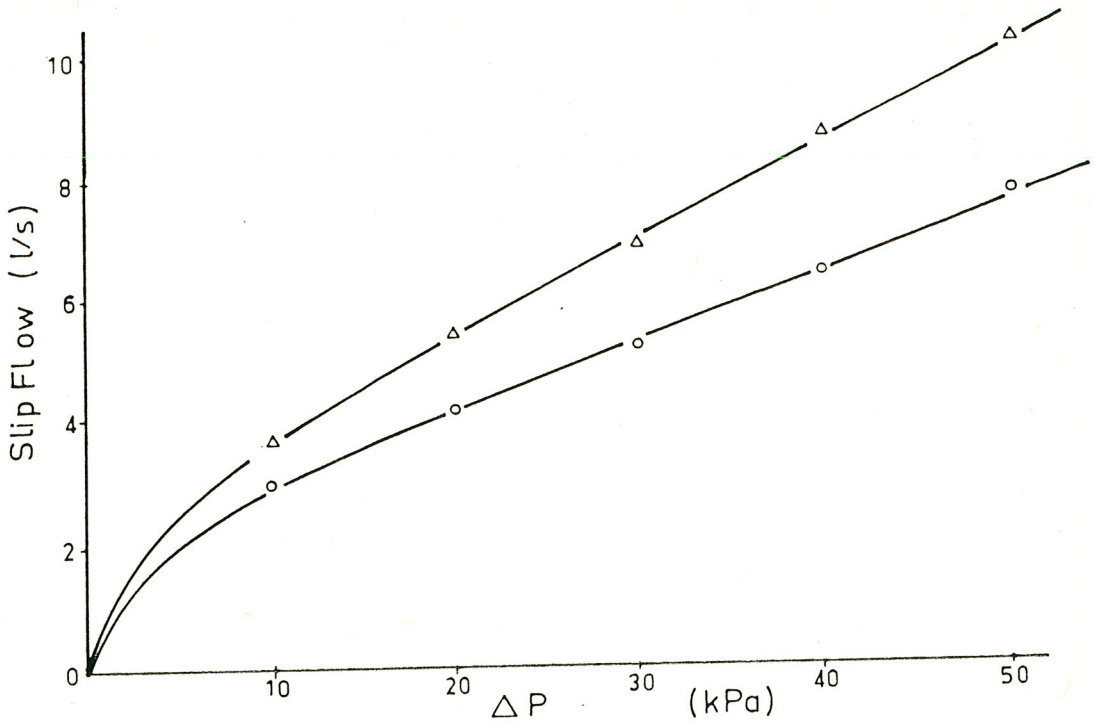

Fig.5. 6. Plot of Leakage Flowrate against Pressure Difference

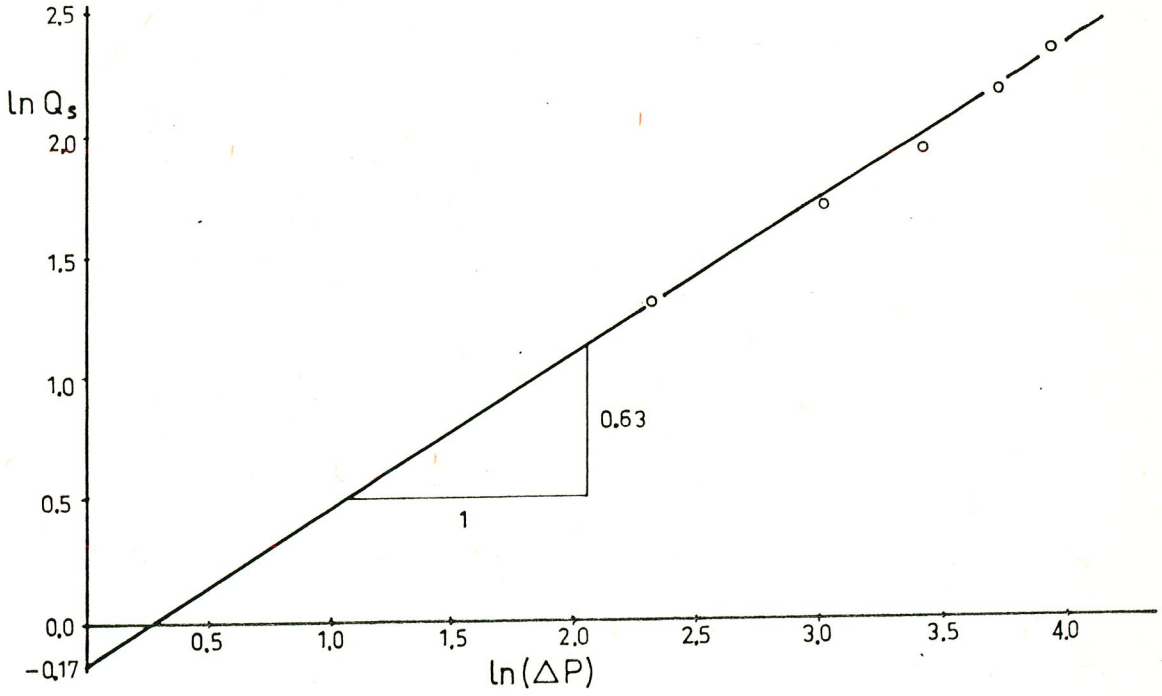

Fig.5. 7. Plot of Leakage Flowrate against Pressure Difference on Logaritmic Scale

different slopes due to the variation of leakage with the rotor speed. In order to determine the value of the leakage flow coefficient that was explained in theoretical analysis; it was necessary to determine an average amount of leakage for each pressure difference. This average leakage flowrates were taken to be the ones corresponding to 1250 rpm. These leakage flowrates are then plotted against difference which cause them. As is seen from Fig.5.6 the leakage flowrate does not vary linearly with the pressure difference as expected. On the other hand the plot of this curve on a logaritmic scale enabled the fitting of a straight line to the experimental results. This is shown in Fig.5.7 . The slope of this line is 0.63 and its' intercept is -0.17 . The value of the intercept , -0.17, is equal to ln(C_s x V_{dc}). Thus, now C_s can be determined :

$$C_s = \exp(\text{ intercept }) / V_{dc} = e^{-0.17} / 1.32 = 0.64 \qquad 5.2$$

This C_s value is valid if the units of the pressure is in kPa , the units the volume is in l and the units of the volume flowrate is in l/s .

The slope of the line shown in Fig.5.7 was expected to be 0.5 but due to the reasons mentioned in the analysis of the volumetric efficiency in section 3.4.2 , the exponent of the pressure difference term i.e; the slope of the above

mentioned line, was found to be 0.63 .

The variation of the leakage flowrate with speed originates from the residual gases whose amount increase with the increasing of the rotational speed of the rotor. Increasing the angular speed of the rotor reduces the time for exhausting the gas in the discharge side. This makes the transfer of the compressed gas difficult, and mass of the residual gas increase followed by ar increase of the pressure high above the discharge pressure. The residual gas at high pressure leaks to the intake side and occupy a space at intake chamber, thus reducing the amount of fresh charge.

The torque input to the compressor for constant pressure differences are plotted against speed in Fig.5.8 . Altough the slopes of the lines fitted to the experimental points should be the same according to the theoretical analysis, the independent fitting of lines for each pressure difference does not satisfy the parallelism. In order to determine the speed dependent drag coefficient, C_r , the average slope of the torque versus speed lines was taken and the lines which have this average slope were plotted . These are shown in Fig.5.8 .

The slope of these lines is 1.26×10^{-3} and C_r can be determined as follows,

$$C_r = \text{Slope} / (V_{dc} \times 60) = 1.26 \times 10^{-3} / (1.32 \times 60)$$

$$= 0.016 \qquad 5.3$$

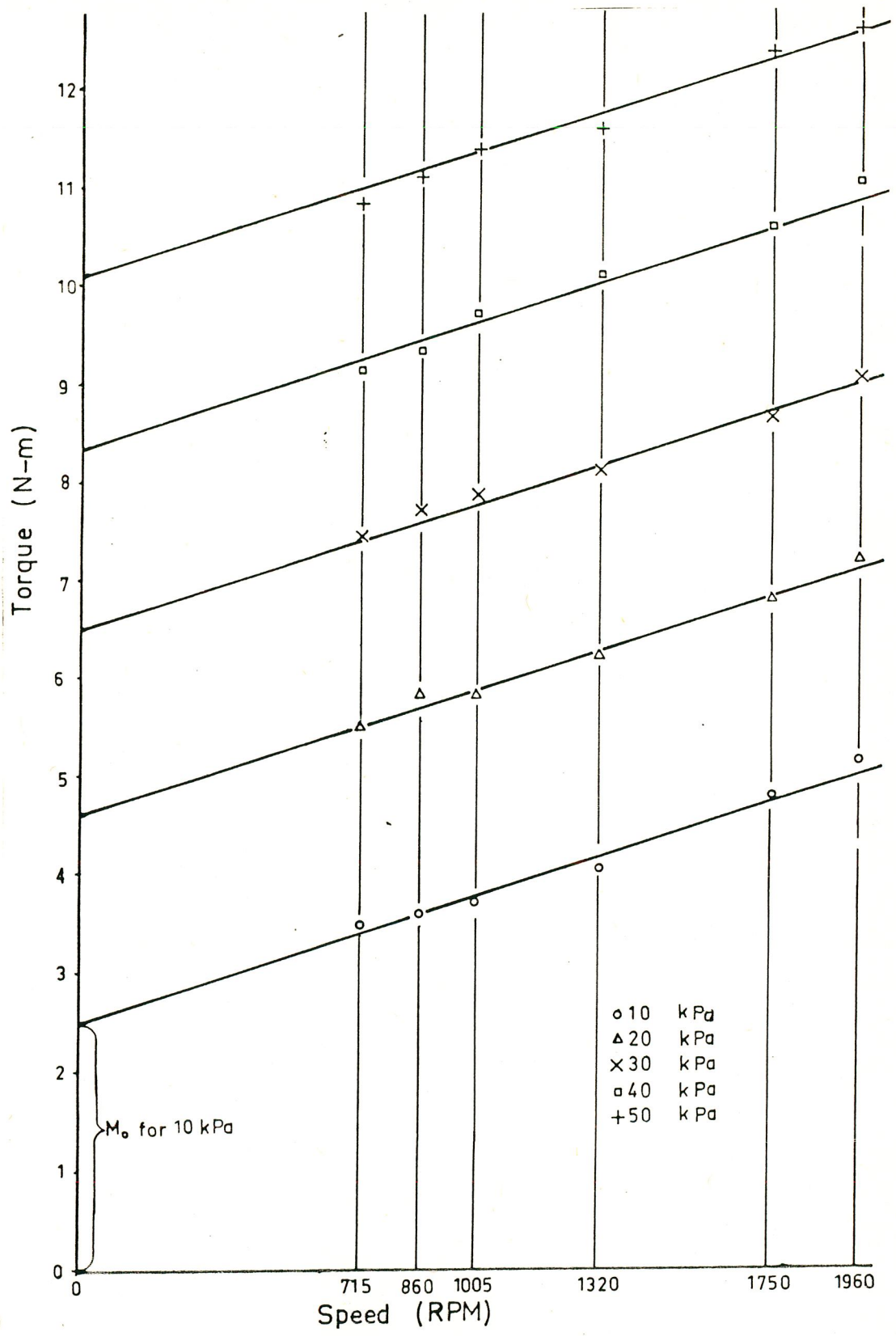

Fig.5. 8. Torque Input of the Compressor against Speed

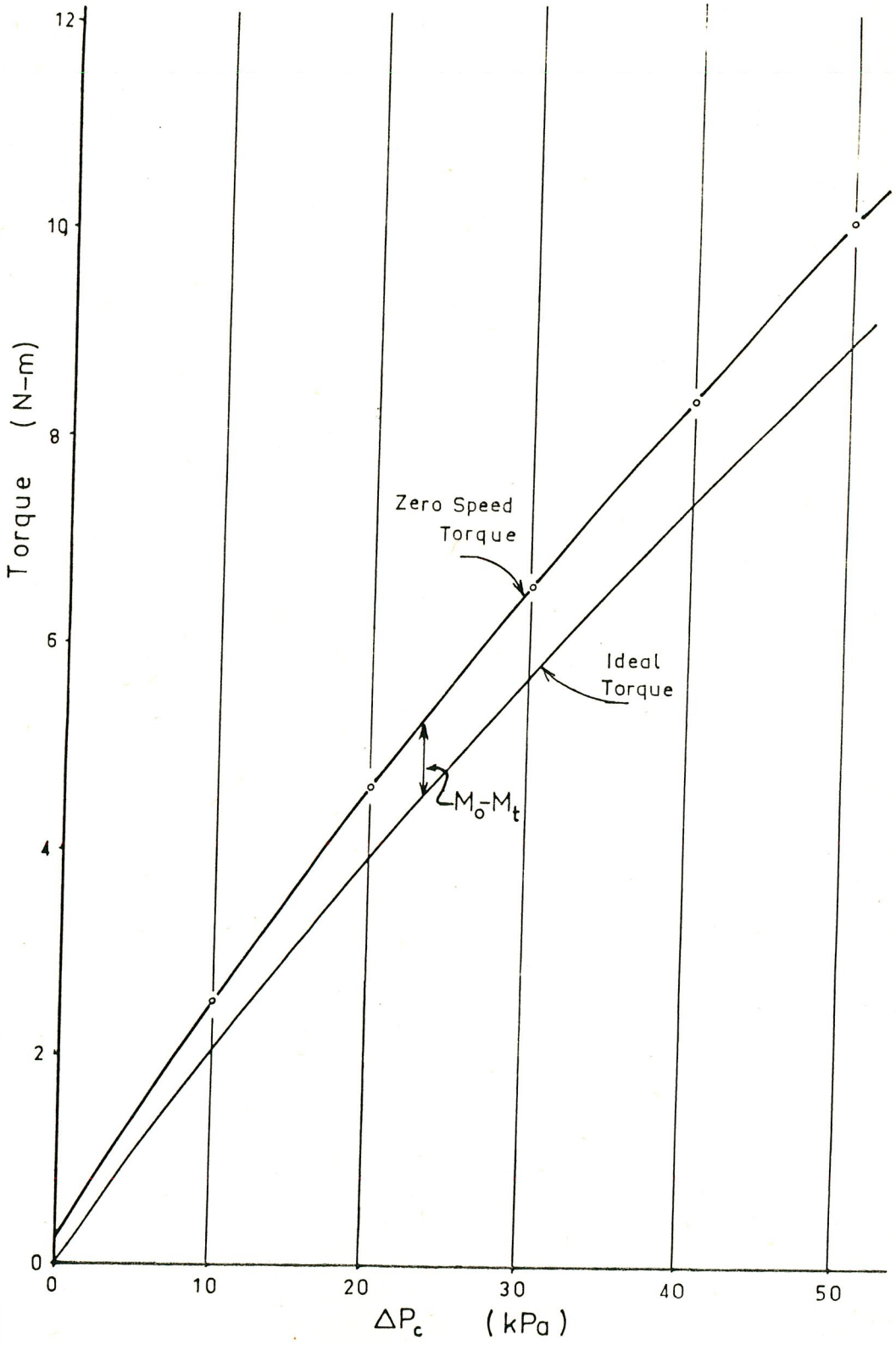

Fig.5. 9. Zero-Speed Torque versus Pressure Difference

The zero-speed torque values are taken from Fig.5.8 by extrapolating the lines to zero speed. Plot of the zero-speed torque versus pressure difference is shown in Fig.5.9 where the ideal torque is also plotted. The differences between these two curves were taken at constant pressure difference values and they are plotted against pressure differences as shown in Fig.5.10 . The slope of the line in Fig.5.10 is 0.017 which is also equal to C_f . The constant friction torque, M_{cc} , is given by the intercept of the line shown in Fig.5.10 . Therefore :

$$C_f = 0.017 \quad N\text{-}m \ / \ kPa$$

and $$M_{cc} = 0.32 \quad N\text{-}m$$

The plots of the experimentally determined volumetric and overall efficiencies of the compressor are presented in Fig's 5.11, 5.12, 5.13 and 5.14 . From these figures it is seemed that the shape of the curves are as expected. The test results indicate that the maximum overall efficiency was 52 % .

From Fig.5.4 it was observed that the flowrate is very sensitive to the pressure differenceacross the ports. The reason for that behaviour is that the clearances may be large which causes too much internal leakage.

Within the scope of the surveyed literature no concise

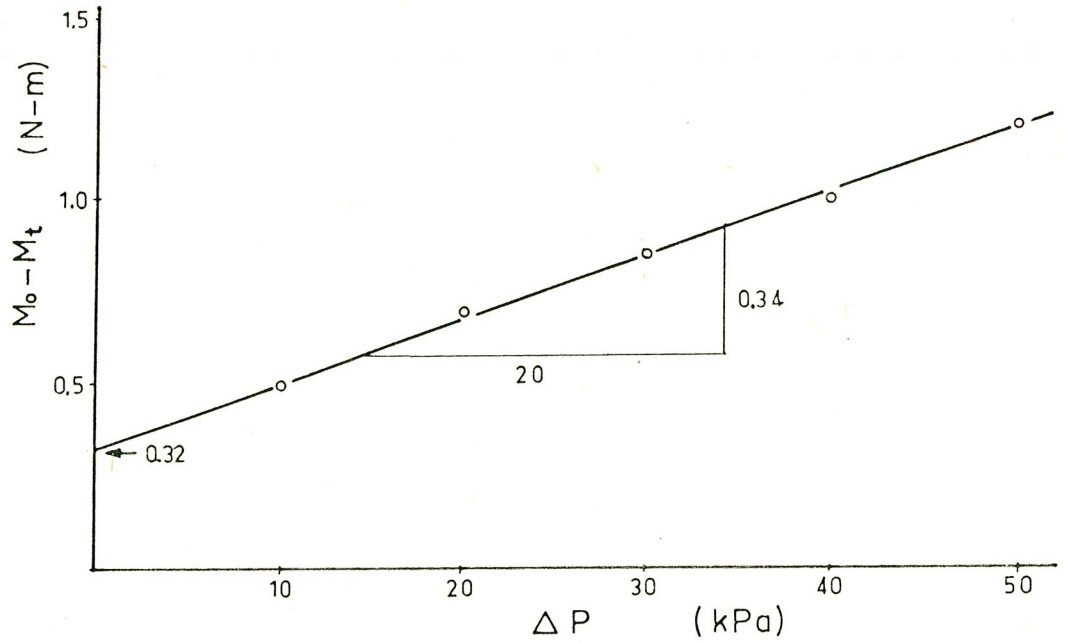

Fig.5.10. Plot of Difference between Zero-Speed Torque and Ideal Torque against Pressure Difference

theory and experimental data for C_s, C_r, C_f and M_{cc} could be found for gas handling positive displacement machinery. However, by the evaluation and estimation from the existing experimental data in the literature on positive displacement gas machinary, the coefficient C_f is found to be in the same order of magnitude as those for the tested compressor. It is not possible to compare the values of C_s and C_r of the tested compressor with those which can be estimated for other positive displacement machinery existing in the literature; because this comparison is only meaningfull when the performance of two geometrically similar machines are compared.

Friction torque, M_{cc}, is found to be 0.32 N-m, which

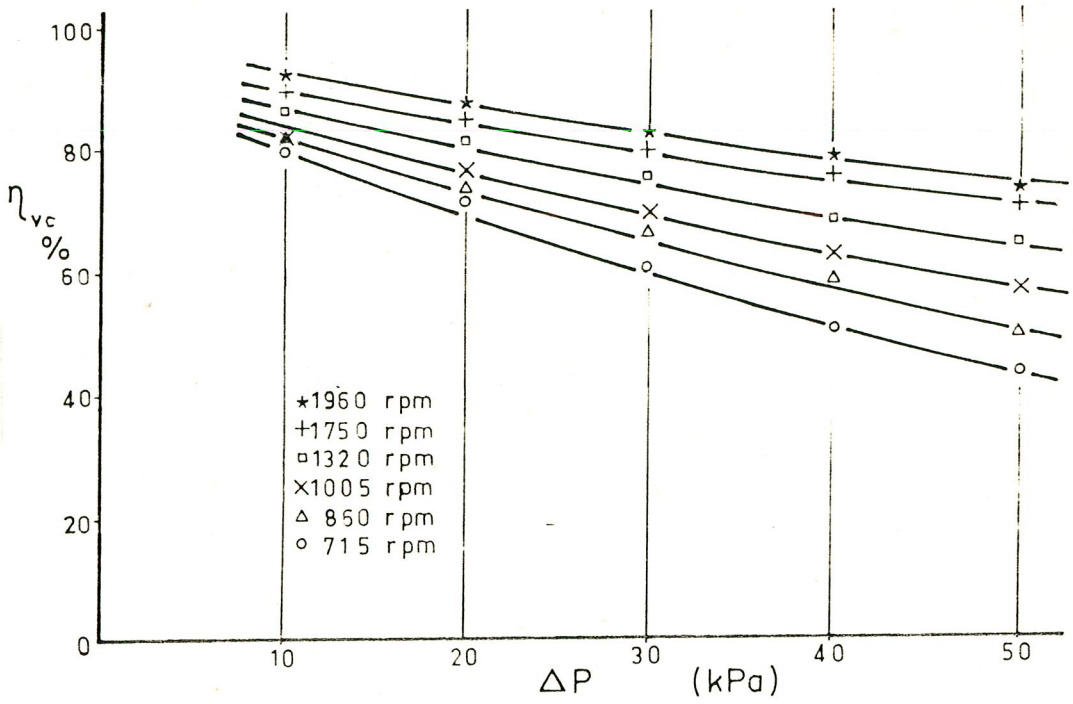

Fig.5.11. Plot of Volumetric Efficiency of the Compressor against Pressure Difference

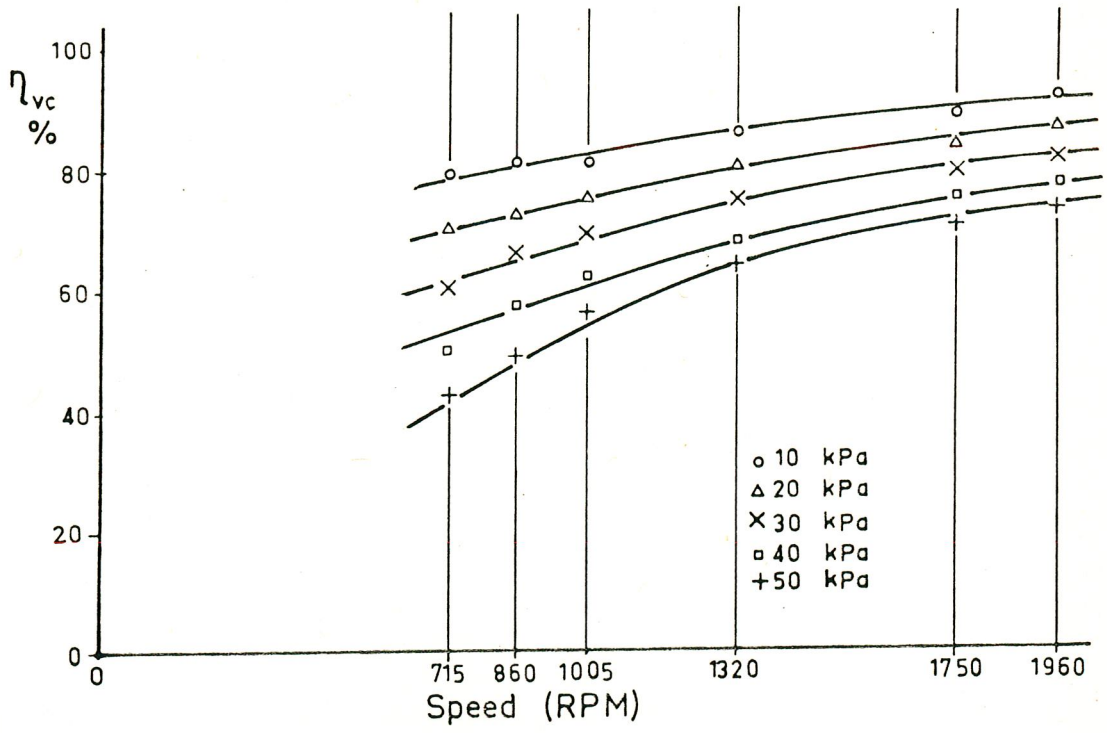

Fig.5.12. Plot of Volumetric Efficiency of the Compressor against Speed

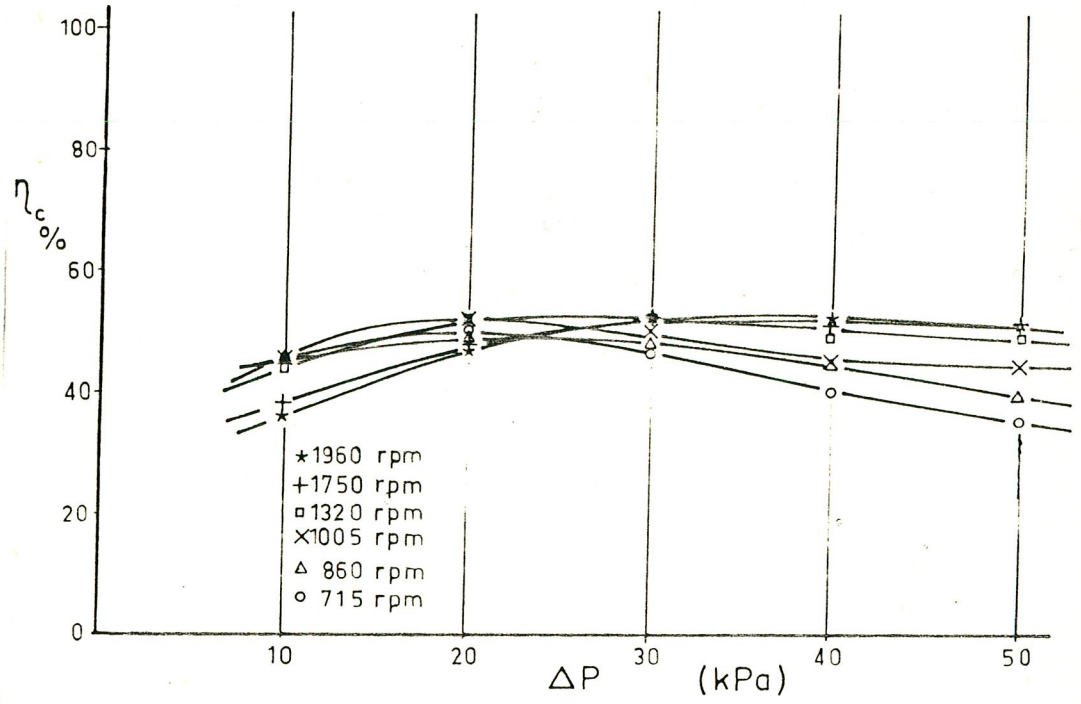

Fig.5.13. Plot of Overall Efficiency of the Compressor against Pressure Difference

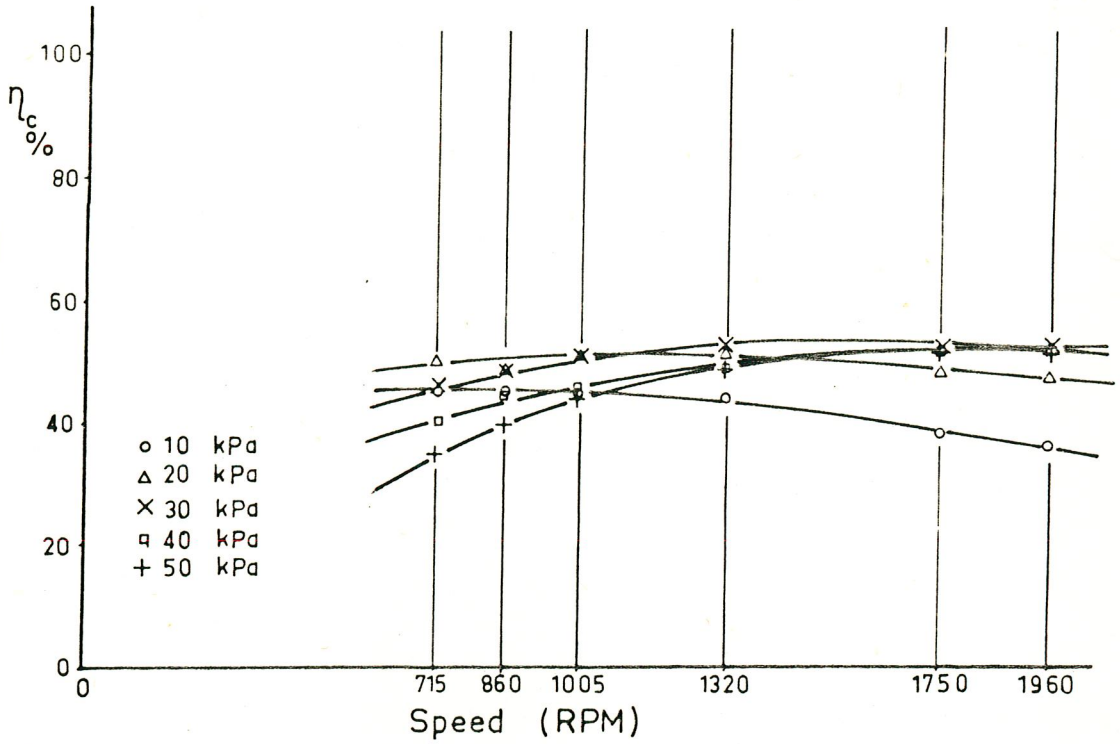

Fig.5.14. Plot of Overall Efficiency of the Compressor against Speed

is insignificiant when compared to the input torque requirements of the compressor. This indicates that the effect of M_{cc} in comparison to the other friction torque terms are small.

The volumetric and mechanical efficiencies of the compressor can also be calculated by using the performance coefficients. Since ;

$$\eta_{vc} = 1 - C_s \Delta P_c^{x} / (N / 60)$$

The exponent of the pressure difference term was determined from the experimental results as 0.63 . The volumetric efficiency at the point which corresponds to the experimentally determined maximum efficiency point becomes ;

$$\eta_{vc} = 1 - 0.64\ (30)^{0.63} / (1320/60) = 75\ \%$$

5.4

and the mechanical efficiency becomes (from Eqn's 3.60, 3.66 and 3.68)

$$\eta_{mc} = \frac{(26.9X1.32/2\pi)}{(26.9X1.32/2\pi) + (0.017X1.32X30) + (0.016X1.32X1320/60) + 0.32} = 75\ \%$$

5.5

The overall efficiency of the compressor car then be calculated as :

$$\eta_c = 0.75\ X\ 0.75 = 57\ \%$$

5.6

This value of efficiency is close enough to the experimentally determined value which is 52 % . This difference between the theoretical experimentally determined values of efficiency is probably due to the errors in determination of the performance coefficients and assumptions made during the theoretical analysis. Another reason may be the occurance of the residual gases in the compressor which was not taken into account in the theoretical analysis.

The assumptions made during the theoretical analysis and the contradictions to these assumptions may be stated as follows :

a) It was assumed that the breathing losses should be ignored when the tangential speed of the vanes were less than 30 m/s . However, the resistance coefficients of the flow at the ports, K_{ic} and K_{dc} may be large enough to increase the breathing losses to a level where they could no longer be considered as insignificiant in magnitude.

b) The leakage flowrate assumed that it remains unchanged with rotational speed of the rotor. But increasing the speed reduces the amount of fresh charge as a result of increase in the amount of residual gases.

c) It was assumed that the equation for volumetric efficiency, Eqn.3.45 , could be modified to the form of Eqn.3.46 . The modified equation may not always satisfy the

conditions imposed by Eqn.3.45 .

By using the experimentally determined performance coefficients, the performance graphs of the compressor and the expander can be plotted. In these performance graphs ; the flowrate, the torque and the efficiency curves are plotted against the pressure difference for various speeds. The performance graphs were plotted by using experimentally determined coefficients are shown in Fig.5.15 and Fig.5.16 for the compressor and the expander respectively. The theoretically determined values of torque, flowrate and efficiency for the compressor are nearly the same as the experimentally measured ones.

The results obtained from the experiments of the circulator were not expected. The aimed cooling capacity have not been reached. If Fig.5.17 is examined throughly, it seemed that, even though the circulator discharge air starts to cool after a certain speed, the torque input increases so much that this increase in torque prevents the increasing of C.O.P. of the system. It was also noticed that the pressure at the inlet of the expander and the flowrate increase almost linearly with increasing rotational speed.

The swept volume of the expander was defined as the vane number times the maximum chamber volume which corresponds to the volume of the chamber just before the discharge port is reached. Even though the free air

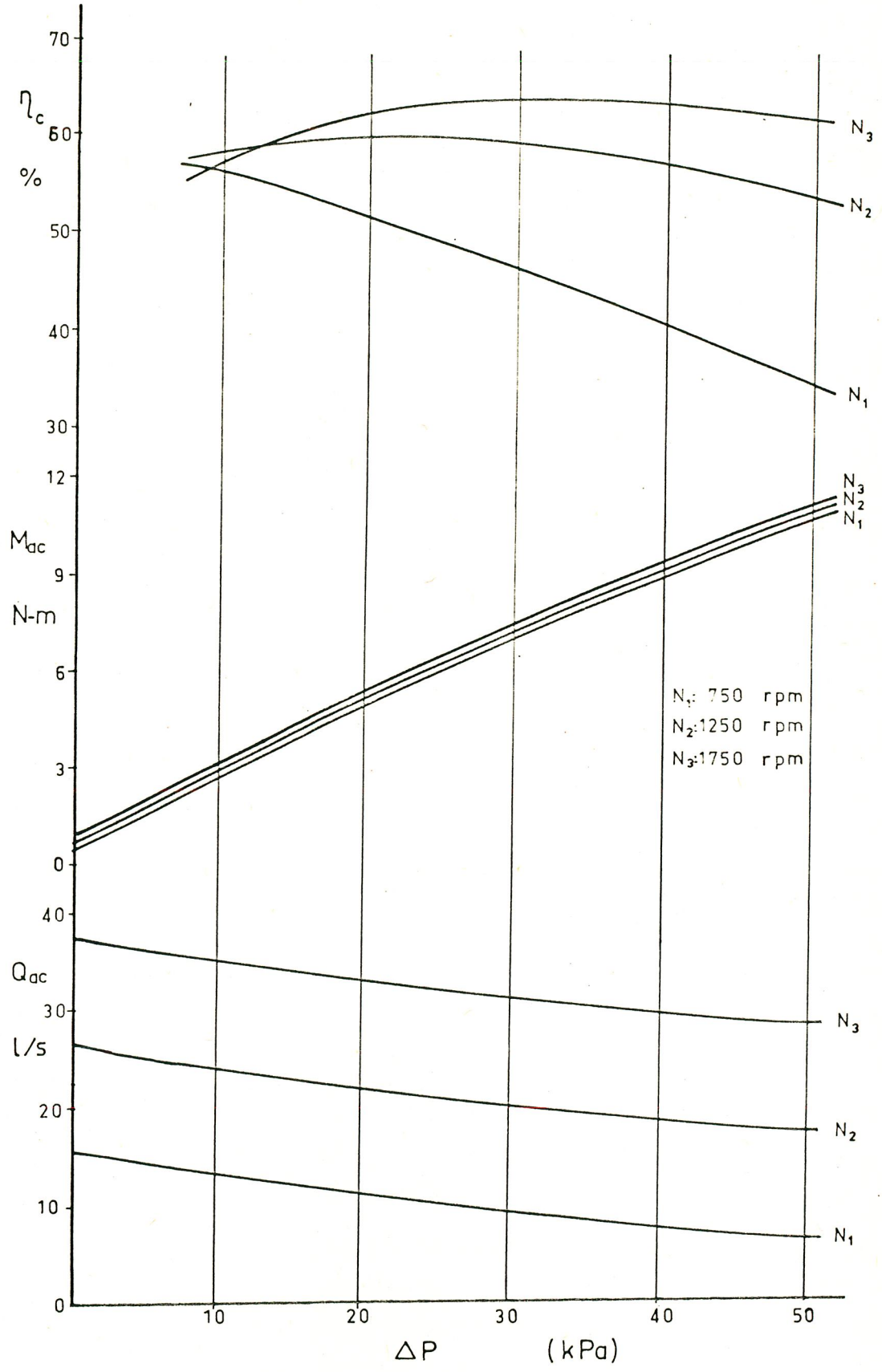

Fig.5.15. Performance Graph of the Compressor

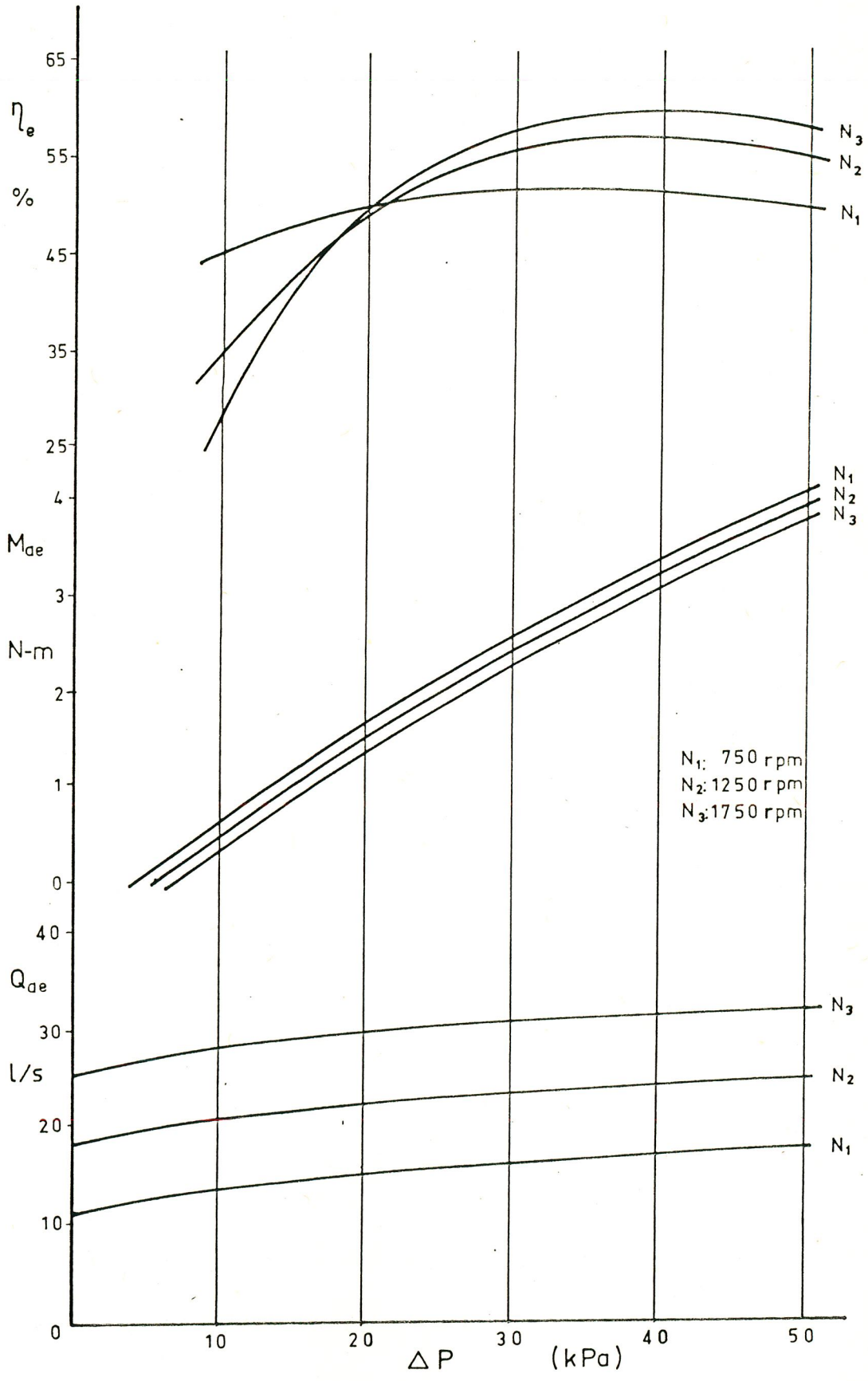

Fig.5.16. Performance Graph of the Expander

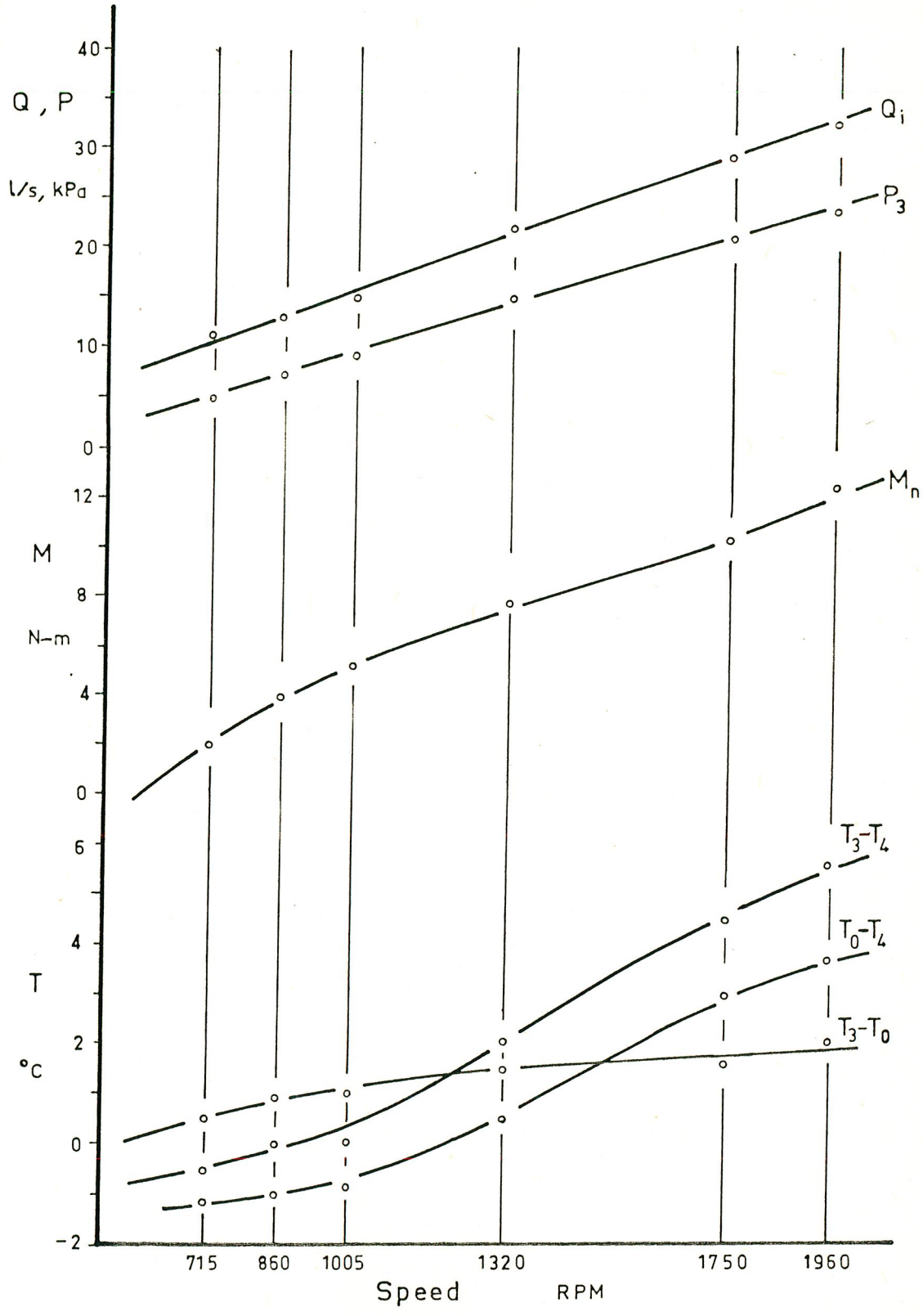

Fig.5.17. Performance Graph of the Circulator

volumetric flowrate of the expander was defined as the number of revolution per second times the above defined swept volume ; the free air volumetric flowrate passing through the expander depends on the inlet chamber volume and the inlet pressure of the expander.

If the internal pressure ratio of the expander and the ratio of the inlet to exhaust pressure of the expander were equal, there would be no difference between the above defined free air volumetric flowrates. Therefore, the swept volume of the expander changes with the change in the position of the inlet port and consequently the flowrate changes for a given rotational speed. An inrease in the expansion ratio decreases the swept volume or vice versa. The experimental data shown in Fig.5.17 were recorded while the compression and expansion ratios of the units were 1.3 .

Now, by using the calculated performance parameters of the compressor and the expander, the operation of the circulator can be predicted. As is shown in Fig.5.18 the measured values for the pressure drop across the heat exhanger were plotted against flowrate. This pressure drop was denoted by ΔP_{hx} which also includes the pressure losses in the pipes connected to the heat excharger.

In Fig.5.18 the pressure differences across the compressor and the expander were also plotted against the flowrate for a rotational speed of 1750 rpm. The calculated

ΔP - Q characteristics of the compressor and the expander are denoted by ΔP_c and ΔP_e respectively.

The equation of these curves are :

$$\Delta P_c = \left(\left(N / 60\ C_s \right) - \left(Q / V_{dc}\ C_s \right) \right)^{1/x} \qquad 5.7$$

$$= \left(\left(1750 / 60 \times 0.64 \right) - \left(Q / 1.32 \times 0.64 \right) \right)^{1/0.63}$$

$$\Delta P_e = \left(\left(N / 60\ C_s \right) + \left(Q / V_{de}\ C_s \right) \right)^2 \qquad 5.8$$

$$\left(\left(1750 / 60 \times 0.64 \right) + \left(Q / 0.87 \times 0.64 \right) \right)^2$$

$$\Delta P_{hx} = k\ Q^2 = 0.005\ Q^2 \qquad 5.9$$

The constants in the above equations were determined from experimental results.

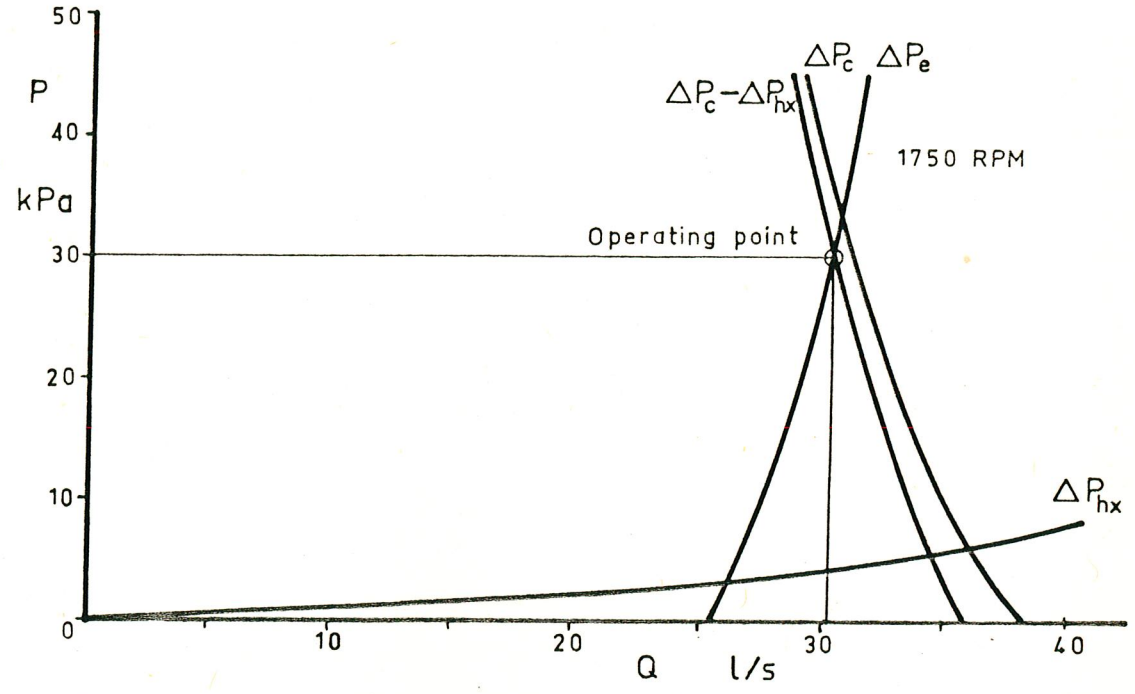

Fig.5.18. Operating Characteristics of the System

The pressure at the inlet of the expander is equal to the pressure supplied by the compressor minus the pressure loss in the heat exchanger and the pipes. Thus a plot of $\Delta P_c - \Delta P_{hx}$ is also drawn in the same figure. Since there are no leakage losses in the pipes and in the heat exchanger the flowrates must be equal for the compressor and the expander. The intersection of ΔP_e curve with $\Delta P_c - \Delta P_{hx}$ curve gives the operating point of the system. The reduction in the swept volume of the expander results in shifting of ΔP_e curve to the left which moderately increases the operating pressure with a slight decrease in the flowrate.

The torque input of the compressor and the torque output of the expander for this operating point can be found from Fig.5.15 for the compressor as ;

$$M_{ac} = 7.8 \text{ N-m}$$

from Fig.5.16 for the expander, as ;

$$M_{ae} = 2.2 \text{ N-m}$$

The net torque input to the circulator is found as ,

$$M_n = M_{ac} - M_{ae} = 5.6 \text{ N-m} \qquad 5.10$$

which is different from corresponding experimentally measured value of net torque input.

In addition to the comments mentioned in the discussion of the experimental results of the compressor, there are certain reasons for explaining the difference between the experimentally measured and calculated performance of the circulator. These are :

a) The performance coefficients of the expander were assumed to be the same of those for the compressor. As it was mentioned in Appendix A in the evaluation of the performance coefficients, the leakage flowrate is very sensitive to the manufacturing tolerances and it changes with the cube of the height of clearances. Therefore, the assumed internal leakage flowrate for the expander may be quite different from the actual leakage flowrate.

b) The insignificiant amount of leakage flow from the compressor to the outer space was neglected, but it may be more probable to expect a leakage from the expander to the outer space. The expander has a bushing to allow the drive shaft to pass through the circulator, this may cause a certain amount of leakage.

c) The expander was designed to operate at pressure ratios of 1.4 to 2.0 . Such an expander inlet pressure to satisfy the 1.4 pressure ratio could never be reached. The reason for this is the leakage flow which greatly affected the pressure differences across the compressor and the expander. The pressure at the inlet of the expander could be

increased by decreasing its' swept volume. A slight decrease of the expander swept volume was possible by increasing the expansion ratio, but the increase in the expansion ratio was much higher than the increase in the inlet pressure of the expander. Thus the pressures in the intake and exhaust ports of the expander could never be acjusted. This pressure ratio mismatch prevents the efficient operation of the expander and thus in turn , causes a poor performance of the circulator.

d) The mesured gage pressures at the inlet of the expander which corresponds to the actual operating conditions were relatively small. Thus, the adverse effect of the pressure drop across the heat exchanger on the system performance becomes relatively large.

e) The measured maximum overall efficiency of the compressor was 52 % which was below the design assumption of 85 % . The calculated C.O.P. for the 52 % overall compressor efficiency and an assumed expander efficiency of 50 % is about 0.30 . This C.O.P. value is not adequate for an efficient operation of the circulator. However, measured C.O.P. is smaller than 0.30 which indicates that the expander efficiency is less than 50 % .

Of all the reasons mentioned above, the effects of the clearances on the performance of the compressor, of the expander and hence of the circulator are the most important

one. If the leakage losses are reduced a sharp increase in the performance of the units and consequently a significiant increase in C.O.P. of the air-conditioning system may be expected.

C H A P T E R S I X

CONCLUSIONS AND RECOMENDATIONS

In this work an unfamiliar type of construction was used to manufacture a positive displacement rotary vane type air compressor. Furthermore, by designing and coupling an expander to the compressor, the feasibility of the compressor-expander couple as an air concitioning unit was investigated.

In order to assist the design of the compressor and the expander, a new method for the prediction of the performance characteristics of the positive displacement gas machinery was developed. Even though the derived theory was proved satisfactory for the prediction of the performance characteristics of the compressor, the designed compressor gave a performance which is below the aimed goal for operation as a component of an air-conditioning unit. Similarly the designed expander was not suitable for the above mentioned purpose either.

The addition of the roller follower at the root of the

vanes significantly reduced the mechanical losses; however the prototype suffered from significant leakage losses. The leakage losses originated from excessive clearances which could be reduced by using better manufacturing techniques.

On the other hand, the addition of roller followers brings the need for extreme manufacturing tolerances while reducing the frictional power losses. The leakages, especially the internal leakage, are highly dependent upon the magnitude of the clearances which causes a sensitive variation of leakage flowrate with the pressure difference across the unit. Even though the prototype has a versatile design, the system did not meet the assumed operation range. The versatile design of the protype increase the shortcomings. The design for a variable pressure ratio operation resulted in the loss of accuracy in marufacturing of the cam which restricted the operation of the units at high speeds. The variable volume ratio design also increase the losses in the ports during the charging and exhausting of air.

It is also very important to manufacture the surfaces, which is rubbing to each other, as smooth as possible. In the machining of the prototype parts this requirement could not be met accurately especially for the parts manufactured from non-metallic materials.

The method of determination of the performance

coefficients for the positive displacement gas machinery is a new concept. If the values of these coefficients were available for similar types of machinery, more realistic assumptions could be made in the design of the units.

It was observed that, if the design were carried out for a certain speed and pressure with some additional information about the performance coefficients the prototype may operate satisfactorily. The most important achievement of this work is that the necessary theoretical and experimental information on performance coefficients are given.

The aim of the further work on the compressor and the expander should be concentrated on recucing the leakage losses and increasing the rotational speed. It is belived that, in accordance with the results of this work, a new prototype can function properly if more appropriate materials are used, such as carbon vanes with a metal rotor providing that they are produced with good manufacturing tolerances and good surface finish.

LIST OF REFERENCES

1) ALAKÖK Nejat , ' Design , Construction and Testing of a Test Set-Up for Evaluating Performance of Hydraulic Pumps ', M.S. Thesis ,1979 .

2) ASHRAE Handbook of Fundamentals , ASHRAE Inc.NYC, 1972 .

3) BAMYACIOGLU Ahmet,'A new Vane-Type Positive Displacement Pump', M.S. Thesis , 1975 .

4) CLAUS F.J.,' Solid Lubricants & Self Lubricating Solids' Academic Press. N.Y. 1972

5) COOPER K.W.,SUMNER L.E. ' A Parametric study of an Open Air - Cycle Air - Conditioner using moist air thermodynamics ' ASHRAE Vol.78/2, No 2499 .

6) ECKER A.L.,EDWARDS T.C.,WARD K.' A Tabular Data Boundary State Analysis of the Edward Cycle' ASHRAE Vol.78/2 No 2501 .

7) EDWARDS T.C. ' A new Air-Conditioning , Refrigerating and Heat Pump Cycle ' ASHRAE Vol.78/2, No 2500 .

8) FREDERIC H.R., STAN W. ' Comfort Criteria for Air-Conditioned Automotive Vehicles' SAE paper 790122

9) KARASSIK, KRUTZSCH, FRASER, MESSINA, Pump Handbook

LIST OF REFERENCES (CONT.)

10) LINDSEY E.F. ' Air-Conditioning without a Refrigerant' Popular Science , Agust 1973 60-1

11) ONAT Kemal , ' Soğutma Makinaları ' (Ders Notları)

12) PEASE D.A. ' Basic Fluid Power ' Prentice Hall Inc. 1967

13) REAY D.A. ' Heat Pumps ' Pergamon Press, Oxford, 1979 .

14) ROBINSON C.S., ECKARD S.E. ' Multi-vane Expander , by adding Power,can improve the Fuel economy of Long Haul Diesel Truck', SAE paper 780689 ,1978 .

15) ROTHBART H.A. ' Cams ' John Wiley , 1966 .

16) SCHEEL L.F.' Gas Machinary ' Golf Publishing Company1972

17) STIESS W. ' Pumpen Atlas I '

18) TOSCANO, HARVEY,ERICSON 'Research and Development of Air Cycle Heat-Pump Water Heater ' ASHRAE Vol.82/2 No 4

19) VAN WYLEN , SONNTAG , ' Fundementals of Classical Thermodyramics ', John Wiley, 1973

20) YEAPLE , ' Hydraulic and Pneumatic Power and Control' Mc-Graw Hill , 1973 .

A P P E N D I C E S

A P P E N D I X A

LEAKAGE ANALYSIS

A.1. Definition of Losses

If all of the volumetric flowrates are transformed to flow rate under standart pressure and temperature, namely the free air flow, the volumetric flow rates can be expressed as:

$$Q_{ac} = Q_{tc} - Q_{ic} - Q_{lc} \qquad A.1$$

for the compressor and ,

$$Q_{ae} = Q_{te} + Q_{ie} + Q_{le} \qquad A.2$$

for the expander,

where Q_{ac} :actual free air delivery of the compressor

Q_{ae} :actual free air supplied to the expander

Q_{tc} :ideal free air delivery of the compressor, which is a function of its physical dimensions , its shaft speed, and the volume swept by the vanes.

Q_{te} : ideal free air supplied to the expander, which is a function of its physical dimensions, its shaft speed and the swept volume.

Q_{ic} : internal leakage flow in the compressor, which is related to the pressure difference between the inlet and outlet of the compressor.

Q_{ie} : internal leakage flow in the expander, which is also related to the pressure difference between the inlet and outlet of the expander.

Q_{lc} : leakage flow from sealings of the compressor to the atmosphere.

Q_{le} : leakage flow from sealings of the expander to the atmosphere.

The slip efficiency of the compressor can be defined as :

$$\eta_{sc} = \frac{\text{actual flow}}{\text{ideal flow}} = \frac{Q_{ac}}{Q_{tc}} = \frac{Q_{tc} - Q_{ic} - Q_{lc}}{Q_{tc}} \qquad A.3$$

The slip efficiency of the expander becomes

$$\eta_{se} = \frac{\text{ideal flow}}{\text{actual supplied fluid flow}} = \frac{Q_{te}}{Q_{ae}} = \frac{Q_{te}}{Q_{te} + Q_{ie} + Q_{le}} \qquad A.4$$

The internal leakage that takes place in a positive

displacement machinery is caused primarily by the flow through the small clearances between the various parts that seperate high-pressure and low-pressure regions. The small clearances are often referred to as the capillary passages. Most of these leakage paths are essentially two flat parallel plates with the flow occuring through the clearance. It is, therefore, reasonable to apply the fundemental relationships for flow between two parallel flat plates. If the force balance is written for a fluid element in a two dimensional flow where the relative motion of the surface is neglected, the pressure-induced flow rate becomes, (see Fig.A.1)) (1)

$$Q = (h\ w\ \Delta P)/(12\ L\mu)\ X\ 10^{-3} \qquad A.8$$

where Q : leakage flow between two parallel flat plates for zero pressure gradient in the w direction in l/s.

ΔP : pressure difference in Pa.

w : width of the clearance in m.

h : thickness of the clearance in m.

μ : average viscosity of the fluid in cP.

If a series of geometrically similar units is considered, the physical dimensions of any one unit are, by definition, proportional to a characteritic dimension ,Y.

The introduction of an internal leakage coefficient,

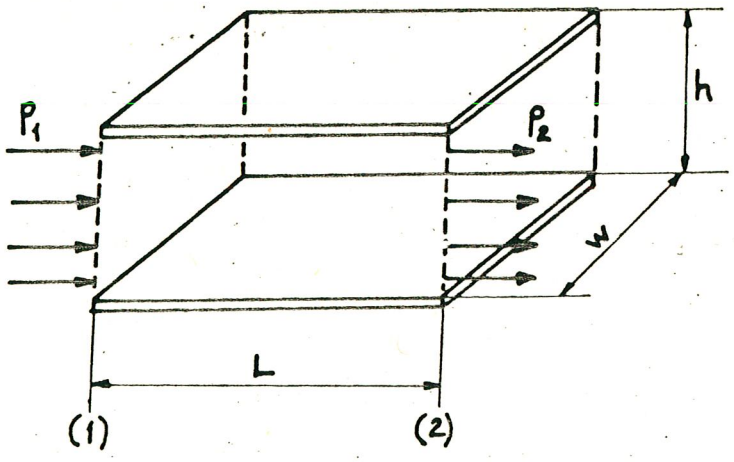

Fig.A. 1. Capillary flow between Flat Parallel Plates

C_i, has been found convenient. It is defined in such a way that the characteristic expression for the capillary flow becomes;

$$Q_i = C_i \, V_d \, \Delta P \qquad \text{A.6}$$

where the coefficient, C_i, is given by

$$C_i = (k/\mu) (h^3 / V_d) \qquad \text{A.7}$$

V_d is the displacement per revolution of the unit and k is a constant. Thus, the displacement V_d is proportional to the cube of the characteristic dimension. By assuming the viscosity remains constant, the internal leakage coefficient becomes;

$$C_i = k' (h / Y)^3 \qquad \text{A.8}$$

Thus, the internal leakage coefficient varies as the

cube of the clearance ratio and can be expected to be very sensitive to manufacturing tolerances. It should be noted that the derivation of the leakage flow and the subsequent definition of the internal leakage coefficient are based on one leakage path. In actual units several different paths exist , each having different dimensions but basically similar characteristics. Therefore, all these paths can be combined into one composite or equivalent path without detraching from the generality of the discussion.

A question may be raised as to the effect of the unit size on the slip coefficient. It appears somewhat farfetched to assume that clearances will be directly proportional to the characteristic dimension. It would be more realistic to state that the clearances will not change with the same percentage as the changes in the unit size. Therefore it seems reasonable that the larger machinery should exhibit consistently lower slip coefficient than smaller machinery.

Since the leakage flow, Q_l, from the sealings to the outer space of the unit has the same characteristics as the viscous internal leakage, it can be expressed by the same theory. The leakage flow from sealings and bushings is proportional to the cube of the clearances and pressure differences. Q_l which is equal to the difference between

inlet and discharge flow rate, becomes;

$$Q_\ell = C_\ell \; V_d \; (P_H - P_o) \qquad \text{A. 9}$$

where $C_\ell = (k / u)\,(h / Y)^3$ A.10

and the P_H is the highest pressure in the unit anc P_o is the athmospheric pressure. In fact, for a well sealed machinery Q_ℓ is very low when compared to Q_i . If the sealing were made satisfactorily the leakage to the outer space can be neglected for low working pressures (less than 3 bar). For the positive displacement machines having one port at zero gage pressure (athmosphere), $(P_H - P_o)$ that is in Eqn.A.9 , can be assumed equal to ΔP that is in Eqn.A.6 . Thus the terms Q_ℓ and Q_i can be combined as,

$$Q_\ell + Q_i = (C_\ell + C_i)\; V_d \; \Delta P \qquad \text{A.11}$$

or, $$Q_\ell + Q_i = C_S \; V_d \; \Delta P \qquad \text{A.12}$$

where $C_S = C_i + C_\ell$ A.13

If the ideal flow is given as :

$$Q_t = V_d \; (N / 60) \qquad \text{A.14}$$

the expression for the delivery of a compressor then becomes

$$Q_{ac} = N \; V_{dc} / 60 - C_S \; V_{dc} \; \Delta P_c \qquad \text{A.15}$$

and for the expander,

$$Q_{ae} = N V_{de}/60 + C'_s V_{de} \triangle P_e \qquad A.16$$

where the prime denotes the values in the expander.

It should be noted that, this expression is based on the assumption that clearances between bearing surfaces remain constant. But in some units the clearances may vary with pressure, speed, temperature and in some cases with position such as that in the vane type machinery. In the vane type machinery, the clearances between the tip of the vane and the casing may vary due to manufacturing and due to variation of contact angle between blade and casing.

These variations are often significiant because C is extremely sensitive to clearances. A further deviation from ideal leakage flow equations results from the occurence of some orifice type leakage in certain gear and vane type machinery. The leakage flow across the vane tips and gear teeth can be expected to vary roughly as the square root of the pressure difference because the length to thickness ratio of these clearance spaces is small, (1) (16) .

So , Eqn's A.15 and A.16 are modified and thus these equations becomes :

$$Q_{ac} = N\ V_{dc}/60 - C_s V_{dc} \Delta P_c^{0.5} \qquad A.17$$

$$Q_{ae} = N\ V_{de}/60 - C\ V_{de} \Delta P_e^{0.5} \qquad A.18$$

A.2. Derivation of Efficiency Equations

The efficiencies, previously defined, can now be derived with the aid of the pertinent dimensionless coefficient, namely C .

a) Slip efficiency of the compressor:

Since

$$\eta_{sc} = \frac{Q_{ac}}{Q_{tc}} = \frac{Q_{tc} - Q_{ic} - Q_{lc}}{Q_{tc}}$$

the slip efficiency of the compressor becomes,

$$\eta_{sc} = 1 - C_s \Delta P_c^{0.5} / (N/60) \qquad A.19$$

b) Slip Efficiency of the Expander:

Since

$$\eta_{se} = \frac{Q_{te}}{Q_{ae}} = \frac{Q_{te}}{Q_{te} + Q_{ie} + Q_{le}}$$

the slip efficiency of the expander becomes,

$$\eta_{se} = \frac{1}{1 + C_s \, \Delta P_e^{0.5} / (N/60)} \qquad A.20$$

As already noted , the slip coefficient is proportional to the cube of the clearance ratio, so the slip efficiency should be expected to be very sensitive to the clearances and it is also expected to be the same in geometrically similar machines, operating with fluids of same viscosity.

A P P E N D I X B

ANALYSIS AND GENERATION OF CAM

The equation of a circle which has a center on X axis is given by :

$$(x - e)^2 + y^2 = R^2 \qquad \text{B.1}$$

where e is the displacement from the origin and R is the radius. This circle can be represented by the following equation in polar coardinates ;

$$r = R (e \cos \phi + (1 - e^2 \sin^2 \phi)^{0.5}) \qquad \text{B.2}$$

In sliding vane type machinery the tip of the vanes follow the contour of the casing. This track is a circle but center of the circle does not coincide with the axis of the rotating shaft. Such an eccentric circle can be defined by equation B.2 . Since the vanes in the rotor, slides in the direction which is perpendicular to the

shaft and since the position of the tip of the vanes are known, the position of the root of the blades at a given angle can be written as,

$$r_o = r - l = R\,(e \cos \phi + (1 - e^2 \sin^2 \phi)^{0.5} - l / R) \qquad B.3$$

where l is the distance between the tip and the root of the vanes and must be greater than 2e. In a similar way the path for the mass center of a vane is:

$$r_g = r - l/2 = R\,(e \cos \phi + (1 - e^2 \sin^2 \phi) - l/2R) \qquad B.4$$

The centerline of the cam which will be manufactured must follow the Eqn.B.3 .

To analyse the forces acting on the roller follower, we must determine the acceleration and pulse ecuation by differentiating the ecuation B.3 . Since ,

$$w = d\phi / d t \qquad B.5$$

$$\alpha = d w / d t = 0 \qquad B.6$$

the velocity equation is

$$v = \dot{r} = d r / d t = w\, d r / d \phi \qquad B.7$$

and acceleration is

$$a = \ddot{r} = d^2r / d t^2 = w^2 \, d^2r / d \phi^2 \qquad B.8$$

and finally the pulse;

$$p = \dddot{r} = d^3r / d t^3 = w^3 \, d^3r / d \phi^3 \qquad B.9$$

where v is velocity, a is acceleration and p is the pulse in radial direction.

The differentiation of r with respect to ϕ results complicated equations. Therefore, the variations of position, velocity, acceleration and pulse with the angular position are given in graphical forms. These were calculated and plotted by using a FORTRAN program. These are shown in Fig's B.2 to B.6 .

The net force acting on the followers which keeps them in contact with the contour of the cam is equal to the centrifugal force minus the inertial force, or

$$F_n = w^2 r_g m - w^2 \ddot{r} m = m w^2 (r_g - \ddot{r}) = m a_n \qquad B.10$$

To prevent the cross-over shock, the follower must be held in contact with the cam at all times. The cross over-shock exist in positive drive cams when the contact of the follower shifts from one side to the other. It occurs at a point where the acceleration of the follower changes from positive to negative or vice versa. This is

also the point of maximum follower velocity. Fig.8.6 shows the net acceleration in a graphical representation, and from this figure it is seen that the cross-over shock does not occur.

The accuracy of the cam surface determines the life of the roller followers and the clearance on the tip of the vanes. Since the acceleration is the second derivative of displacement, the large magnification of the error in the cam surface will manifest itself on the acceleration curve. Also we know that the acceleration curve is proportional to the force acting on the system. Thus the follower feels the acceleration disturbances plus the dynamic disturbances. To obtain a cam with a good acceleration curve and good surface quality , a precise cam must be manufactured. With the present methods of fabrication existing in our machine shop, the precision of the cam was limited by the accuracy of forming or cutting contour. Using the increment cutting method with a number of machine setting does not satisfy our requirements as well as a continuous generation method. A precise cam may be achived only with a tracing method , or by a using CNC machine. If the only requirement were the profile of the centerline, it could be obtained with a copy unit on a lathe, with a high degree of accuracy. Since the contour of the cam should be followed by the roller follower which

is the bearing at the root of the vane, the profile of the cam contour must be produced. The distance between the centerline and contour of the cam varies in the direction of the follower motion. This distance variation which is due to the variation of the angle between the casing and the vane, can be explained by referring to Fig.B.1 .

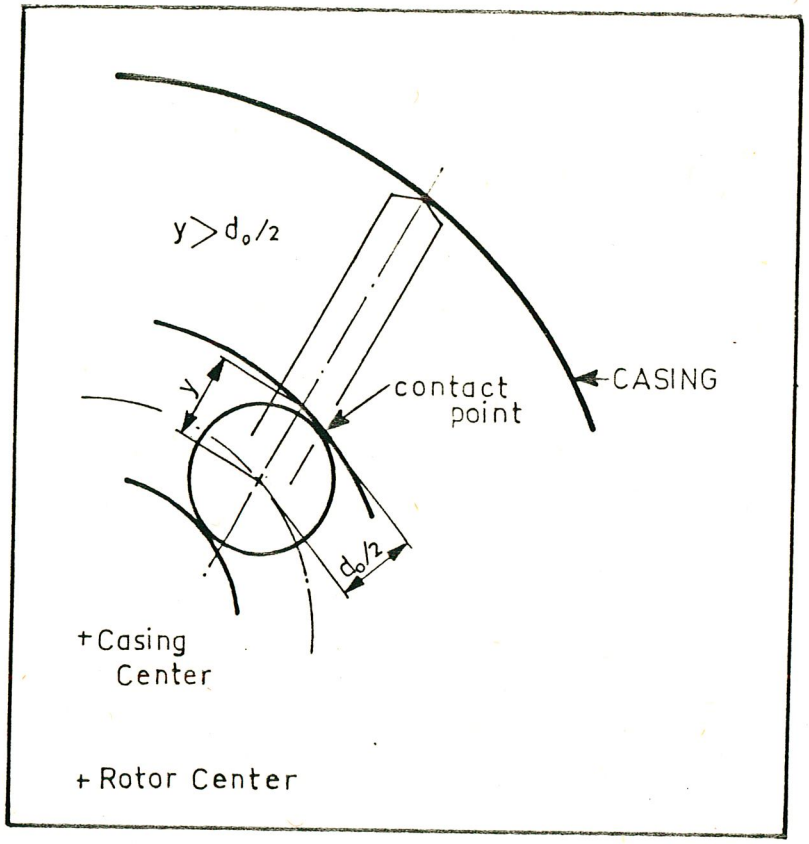

Fig.B. 1. Distance between the Centerline of the Cam and the Casing

Due to the above mentioned reason the cam profile can be obtained by using a cutter which has an equal diameter with the follower, and by moving the cutter on the centerline of the cam profile with an appropriate apparatus.

The path of the centerline of the cutter is formed by the points which are placed on a distance from the

casing in the radial direction. This distance is equal to the root-tip length of the vane. By using a copy unit on milling machine the distance between the outer surface of the cover and the cutter center can be held constant. Since the copy unit of the milling machine enables us to move the table in the vertical direction, the cutter kept a constant position and the working part was revolved. The rotation of the working part was satisfied by using the power feed motor of the machine. During this operation power feed motor is disengaged from the table and connected to the shaft of the working part via gears. At the beginning, the tracer of the copy unit was setted to the center of the cutter then raised 42.4 mm which is the distance between the center of the roller follower and the tip of the vane. After the above settings were made the working part was moved through the cutter then revolved. As the cover revolves on the eccentric center, the tracer picks up the height of the outer surface. The ascending motion of the outer surface is compensated by descending the table. This motion keeps the cutter center to the outer surface distance constant. The carving of the cam groove is completely done by repeating the above mentioned operations.

But unfortunately, during this machining operations, due to the sudden failure of main power suply, the

tracing stopped while the cutter goes on rotating due to its inertia, thus some imperfections on the cam surface were occured. This portion of the cams were than filled with welding and then machined again.

At later stages of the experimertal investigations the cams were smoothened with sand paper by using a crescent shaped tool in the milling machine.

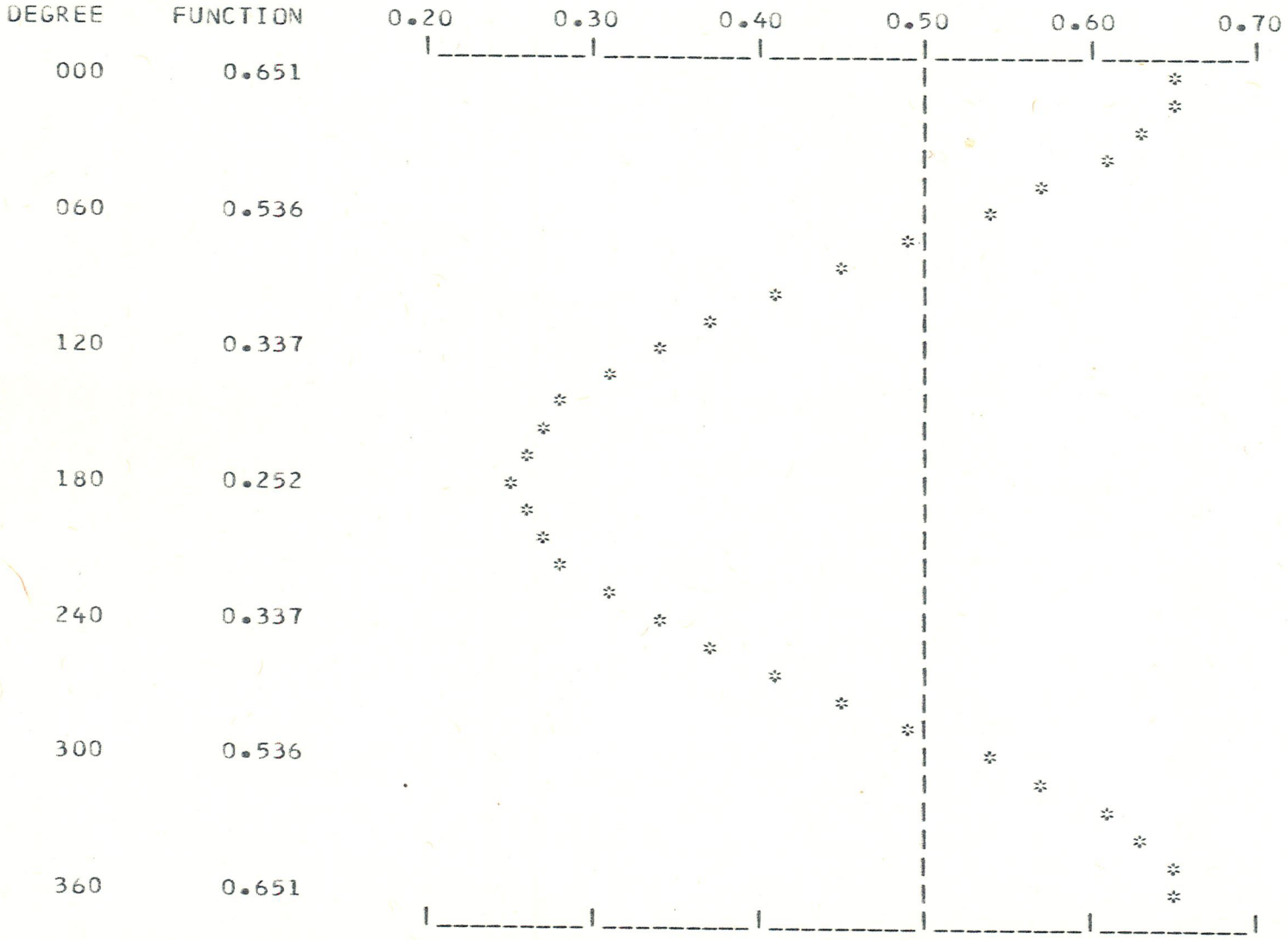

FIG.B.2. VARIATION OF RADIAL POSITION

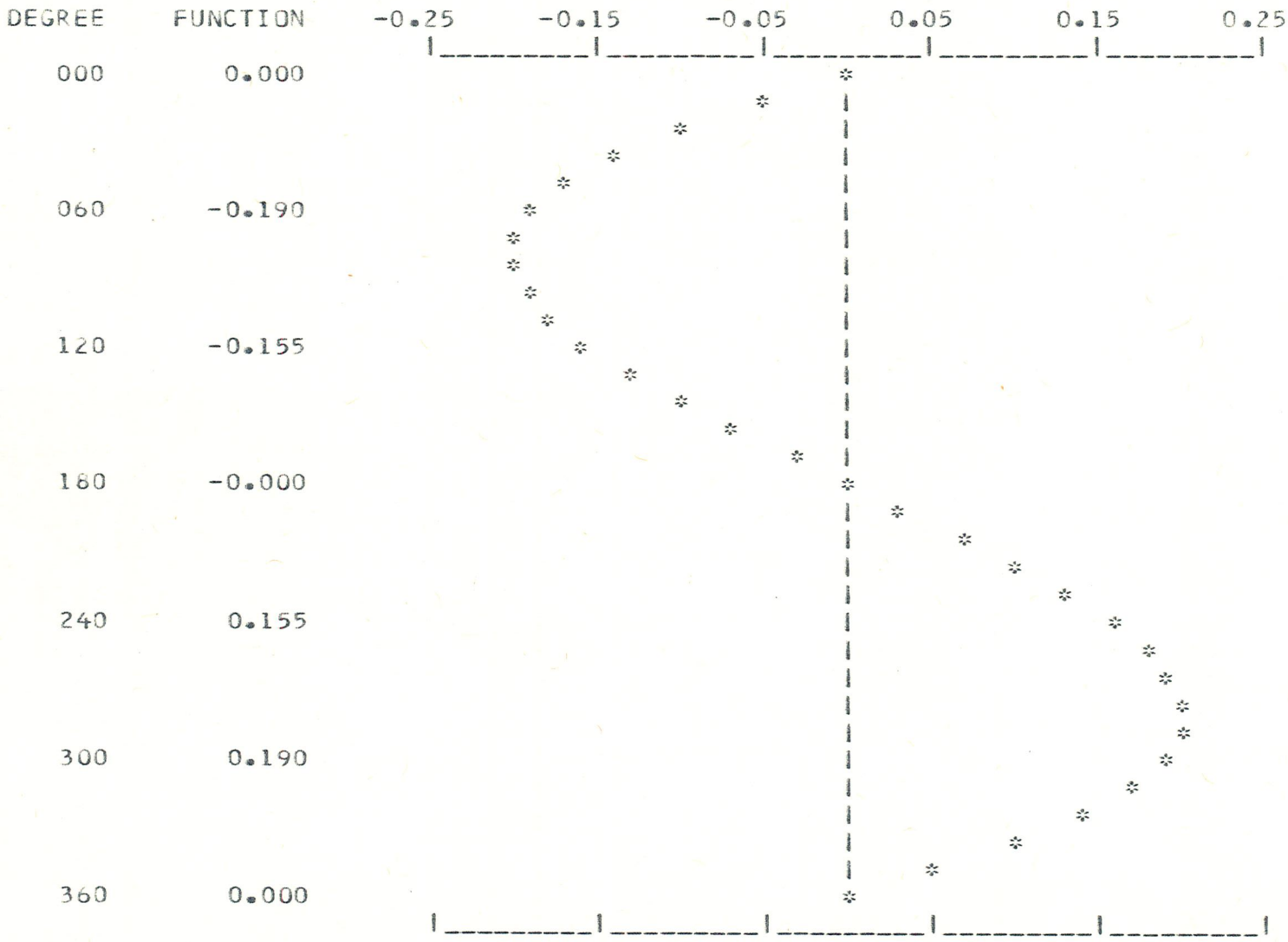

FIG.B.3. VARIATION OF RADIAL VELOCITY

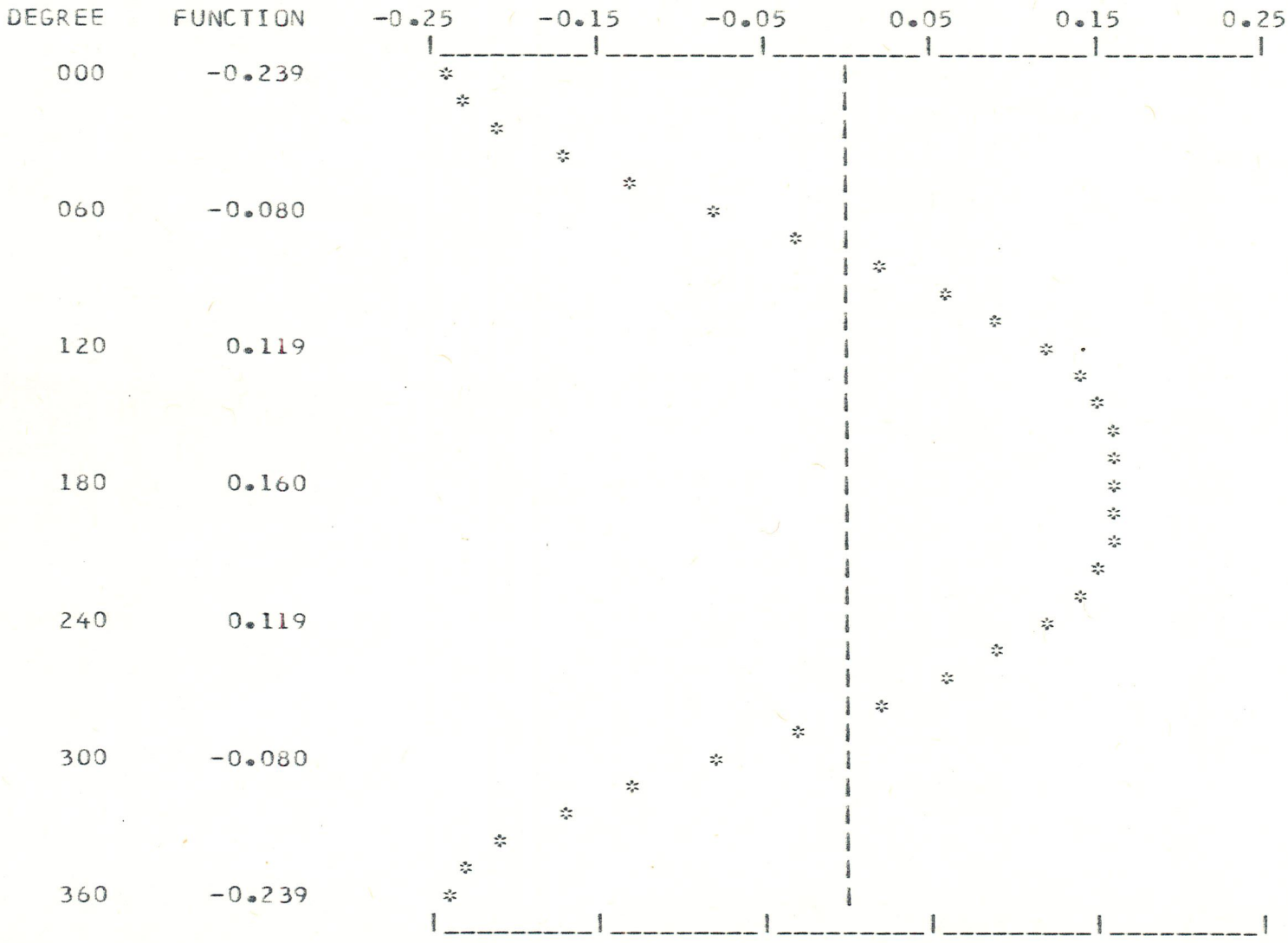

FIG.B.4. VARIATION OF RADIAL ACCELERATION

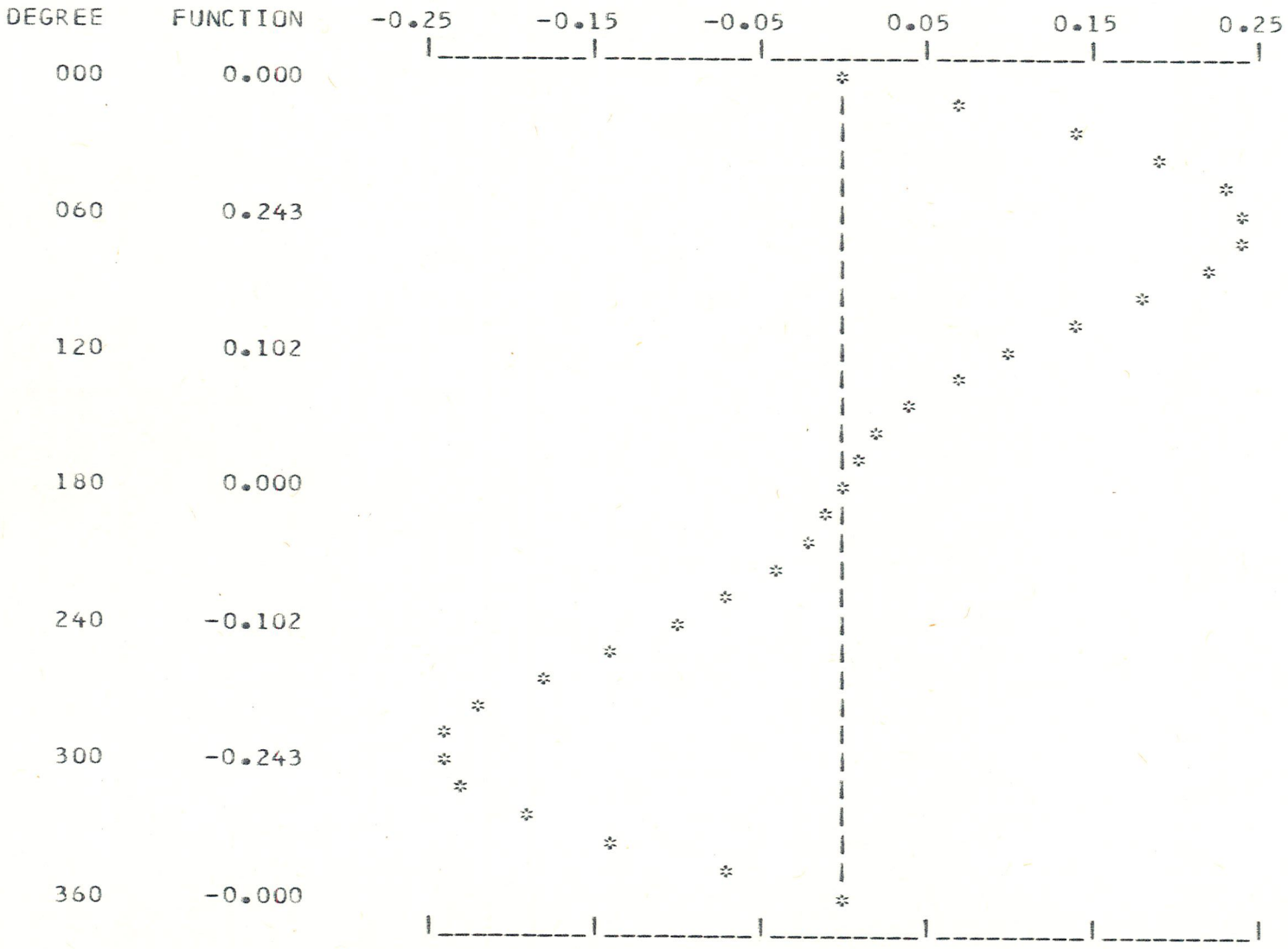

FIG.B.5. VARIATION OF RADIAL PULSE

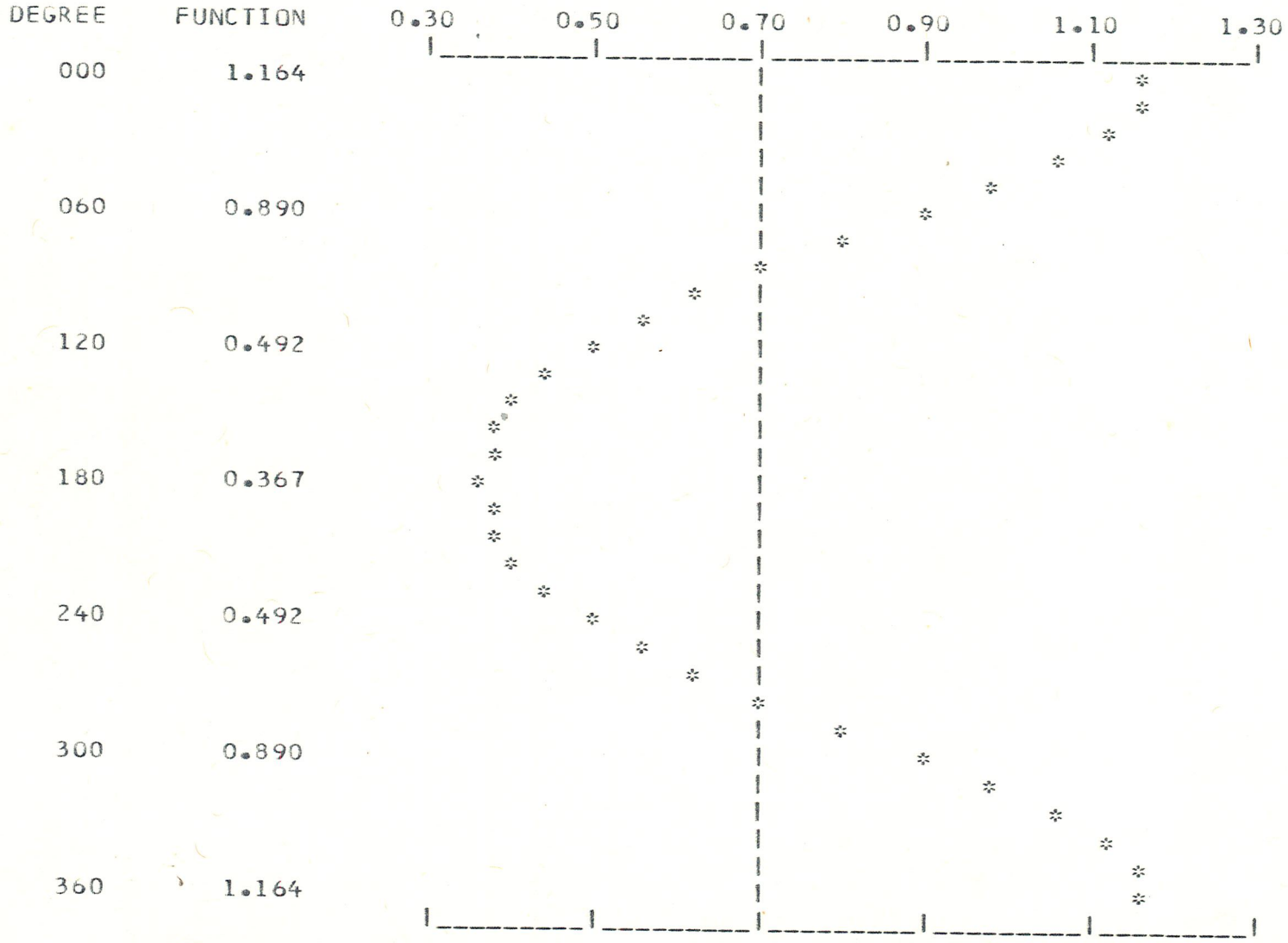

FIG.B.6. VARIATION OF NET ACCELERATION

A P P E N D I X C

SAMPLE CALCULATION

The parameters which are relavent in the determination of the performance characteristics of the compressor and the circulator were calculated from the experimental data as follows :

1) Inlet Pressure , P_1 ,

P_1 (mmHg) = Barometric Pressure (mmHg) -

Pressure Drop across the Nozzle (inches of wc)x 25.4/13.6

P_1 (Pa) = P_1 (mmHg) X 133.3 (absolute)

During the experiments the variation of the barometric pressure was between 682 - 688 mmHg and the pressure drop across the nozzle was about 1.5 inches of wc. Thus taking an average value of P as 91 kPa gave an error less than 0.8 % in the determination absolute inlet pressure.

2) Discharge Pressure, P_2 ,

P_2 (Pa) = P_2 (bar) X 101357 (gage)

3) Volume Flowrate, Q ,

Volume flowrate is found in cfm by using the calibration

curves of the nozzle supplied by the manufacturer.

$Q\ (l/s) = Q\ (cfm) \times 0.472$

4) Torque, M ,

Digital readout value is converted into N-m by,

$M\ (n\text{-}m) = \Omega \times 1.4128 \times 10$

5) Temperature, T ,

Milivolt output of the thermocouple is measured and converted to °C by using the calibration curve.

6) Density of Air, ρ_1 ,

Density of air at inlet is given by,

$\rho_1\ (kg/m\ ) = 0.4643 \times P_1\ (mmHg) / T\ (°K)$

or $\rho_1 (kg/m\ ) = 3.48 \times 10 \times P_1\ (Pa) / T\ (°K)$

7) Input Power, W_i ,

$W_i = 2\pi / 60 \times N \times M_n$

8) Output Power, W_o ,

$W_o = Q\ H\ g\ \rho_1 \times 10^{-3}$

where H is the adiabatic head in m. and calculated for air as follows :

$H = 102.2 \times T_1\ (°K) \times ((P_2 / P_1)^{\frac{k-1}{k}} - 1)$

and $H\ g\ \rho_1 = 3.48 \times P_1\ (Pa) \times ((P_2 / P_1)^{\frac{k-1}{k}} - 1)$

The values of term ($H\ g\ \rho_1$) for different outlet pressures, and 91 kPa inlet pressure are tabulated below.

ΔP_c (kPa)	$\Delta P' = H\ g\ \rho_1$ (kPa)
10	9.6
20	18.5
30	26.9
40	34.8
50	42.3

9) Overall Efficiency , η_c ,

Overall efficiency was found by,

$$\eta_c = \frac{\Delta P' \text{ (kPa)} \times Q \text{ (l/s)} \times 9.55}{N \text{ (rpm)} \times M \text{ (N-m)}}$$

10) Volumetric Efficiency, ,

$$\eta_{vc} = Q \times 60 / (V_{dc} \times N)$$

A P P E N D I X D

VARIATION OF VOLUME INSIDE THE UNITS

VANE NUMBER = 4.
SWEPT VOLUME = 1.321

DEGREE	VOL. RATIO
45.0	1.000
60.0	1.022
75.0	1.091
90.0	1.218
105.0	1.424
120.0	1.746
135.0	2.257

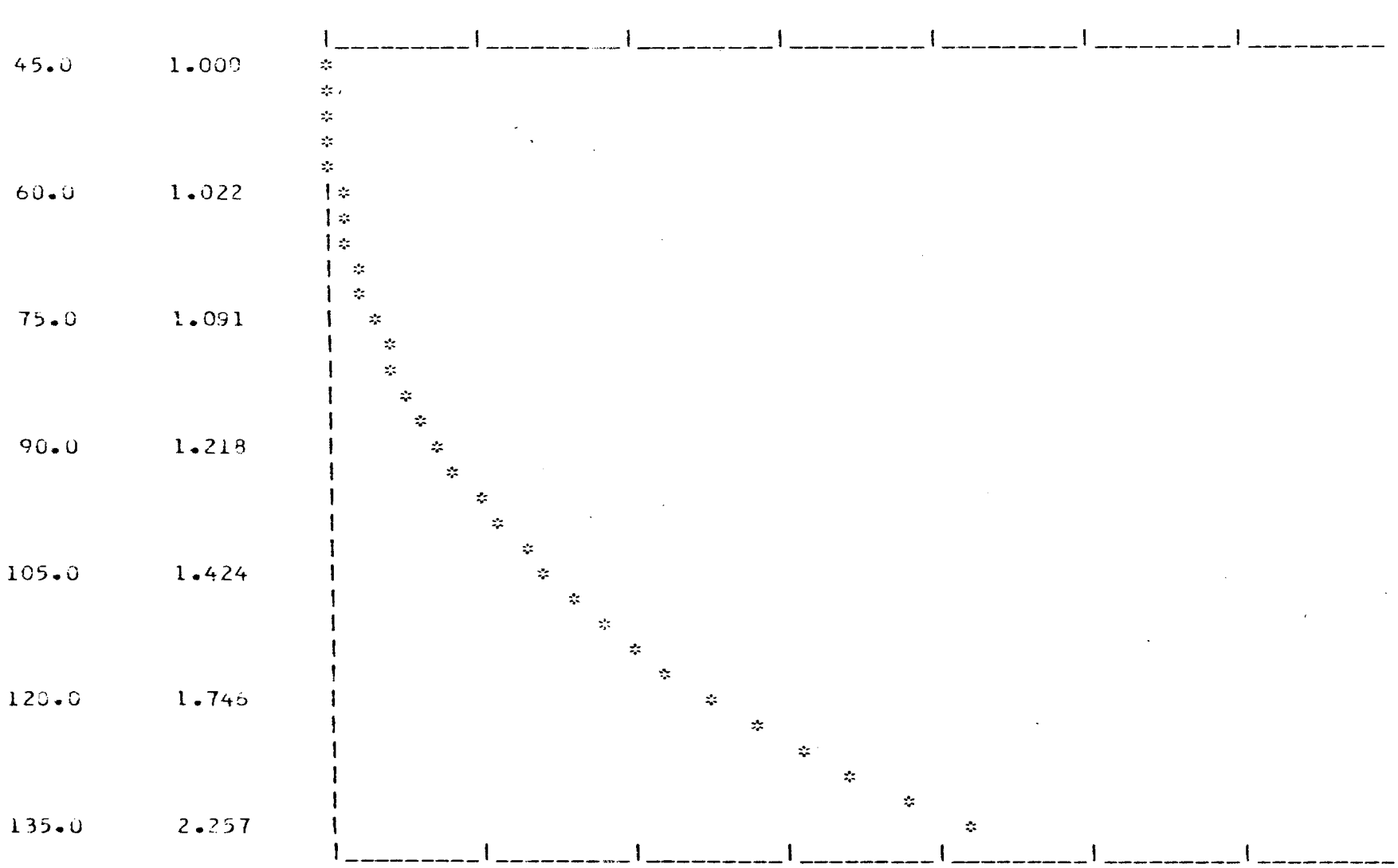

MAXIMUM VOLUME RATIO = 2.257

VANE NUMBER = 5.
SWEPT VOLUME = 1.332

DEGREE	VOL. RATIO
36.0	1.000
54.0	1.034
72.0	1.142
90.0	1.350
108.0	1.714
126.0	2.351
144.0	3.532

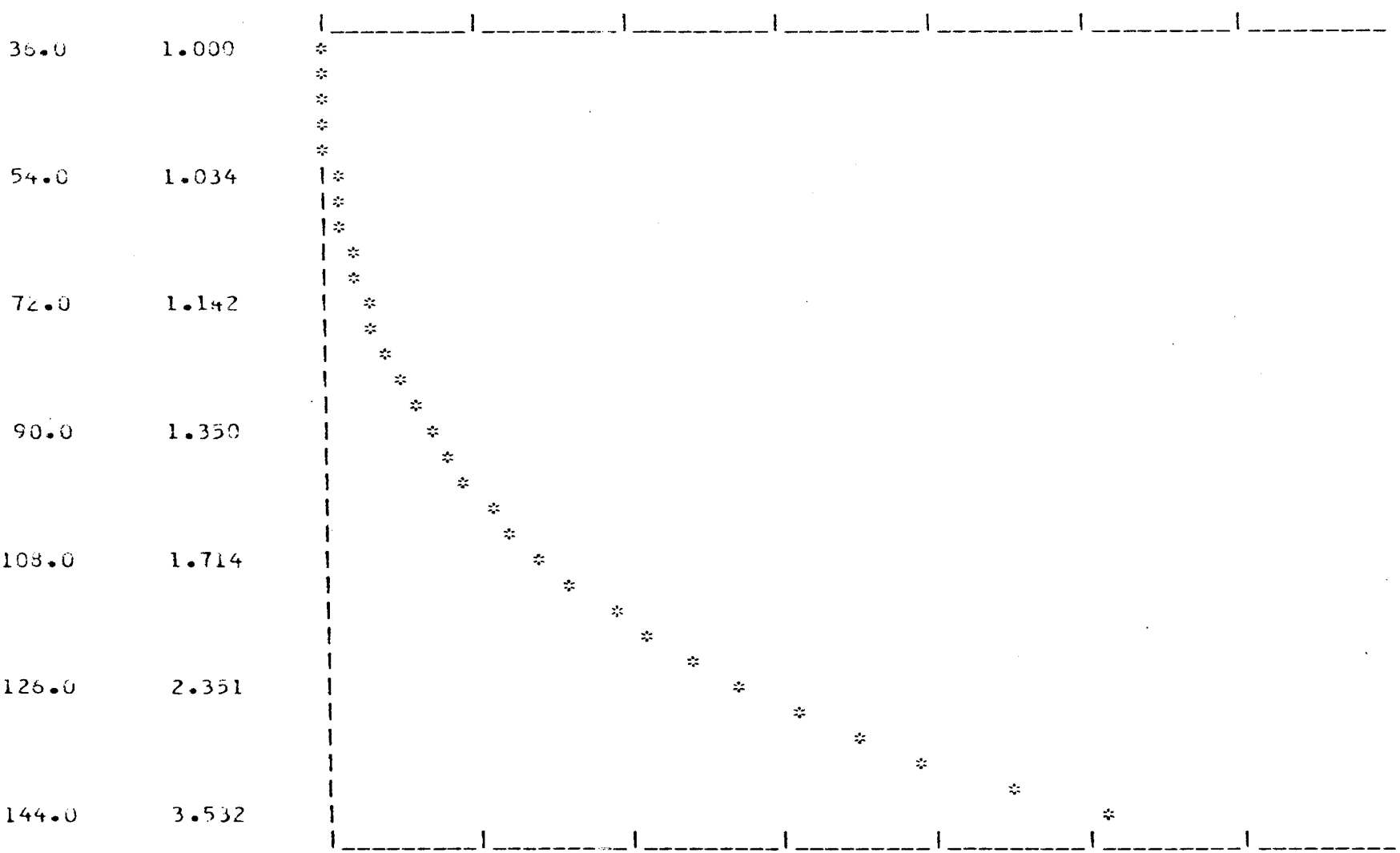

MAXIMUM VOLUME RATIO = 3.532

VANE NUMBER = 6.
SWEPT VOLUME = 1.329

DEGREE	VOL. RATIO
30.0	1.000
50.0	1.043
70.0	1.184
90.0	1.465
110.0	1.989
130.0	2.999
150.0	5.170

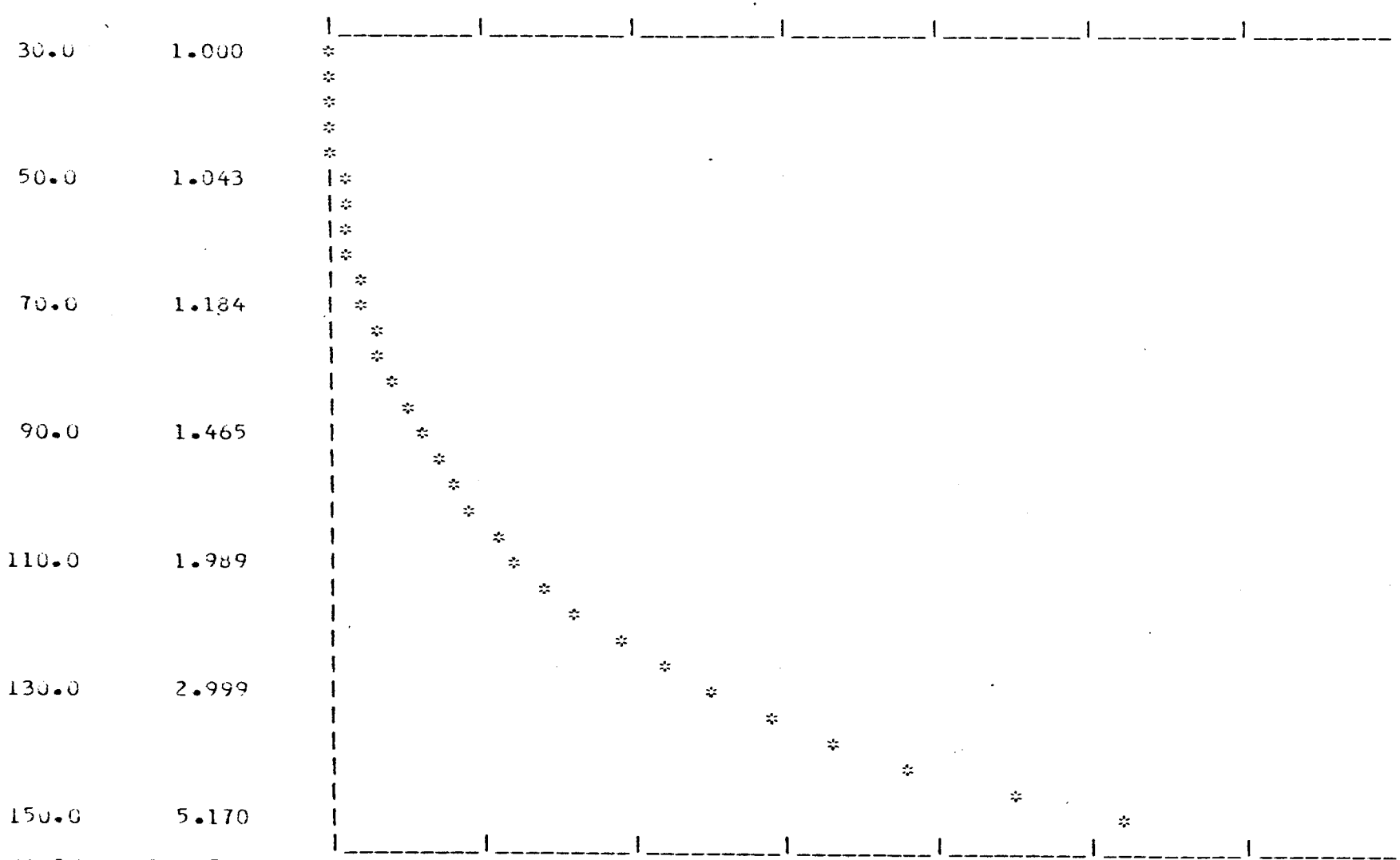

MAXIMUM VOLUME RATIO = 5.170

VANE NUMBER = 8.
SWEPT VOLUME = 1.304

DEGREE	VOL. RATIO
22.5	1.000
45.0	1.056
67.5	1.247
90.0	1.649
112.5	2.472
135.0	4.319
157.5	9.510

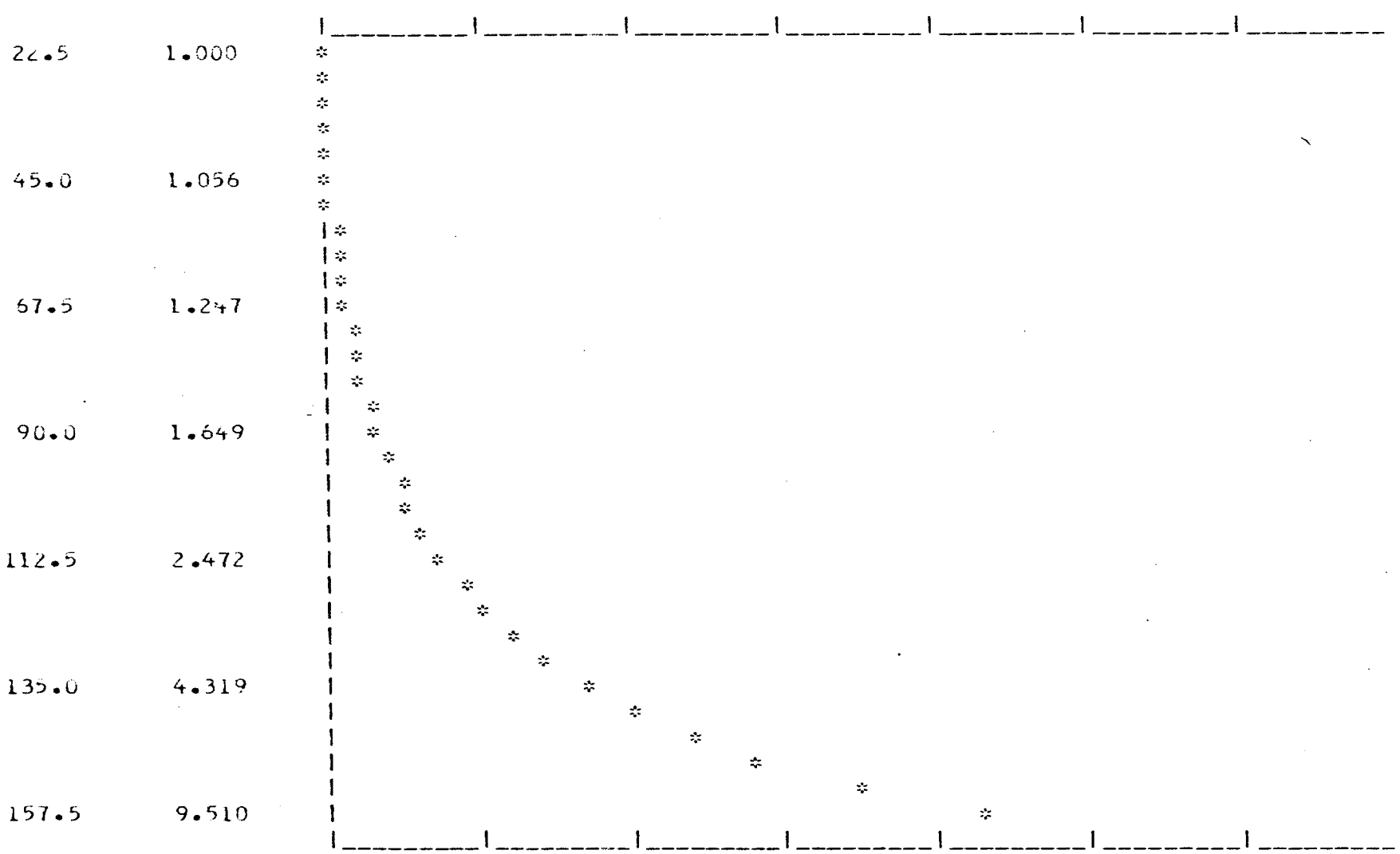

MAXIMUM VOLUME RATIO = 9.510

VANE NUMBER = 10.
SWEPT VOLUME = 1.269

DEGREE	VOL. RATIO
18.0	1.000
42.0	1.066
66.0	1.291
90.0	1.737
114.0	2.869
138.0	5.594
162.0	15.303

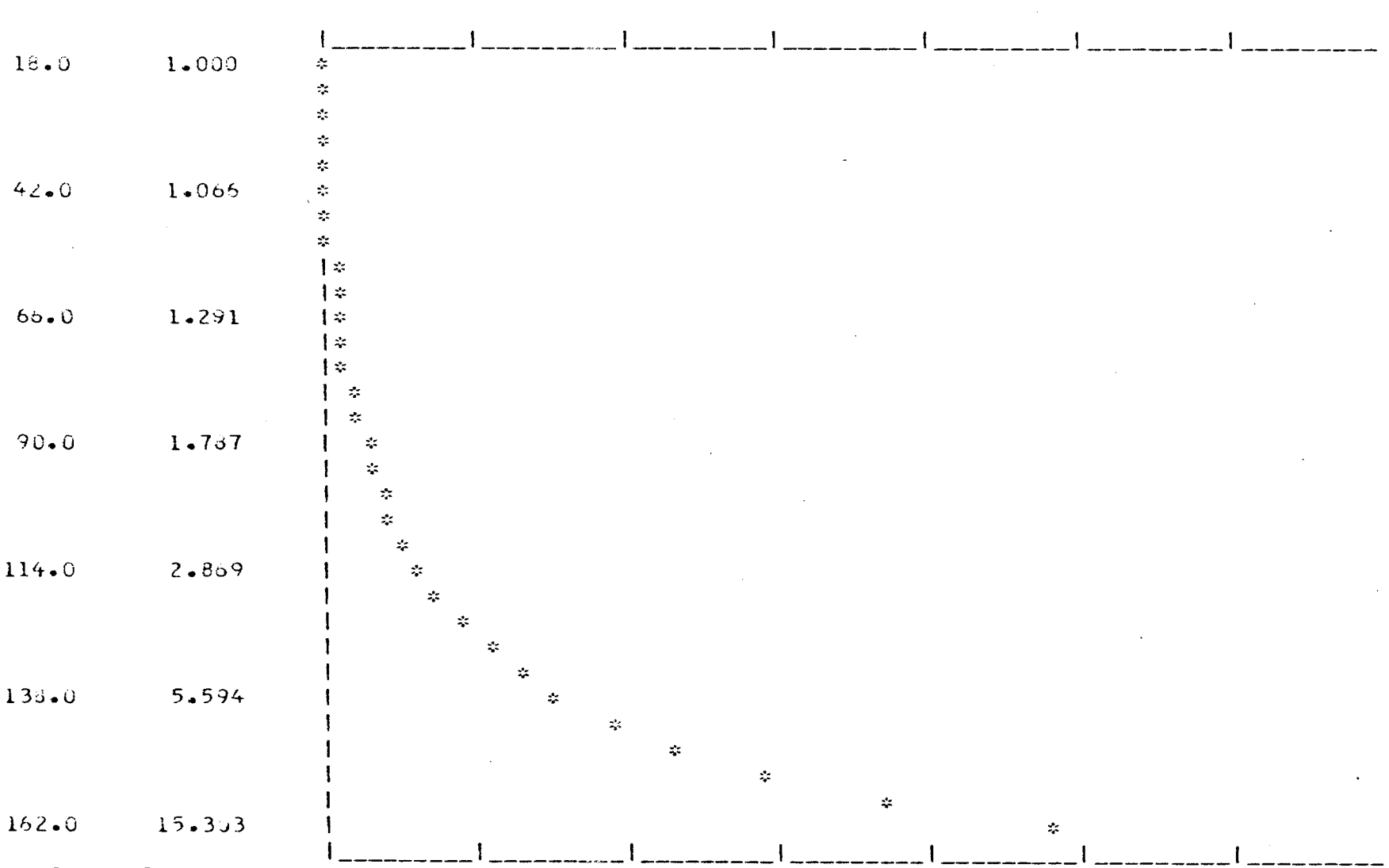

MAXIMUM VOLUME RATIO =15.303

VANE NUMBER = 12.
SWEPT VOLUME = 1.230

DEGREE	VOL. RATIO
15.0	1.000
40.0	1.072
65.0	1.324
90.0	1.894
115.0	3.198
140.0	6.794
165.0	22.634

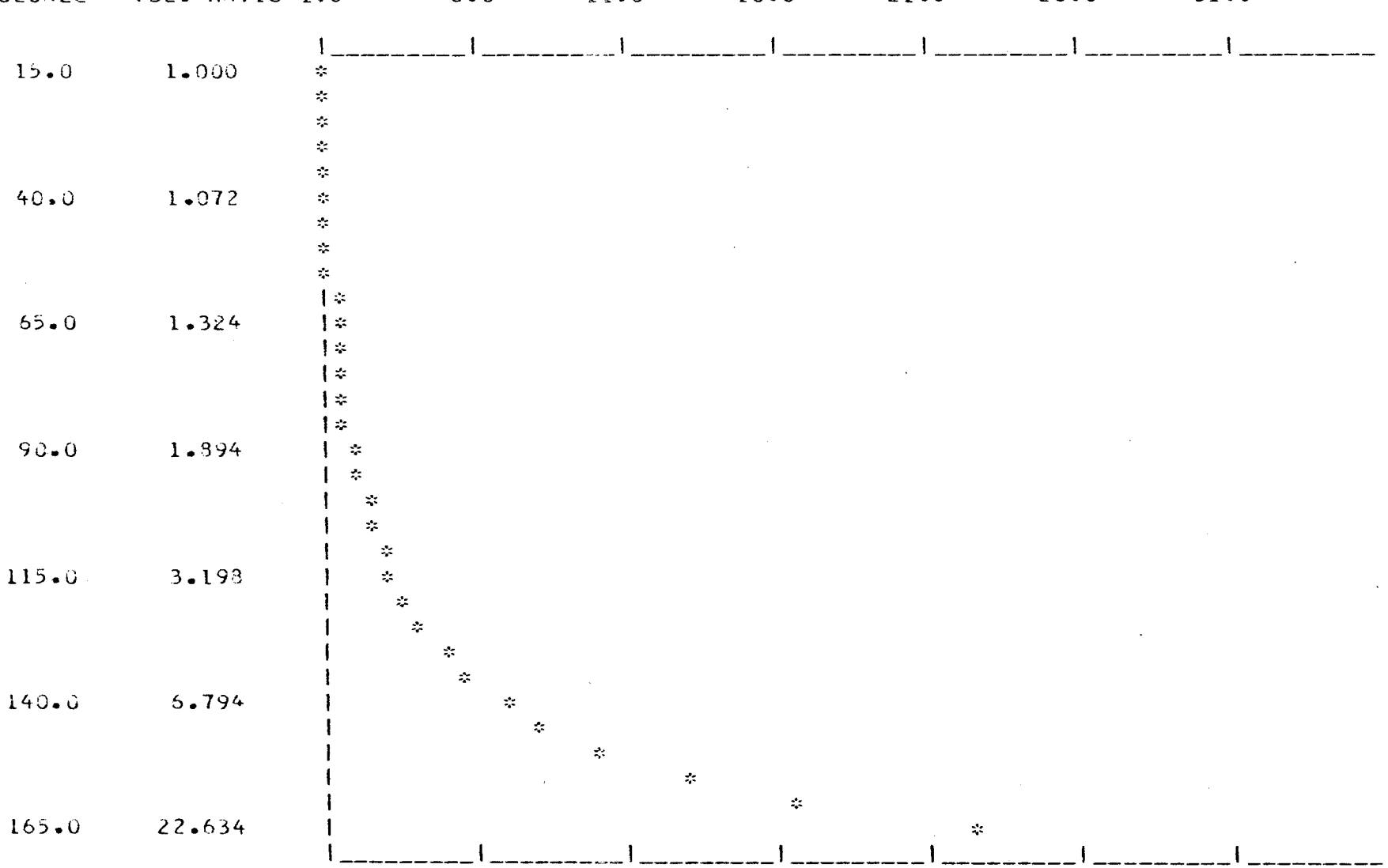

MAXIMUM VOLUME RATIO =22.634

A P P E N D I X E

PROPERTIES OF DELRIN 570x AT 70 F (4)

Ultimate Tensile Strength	8500 psi
Tensile Elongation	7 %
Compressive stress	5400 psi
Flexural Modulus of Elasticity	410000 psi
Specific Gravity	1.56 gr/cm
Rockwell Hardness	M90
Coefficient of thermal expansion	20 /min/in F
Water absorption(24 hr immersion)	0.25 %
Coefficient of friction with steel	0.08
PV Limit (at 800 fpm)	20000 psi-fpm
Wear constant	20X10 in /min ft lb hr

A P P E N D I X F

SPECIFICATIONS OF TORQUE TRANSDUCER

AND

INDICATOR

I) TORQUE TRANSDUCER

Trade Mark	:	BLH Electronics, Irc. Torque Sensor
Type	:	A-1
Capacity	:	100 in-lb (11.3 N-m)
Maximum Speed	:	7000 rpm
Weight	:	5.5 lb (2.5 kg)
Flexural Natural Frequency	:	46600 rpm
Output at Rated Torque	:	1.5 mV/V
Calibration Accuracy	:	0.25 % R.T. Cw or CCw
Nonlinearity	:	0.05 % R.T.
Repetabilty	:	0.05 % R.T.
Hysterisis	:	0.05 % R.T.
Safe Temperature Range	:	-50 to 140 F

Exitation Recomended : 12 V, AC or DC

Maximum : 25 V, AC or DC

Terminal Resistance Input : 350 + 1.5 ohm

Output : 350 + 3.0 ohm

Overload Ratings Safe : 120 %

Electrical Failure : 300 %

Allowable Axial Load Press Fit : 1000 lbs (454 kg)

Insulation Resistance : Bridge to Ground 2000 Mohms

Shield to Ground 1000 Mohms

Termination : MS3102A-18-85-A105 connector with mating 15 ft cable assembly.

II) STRAIN INDICATOR

Input : + 1 mV/V = 10000 counts

Display : 5 active digits

Resolution : + 0.01 %

Bridge Excitation : 10.0 Vdc at 350 mA

System Accuracy : 0.05 % at 50 % of full scale

Measuring Speed : from 3 reading per secondto 1 reading at every 2 second

Power : 115 V or 230 V, 25 W

Temperature Effect On Zero : 0.001 % of full scale

Amplifier Input Impedance : 50 M ohm

A P P E N D I X G

CALIBRATION CHARTS OF THE FLOW NOZZLE AND THERMOCOUPLE

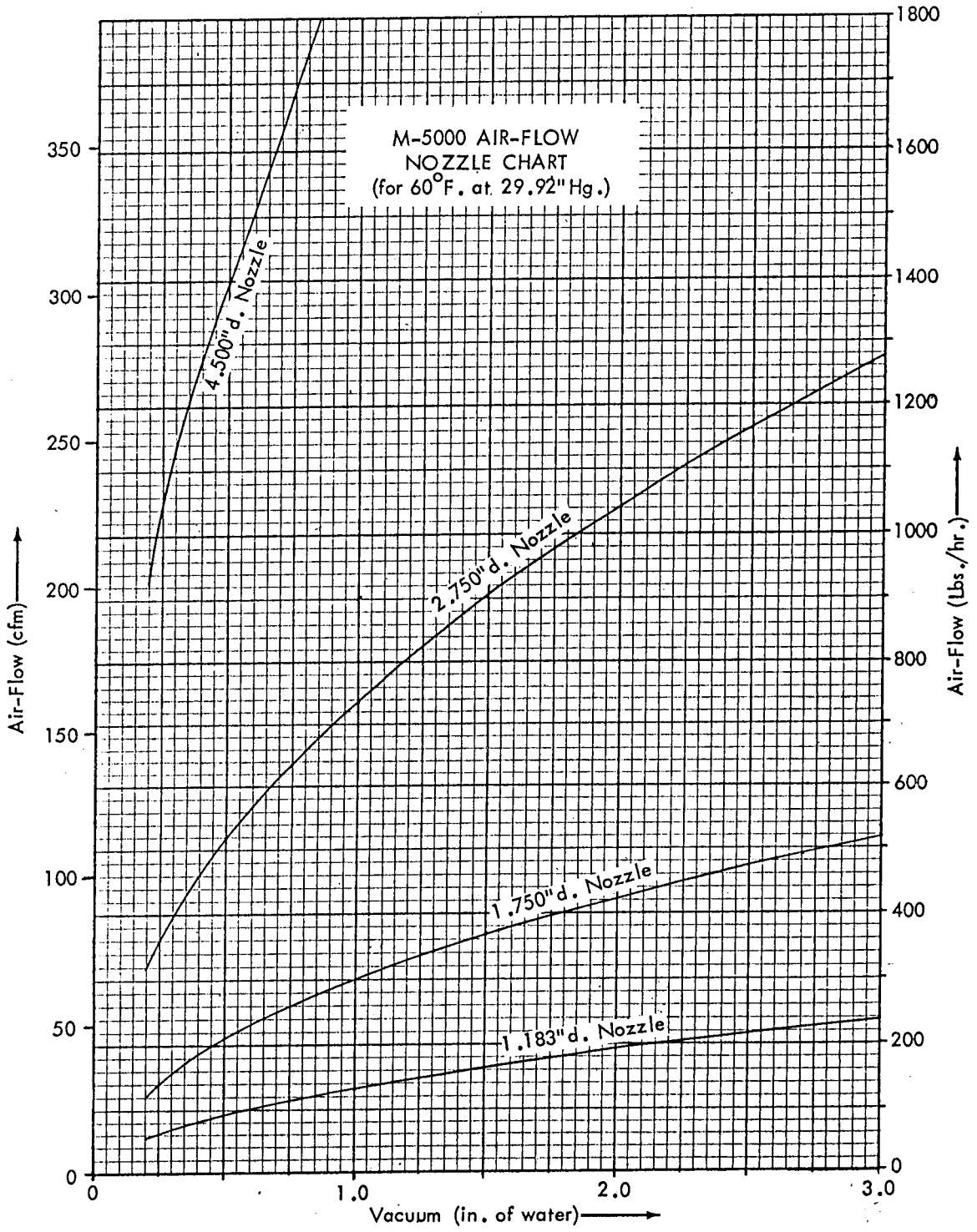
M-5000 AIR-FLOW
NOZZLE CHART
(for 60°F. at 29.92" Hg.)
4.500" d. Nozzle
2.750" d. Nozzle
1.750" d. Nozzle
1.183" d. Nozzle
Air-Flow (cfm)
Air-Flow (Lbs./hr.)
Vacuum (in. of water)
0
50
100
150
200
250
300
350
200
400
600
800
1000
1200
1400
1600
1800
1.0
2.0
3.0

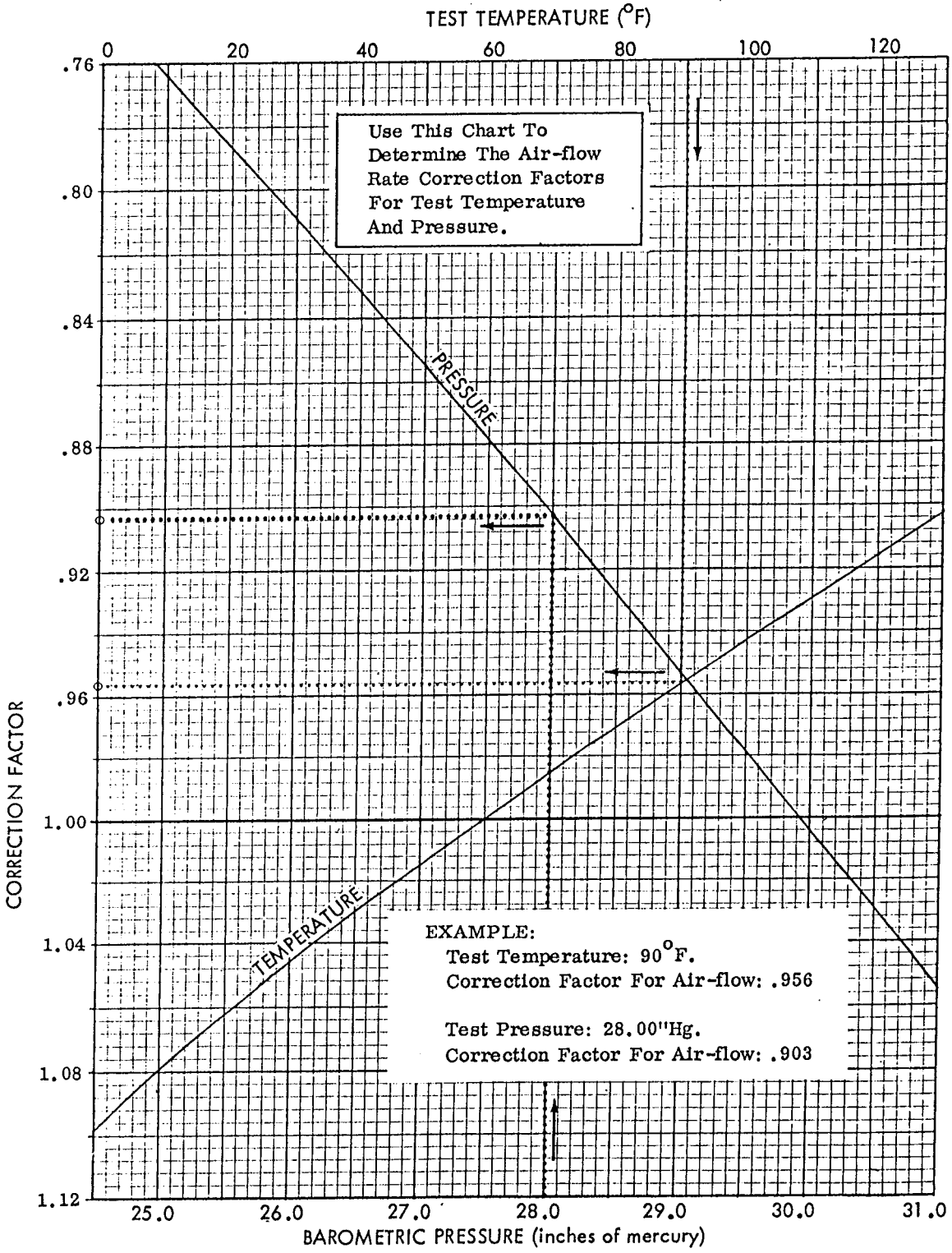
TEST TEMPERATURE (°F)
0
20
40
60
80
100
120
.76
.80
.84
.88
.92
.96
1.00
1.04
1.08
1.12
CORRECTION FACTOR
Use This Chart To Determine The Air-flow Rate Correction Factors For Test Temperature And Pressure.
PRESSURE
TEMPERATURE
EXAMPLE:
Test Temperature: 90°F.
Correction Factor For Air-flow: .956
Test Pressure: 28.00"Hg.
Correction Factor For Air-flow: .903
25.0
26.0
27.0
28.0
29.0
30.0
31.0
BAROMETRIC PRESSURE (inches of mercury)

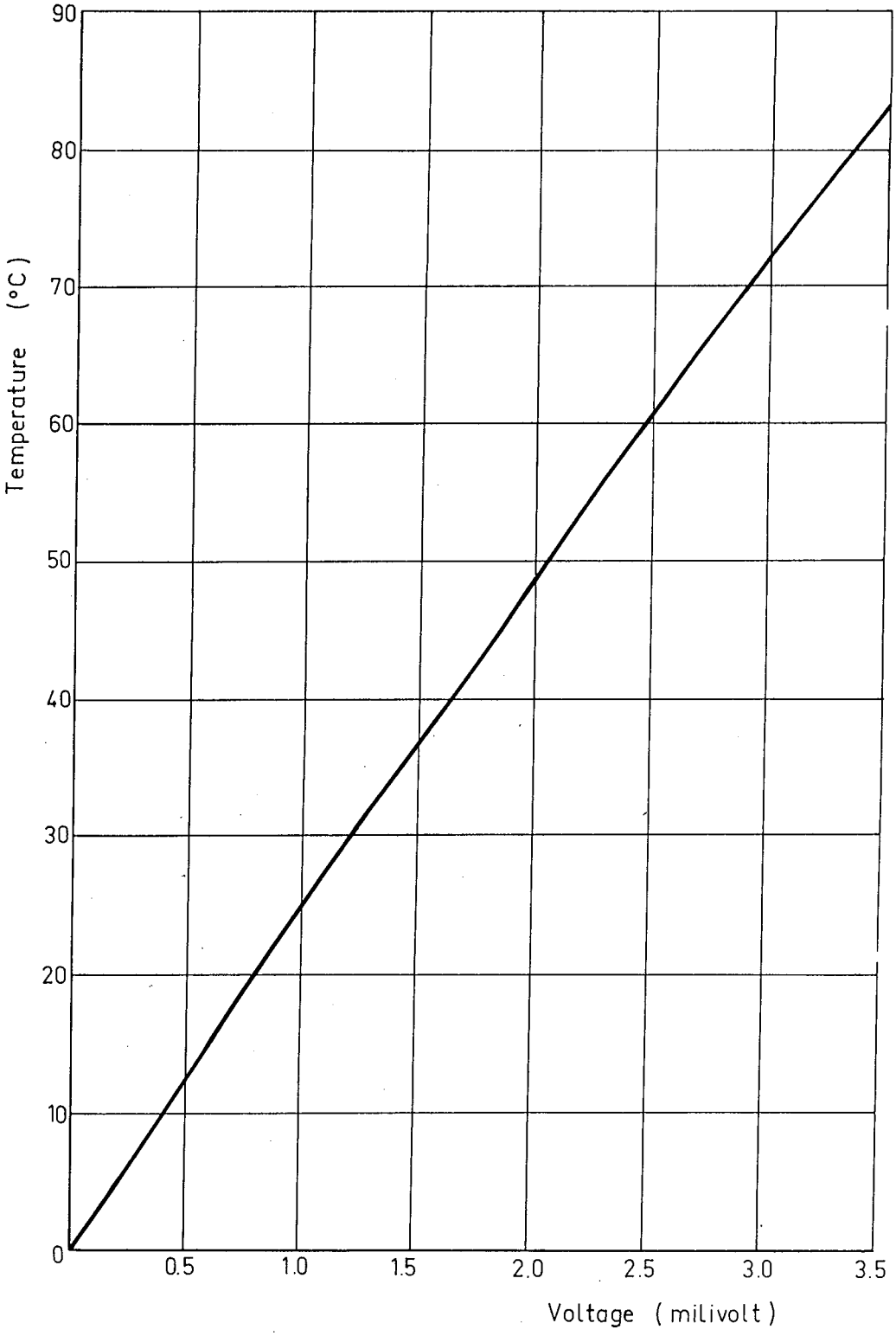
90
80
70
60
50
40
30
20
10
0
Temperature (°C)
0.5
1.0
1.5
2.0
2.5
3.0
3.5
Voltage (milivolt)

A P P E N D I X H

TECHNICAL DRAWINGS

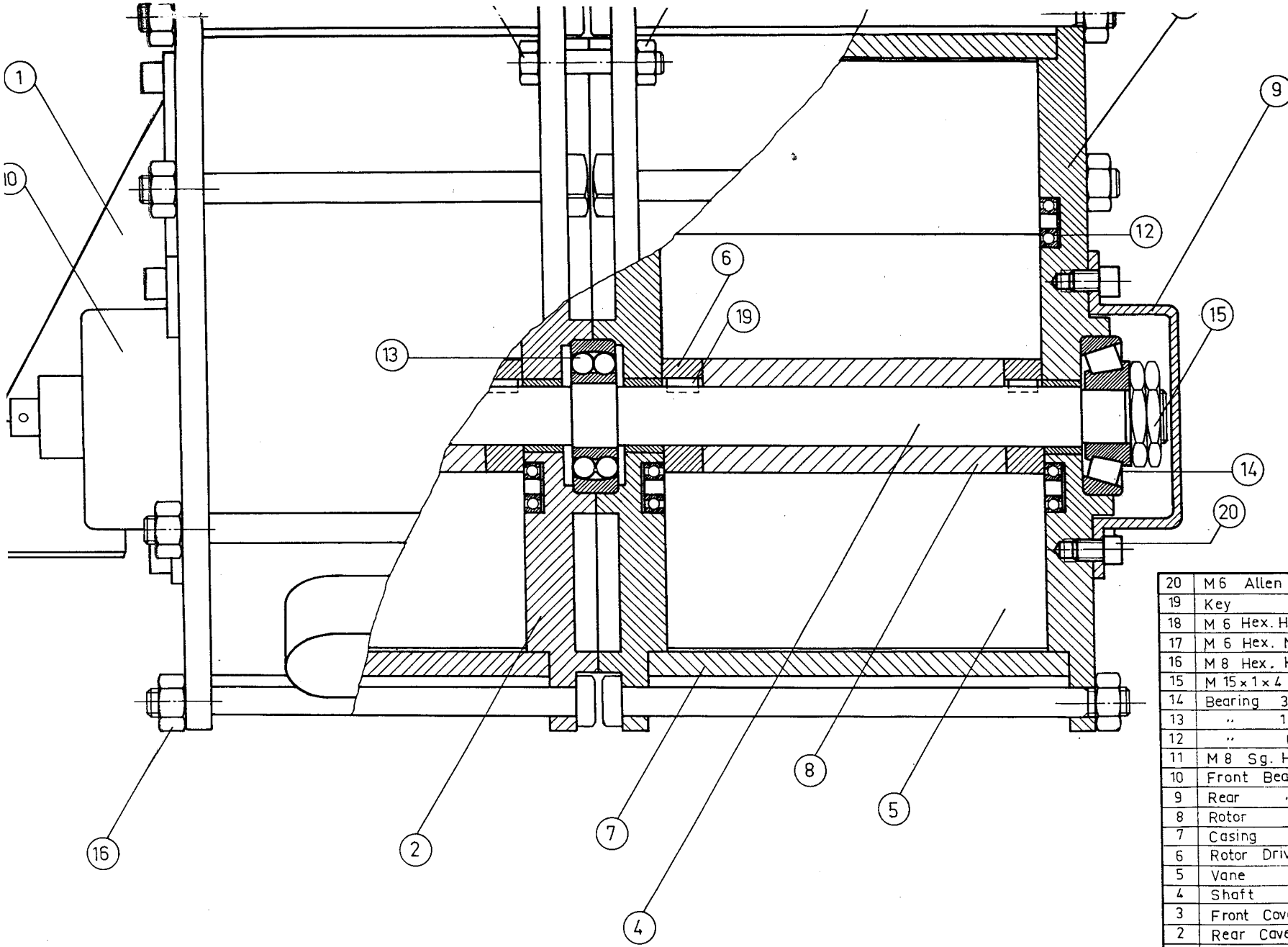

No	Name of part	Quantity	Material
20	M 6 Allen Head Bolt	10	Standard
19	Key	4	Steel
18	M 6 Hex. Head Bolt	6	Standard
17	M 6 Hex. Nut	6	Standard
16	M 8 Hex. Head Bolt	12	Standard
15	M 15 x 1 x 4 Hex. Nut	4	Steel
14	Bearing 30302	2	Standard
13	" 1203	1	Standard
12	" 624	16	Standard
11	M 8 Sg. Head Bolt	12	Steel
10	Front Bearing Cap	1	Steel-Bra
9	Rear " "	1	Steel
8	Rotor	2	Delrin
7	Casing	2	Steel
6	Rotor Driver	4	Brass St
5	Vane	8	Steel
4	Shaft	1	Steel
3	Front Cover	2	Steel
2	Rear Cover	2	Steel
1	Hose Adapter	2	Steel

Drawn by	Selim Okutur	Name of part or Assembly	METU GAZIANTI ENGINEERING FACU
Control		CIRCULATOR	
Date	22-6-982	1/1	Drawin No
Scale			

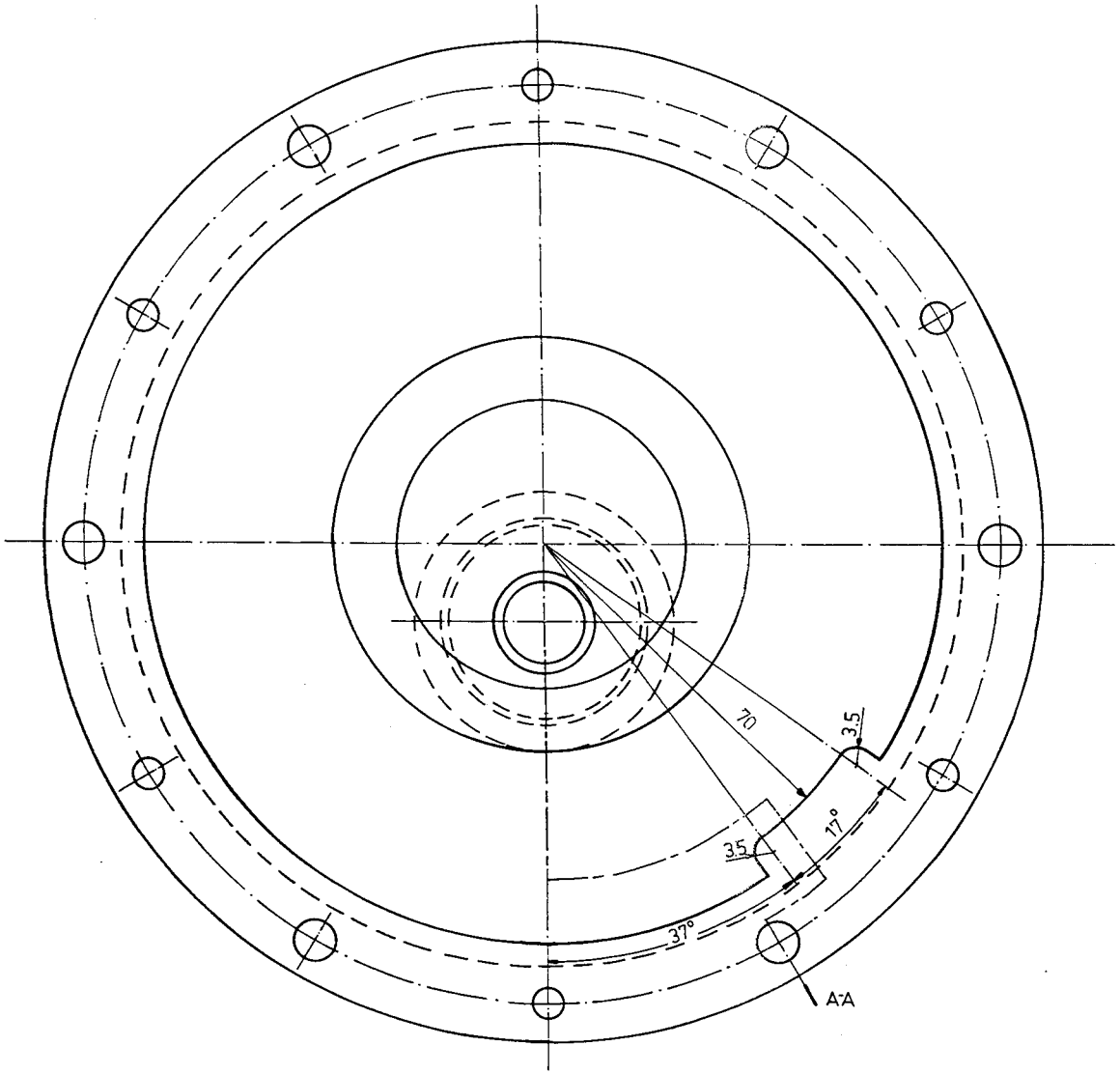

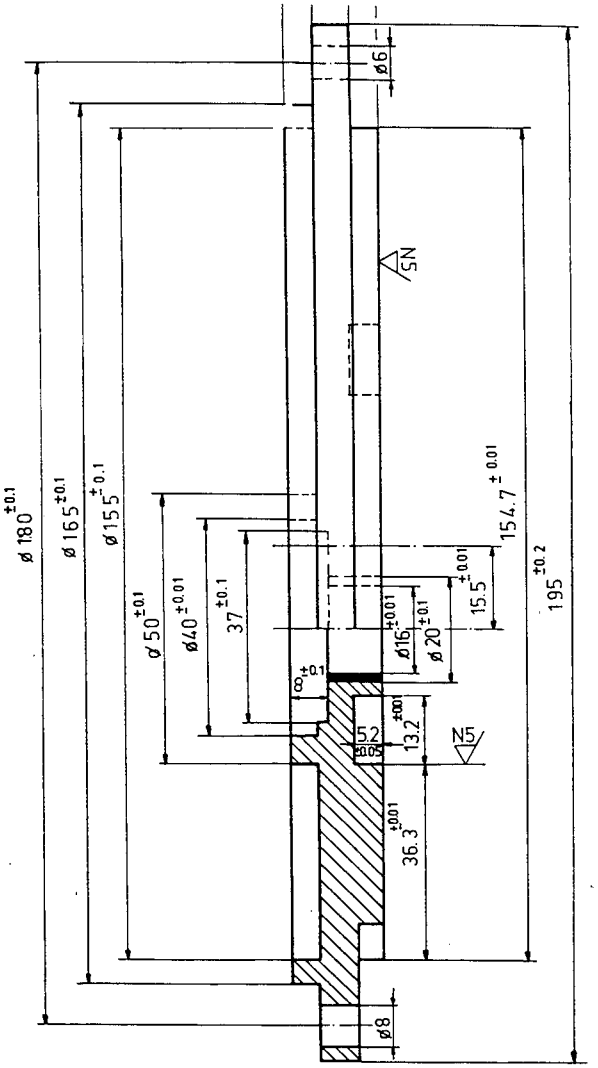

Section A-A

Unspecified tolerances ±0.5

Drawn by	Quantity	Scale	Material	Part Name	Date	Drawing No
Selim Okutur	2	1/1	St 30	Back Cover	22.6.1982	2

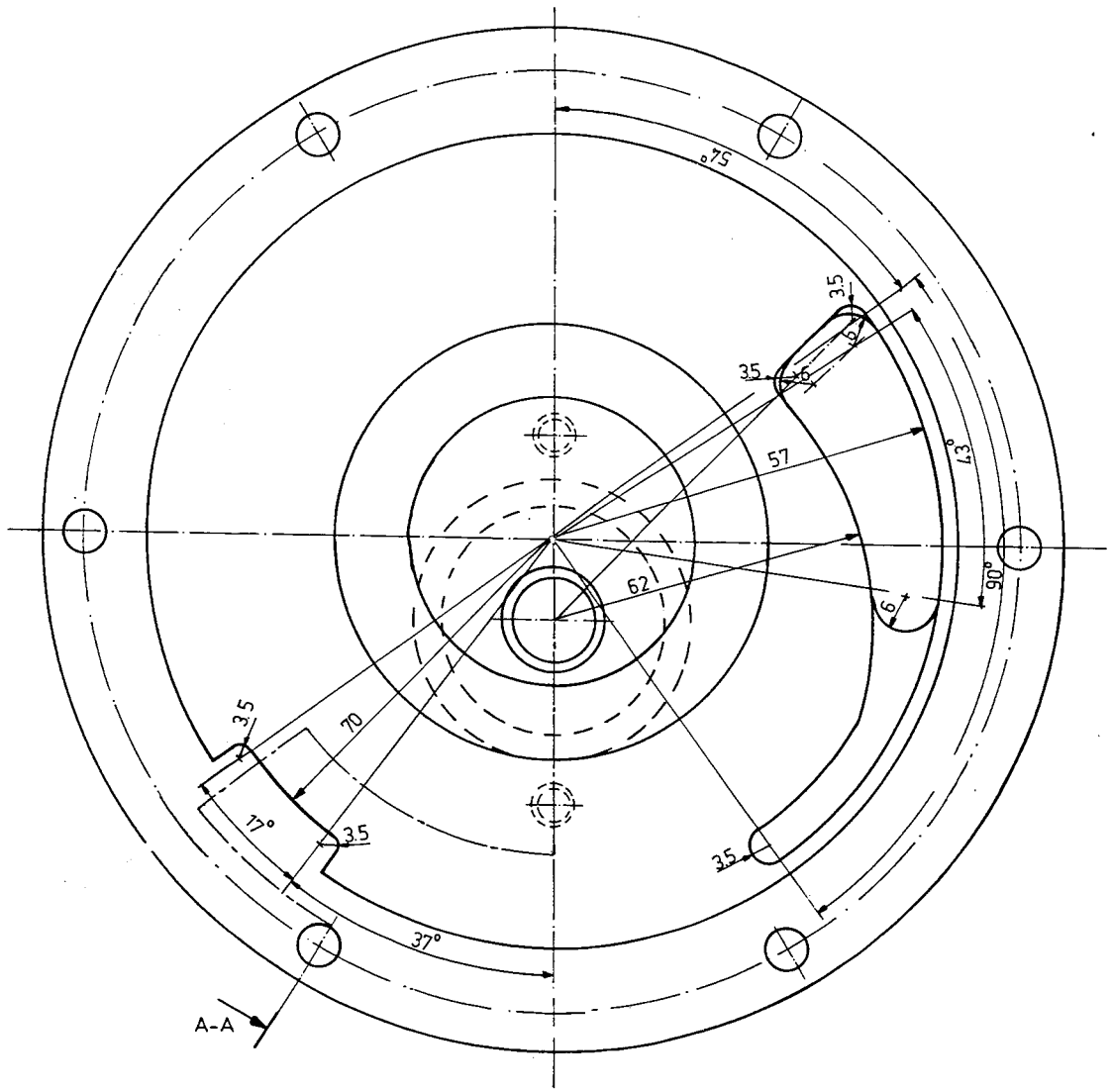

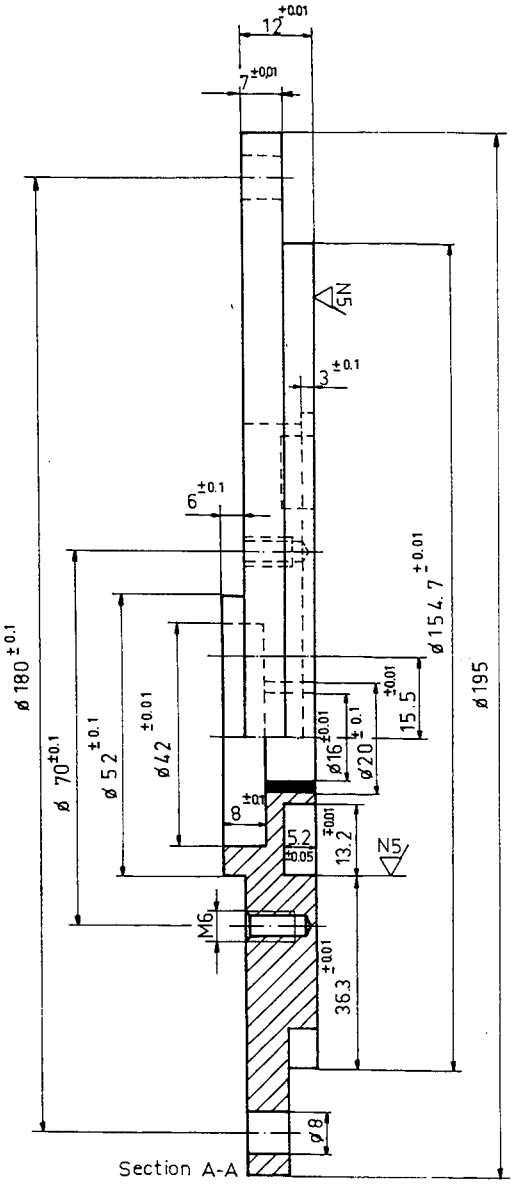

Unspecified tolerances ± 0.5

Drawn by			Material	Part Name	Date	Drawing No.
Selim Okutur	2	1/1	St 30	Front Cover	22-6-1982	3

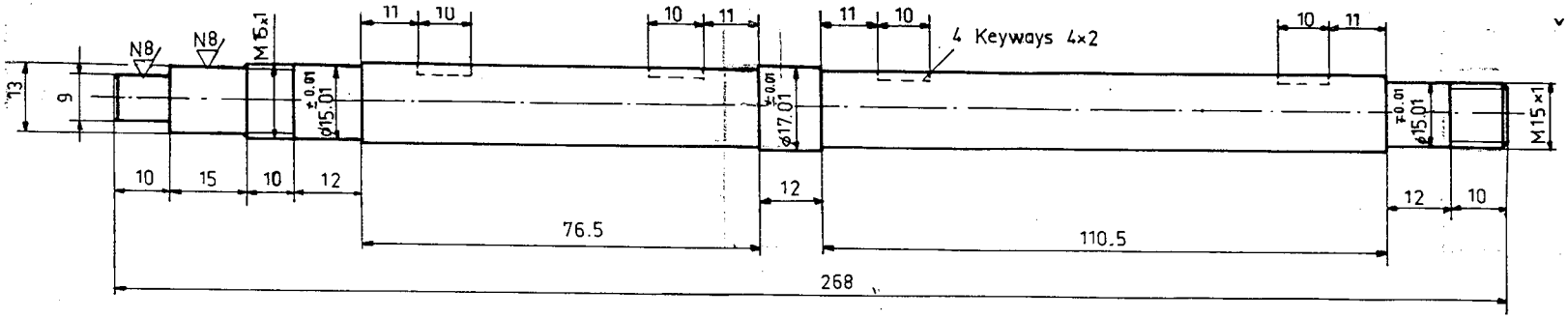

Unspecified tolerances ± 0.1

Drawn by	Quantity	Scale	Material	Part Name	Date	Drawing No
Selim Okutur	1	1/1	St 70	Shaft	15.6.1983	4

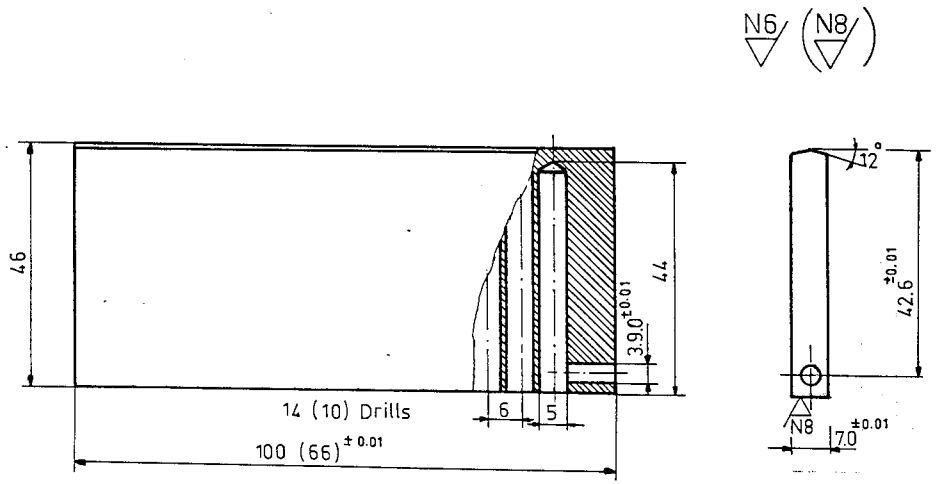

Number in paranthesis designates the dimensions in the expander part.

Unspecified tolerances: ± 0.1

Drawn by	Quantity	Scale	Material	Part Name	Date	Drawing No
Selim Okutur	4+4	1/1	St 40	Blade	15.6.1983	5

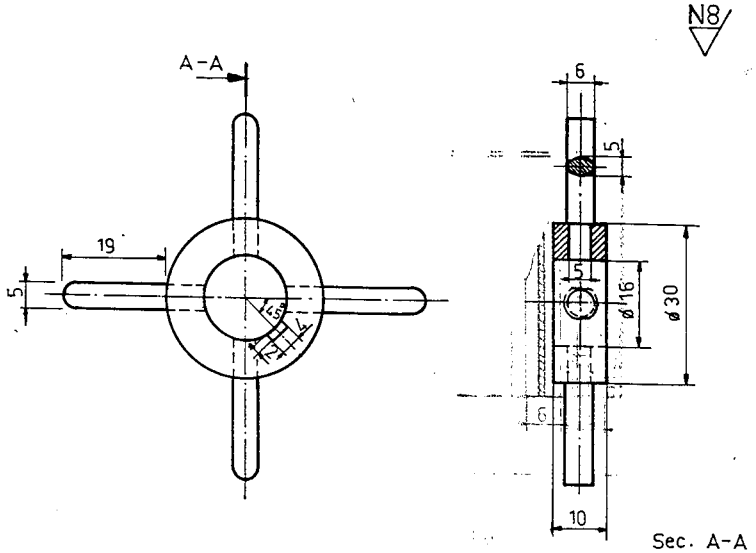

Unspecified tolerances ± 0.1

Drawn by	Quantity	Scale	Material	Part Name	Date	Drawing No
Selim Okutur	4	1/1	Brass Steel	Rotor Driver	15.6.1983	6

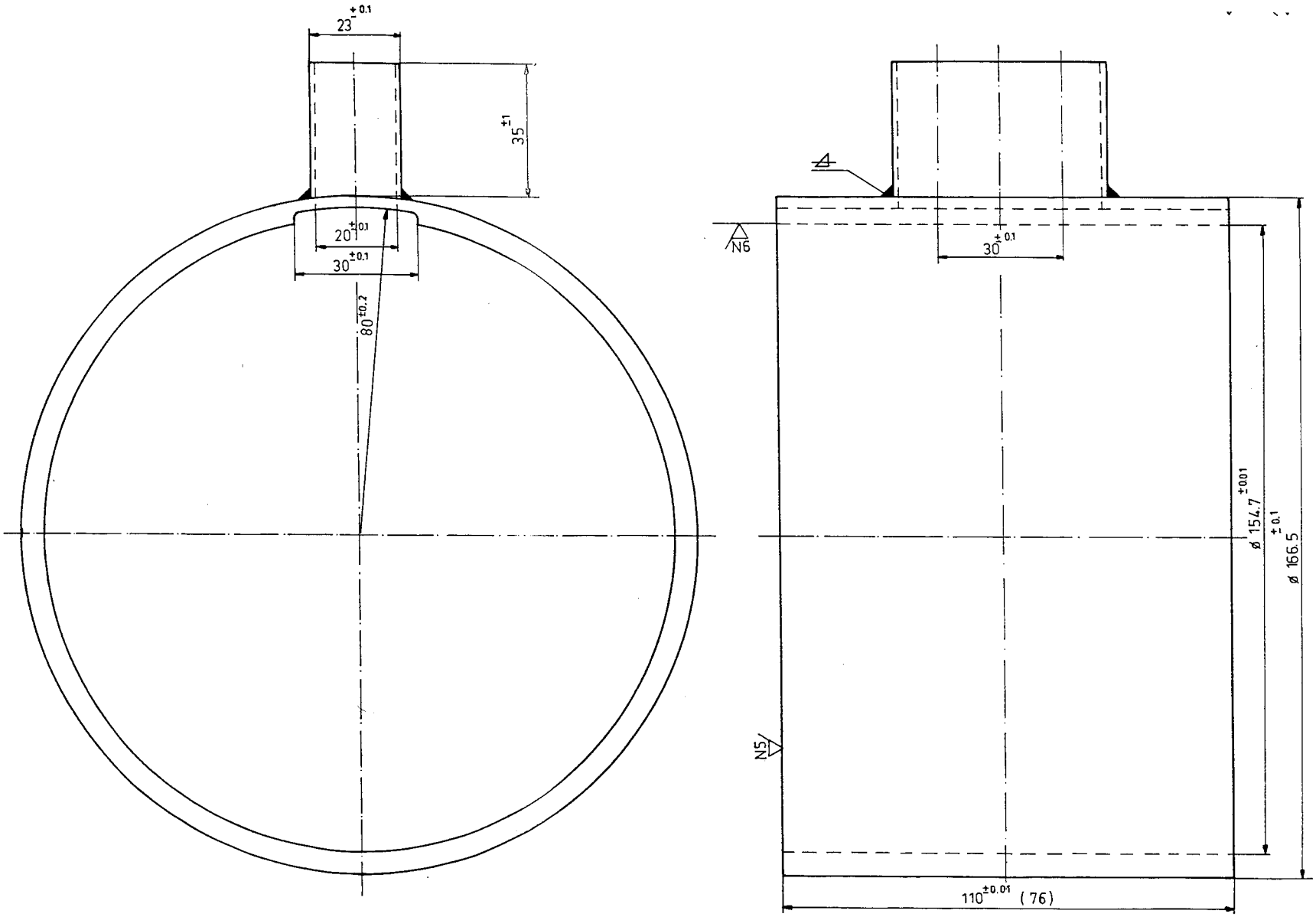

Number in paranthesis designates the dimensions in the expander part.

Drawn by	Quantity	Scale	Material	Part Name	Date	Drawing No
Selim Okutur	-	1/1	St 40	Casing	22.6.1982	7

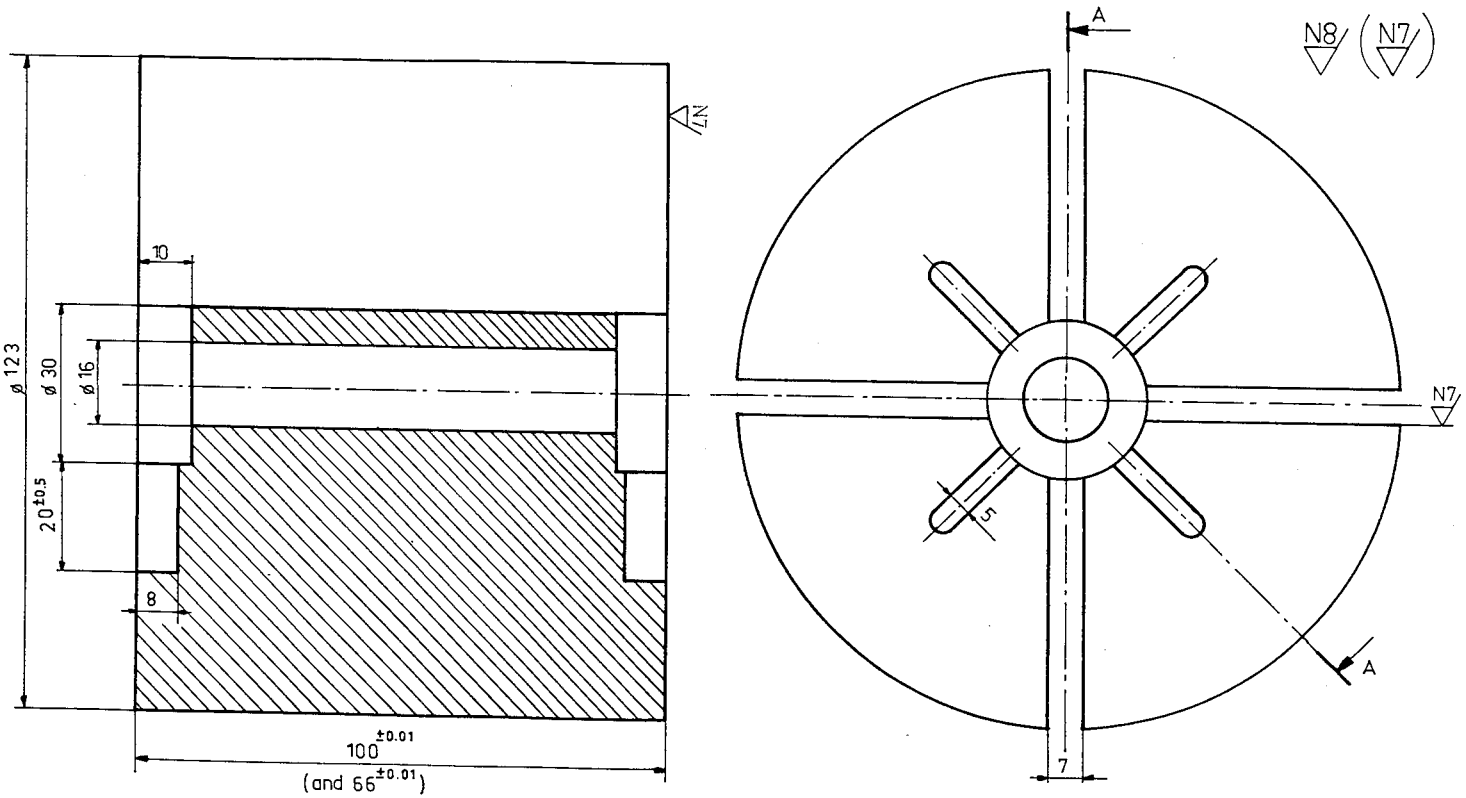

Section A-A

Unspecified tolerances ±0.02

Drawn by	Quantity	Scale	Material	Part Name	Date	Drawing No
Selim Okutur	2	1/1	Delrin 570X	Rotor	21.6.1983	8